# Reference Handbook of Gynecologic Pelvic MRI

*Lauren F. Alexander, MD*[1] • Stephanie Nougaret, MD, D*[2] • Krupa Patel-Lippmann, MD[3] • Aradhana M. Venkatesan, MD[4] • Pamela I. Causa-Andrieu, MD[5]*
*Myra K. Feldman, MD[6] • Madhura Desai, MD, D[1] • Wyanne Law, MD[7] • Bahar Mansoori, MD[8] • Refky Nicola, MSc, DO[9]*
*Elizabeth A. Sadowski, MD**[10] • Yulia Lakhman, MD**[7,11]

*L.F.A. and S.N. contributed equally to this work.
**E.A.S. and Y.L. are co–senior authors.
Author affiliations, funding, and conflicts of interest are listed at the end of this article.
See the invited commentary by Ghafoor and Stocker in this issue.

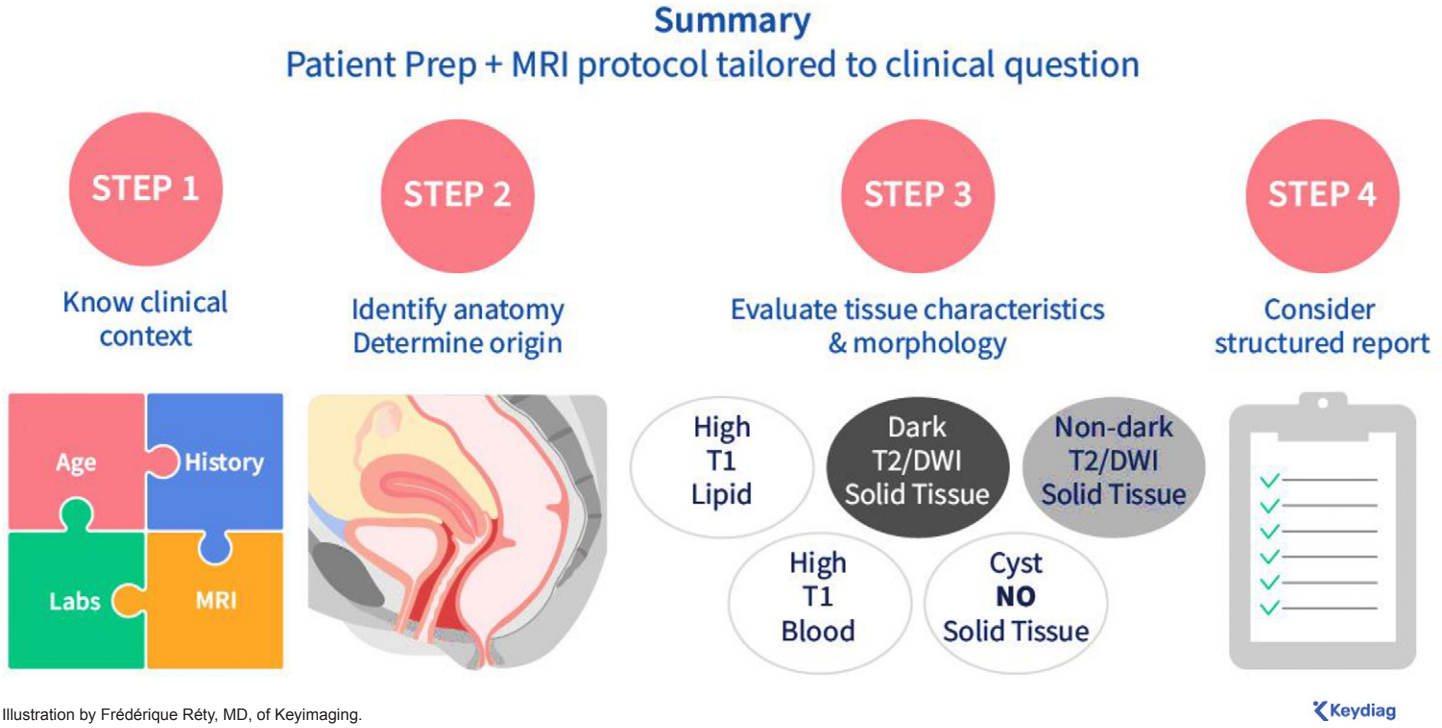


Illustration by Frédérique Réty, MD, of Keyimaging.

Gynecologic pelvic MRI is a crucial imaging modality for problem solving, offering superior soft-tissue contrast and multiplanar capabilities for the detailed evaluation of female patients across a range of indications. Accurate interpretation of gynecologic pelvic MRI depends on using protocols tailored to the clinical indication, reviewing the patient's clinical history (such as age, symptoms, medical and surgical history, and genetic mutations), and considering laboratory data. A comprehensive understanding of the female pelvic anatomy, best visualized on high-resolution multiplanar T2-weighted images, is also essential. A systematic step-by-step approach to lesion evaluation further contributes to accurate interpretation. This process begins with determining lesion origin. Once identified, evaluating lesion tissue composition and assessing solid tissue morphology enables lesion classification into one of the following categories: *(a)* T1-hyperintense lipid-containing lesions, *(b)* T1-hyperintense blood-containing lesions without solid tissue, *(c)* cysts (simple or proteinaceous fluid) without solid tissue, *(d)* cystic or solid lesions with dark T2/dark diffusion-weighted imaging (DWI) solid tissue, and *(e)* cystic or solid lesions with non-dark T2/non-dark DWI solid tissue. Based on lesion origin and these categories, the differential diagnosis can be developed and communicated in a structured radiology report, ensuring clear and concise communication with the treatment team.



## Introduction

MRI is used routinely in patients with gynecologic conditions due to its superior soft-tissue contrast and multiplanar capability. It can provide a detailed assessment of pelvic anatomy, lesion origin, tissue characteristics, and disease extent. Its indications include *(a)* characterizing US-indeterminate adnexal masses, *(b)* evaluating the cause of pelvic pain and abnormal uterine bleeding, *(c)* mapping symptomatic uterine leiomyomas and differentiating them from uterine sarcomas, *(d)* staging gynecologic cancers, and *(e)* addressing complex

RG
OBSTETRIC AND GYNECOLOGIC IMAGING

Invited Commentary TestYour Knowledge CME

**RadioGraphics 2026; 46(2):e250029**
**https://doi.org/10.1148/rg.250029**

**Content Codes:** MR, OB

**Abbreviations:** ADC = apparent diffusion coefficient, CSF = cerebrospinal fluid, DWI = diffusion-weighted imaging, LN = lymph node

## TEACHING POINTS

- MRI offers exceptional anatomic detail, with multiplanar T2-weighted imaging serving as the cornerstone of anatomic assessment. Radiologists must have a thorough understanding of female pelvic anatomy to interpret pelvic MRI effectively.
- Before interpretation, radiologists should review the clinical information, including patient age and indications for MRI. Key clinical details include symptoms such as pelvic pain, amenorrhea, abnormal bleeding or discharge, virilization, or precocious puberty; duration of symptoms; and signs of infection.
- Characterizing a lesion begins with identifying normal structures and the likely origin, guided by the clinical history. Start by locating the ovaries and uterus.
- A systematic review of in- and opposed-phase and fat-saturated T1-weighted images to assess for lipid versus blood content, followed by review of T2-weighted and contrast-enhanced images to distinguish cysts from cystic and solid lesions based on the presence of solid tissue in the latter two, along with evaluation of diffusion-weighted images and the ADC map, enables categorization of lesions into five groups: *(a)* T1-hyperintense lipid-containing lesions, *(b)* T1-hyperintense blood-containing lesions without solid tissue, *(c)* cysts (simple or proteinaceous fluid) without solid tissue, *(d)* cystic or solid lesions with dark T2/dark DWI solid tissue, and *(e)* cystic or solid lesions with non-dark T2/non-dark DWI solid tissue.
- *Solid tissue* is defined as a solid component that demonstrates enhancement.

congenital müllerian duct anomalies. Additional indications include evaluating for pelvic floor dysfunction, fistulas, or placental abnormalities.

This article aims to enhance the interpretation of female pelvic MRI for gynecologic conditions. After outlining patient preparation, tailored MRI protocols, and the normal female pelvic anatomy, a step-by-step approach to interpretation is presented, focusing on evaluating lesion origin, lesion tissue composition, and solid tissue morphology (Fig 1). The review also emphasizes the importance of incorporating the patient's clinical history to narrow the differential diagnosis and the role of disease-specific structured reporting in improving communication (Fig 1).

## Patient Preparation and Tailored MRI Protocols

Proper patient preparation is crucial to minimize artifacts. Patients should empty their bladder approximately 1 hour before scanning for partial filling to help achieve the optimal uterine position for imaging (1–4). Administering an antiperistaltic agent (such as glucagon 1 mg intramuscularly or intravenously), if not contraindicated, can improve image quality by reducing peristalsis-related motion artifacts (5,6). A microenema can help evacuate rectal contents, minimizing rectal gas and reducing distortion at diffusion-weighted imaging (DWI) (5–7). Vaginal distention with US gel is considered optional according to consensus statements (4,8,9). However, it may enhance the evaluation of vaginal involvement in deep endometriosis, cervical cancer, and congenital müllerian duct anomalies (10,11). After a 60-mL syringe is filled with US gel and air bubbles are removed to prevent susceptibility artifact, patients can often insert the gel themselves (4).

Examinations are performed at 1.5 T or 3 T with the patient in the supine position, using a pelvic phased-array surface coil to maximize the signal-to-noise ratio. Standard female pelvic MRI protocols include a core set of sequences tailored to clinical indications. These sequences include large field-of-view (FOV) coronal pelvic T2-weighted imaging extending to the kidneys, axial pelvic in- and out-of-phase T1-weighted imaging, and axial pelvic T2-weighted imaging (12,13). High-resolution small FOV multiplanar T2-weighted imaging is performed in at least two orthogonal planes aligned with the organ of interest (Figs 2, 3) (14–16). DWI is performed in at least one plane with $b$ values of 0–50 and 1000 sec/mm$^2$, matched to one of T2-weighted imaging in plane, FOV, and section thickness (17,18). A corresponding apparent diffusion coefficient (ADC) map is then generated. Finally, three-dimensional T1-weighted imaging with fat suppression is performed pre- and postcontrast using dynamic or multiphase techniques depending on the indication (8–10,19–25). Protocol details, the rationale for various sequences, and tips for interpretation are outlined in Table S1 (1–25).

## Key Anatomic Details of the Female Pelvis

MRI offers exceptional anatomic detail, with multiplanar T2-weighted imaging serving as the cornerstone of anatomic assessment. Radiologists must have a thorough understanding of female pelvic anatomy to interpret pelvic MRI effectively.

### Pelvic Compartments

The pelvis is divided into the peritoneal cavity and the subperitoneal space (26–28). The peritoneal cavity is lined by the peritoneum and normally contains minimal fluid. The subperitoneal space houses organs, mesenteries, and connective tissues. The intraperitoneal organs are fully enveloped by the peritoneum, while the extraperitoneal organs lie in the subperitoneal space (Fig 4).

The vesicouterine pouch and rectouterine pouch are formed by the peritoneal reflections over the bladder dome, uterine corpus, and rectum (28,29). The posterior border of the rectouterine pouch is lined by the anterior peritoneal reflection, separating the intra- and extraperitoneal rectum and appearing as a thin T2-hypointense line (Fig 4) (30).

The extraperitoneal organs are divided into the anterior compartment, middle compartment, posterior compartment, and bilateral pelvic sidewalls (Fig 4) (28,29,31). The anterior compartment includes the bladder as well as the prevesical and perivesical spaces (Fig 5) (32,33). The bladder, median umbilical ligament (obliterated urachus), and medial umbilical folds are enclosed by the umbilical fascia, forming the perivesical space. The prevesical space lies anterior and lateral to the bladder, with the retropubic space of Retzius behind the pubic symphysis.

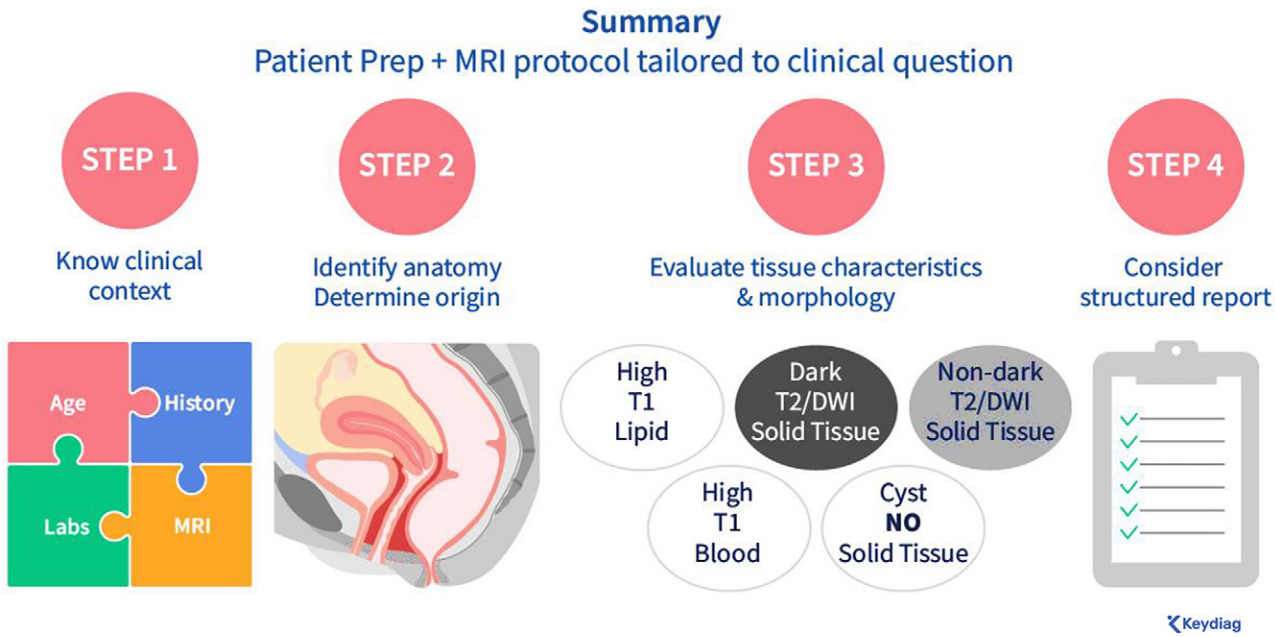


**Figure 1.** Proposed step-by-step approach to interpreting female pelvic MRI. *DWI* = diffusion-weighted imaging, *T2* = T2-weighted imaging.

The middle compartment contains the uterus and vagina. The uterus is supported by the broad ligaments, paired double-layered peritoneal folds extending to the pelvic sidewalls and floor (Fig 6) (29,34). The broad ligaments, indistinct at T2-weighted imaging unless outlined by ascites, are divided into three parts: mesometrium (laterally, supporting the uterine body), mesosalpinx (superiorly, supporting the fallopian tubes), and mesovarium (posteriorly, supporting the ovaries). They enclose the uterus, fallopian tubes, proximal round ligament, and ovarian ligament, as well as uterine and gonadal (ovarian) vessels. The round ligaments, T2-hypointense ropelike fibromuscular structures, extend from the uterine cornua along the anteromedial aspect of the external iliac vessels, passing through the inguinal canal and reaching the anterior labia majora and mons pubis (Fig 5) (29,34). The uterosacral and cardinal ligaments attach the torus uterinus (posterolateral uterocervical junction), cervix, and superior vagina to the presacral tissues and pelvic sidewalls, respectively (29,34). The cardinal ligaments, indistinct at T2-weighted imaging, enclose the uterine vessels, while the uterosacral ligaments, thin paired T2-hypointense bands, extend from the torus uterinus to the presacral tissues (Fig 5) (29).

The posterior compartment includes the rectum, anus, mesorectal fat enclosed by the mesorectal fascia, and the presacral space (Figs 4,5) (28,29,31). The mesorectal fascia, a thin T2-hypointense fibrous structure, is composed of the rectovaginal fascia anteriorly, uterosacral ligaments laterally, and pelvic fascia posteriorly. The presacral space lies between the mesorectal and presacral fascia.

The pelvic sidewalls, bordered by the obturator internus and piriformis muscles, house the iliac vessels, ureters, and lateral pelvic lymph nodes (LNs) (35). Inferior support for the pelvis is provided by the pelvic diaphragm (levator ani and coccygeus muscles), perineal membrane, urogenital triangle, and external anal sphincter (31).

## Ovaries and Fallopian Tubes

***Ovaries.***—The ovaries are mobile intraperitoneal organs supported by the ovarian ligament (connecting the ovary to the uterine cornua), the mesovarium (anchoring the ovary to the broad ligament), and the suspensory ligament (connecting the ovary to the pelvic sidewall and enclosing gonadal vessels) (Fig 6) (36). The gonadal arteries arise from the abdominal aorta below the renal arteries; the right gonadal vein drains into the inferior vena cava and the left into the left renal vein. A gonadal vein diameter greater than 0.8 cm is abnormal, although the correlation between gonadal vein diameter and venous reflux is poor (37). Gonadal vessels travel anterior to the psoas muscles and lateral to the ureters.

Ovarian appearance varies depending on the phase of the menstrual cycle and menopausal status. Premenopausal ovaries are larger oval-shaped structures, with zonal anatomy best seen at T2-weighted imaging, including a T2-hypointense cortex, a T2-intermediate medulla with loosely packed stroma and vessels, T2-hyperintense thin-walled follicles, and occasionally a corpus luteum (19,38). A corpus luteum shows a thick T2-intermediate wall due to luteinized theca cells, which becomes crenulated during involution. A nonhemorrhagic corpus luteum appears centrally T1 hypointense and T2 hyperintense, whereas a hemorrhagic corpus luteum shows central T1 and T2 hyperintensity, sometimes exhibiting a hematocrit level. Following intravenous contrast material administration, the ovarian cortex and stroma enhance mildly, less intensely than the myometrium, whereas the corpus luteum wall demonstrates early avid enhancement (38). Postmenopausal ovaries are smaller than premenopausal ovaries, with a T2-intermediate-to-hypointense cortex and medulla, and occasional small cysts (38). Table S2 and Figures 7–10 detail MRI features of common physiologic and other benign ovarian observations (19,38–42).

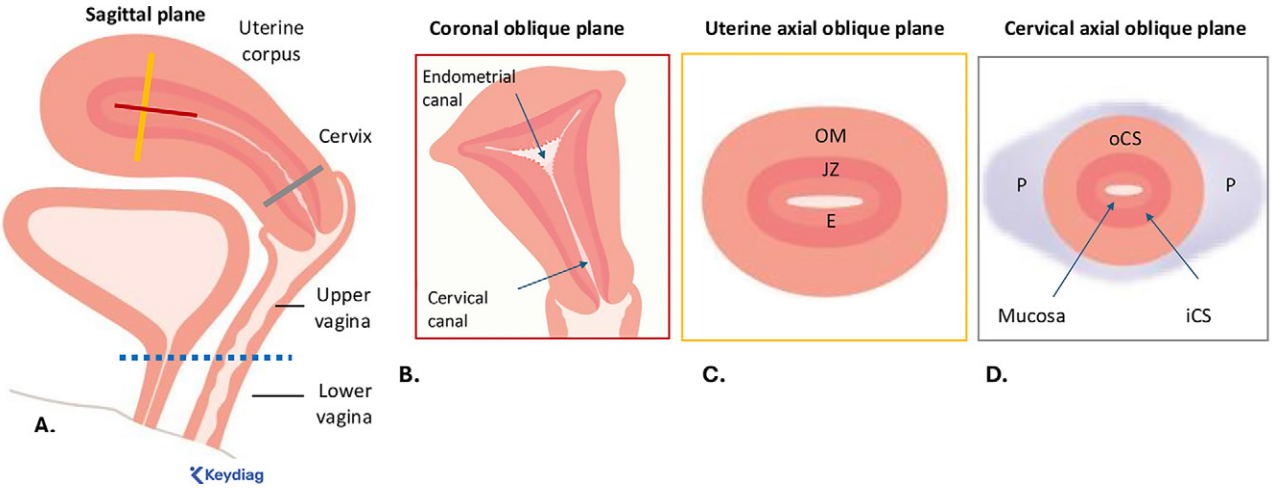


**Figure 2.** Illustrations depict the imaging planes commonly used in MRI evaluation of the female pelvis. Midsagittal illustration **(A)** through the uterus shows key MRI plane prescriptions. The red line in **A**, parallel to the uterine corpus, indicates the prescription of the coronal oblique or ovarian axis (illustrated in **B**; red box), which helps differentiate between uterine and ovarian origin of an adnexal mass and outlines the outer contour of the uterine fundus, relevant in the evaluation of müllerian duct anomalies. The yellow line in **A**, perpendicular to the uterine corpus, shows the prescription of the uterine axial oblique plane (illustrated in **C**; yellow box). This plane is used to assess the depth of myometrial invasion in endometrial cancer staging or to map the locations of uterine leiomyomas. The gray line in **A**, perpendicular to the cervix, represents the prescription of the cervical axial oblique plane (illustrated in **D**; gray box), which is essential for assessing parametrial invasion in cervical cancer staging. Last, the blue dashed line in **A** placed horizontally at the bladder neck divides the upper two-thirds from the lower one-third of the vagina—an important distinction for cervical cancer staging. *E* = endometrium, *iCS* = inner cervical stroma, *JZ* = junctional zone (inner myometrium), *oCS* = outer cervical stroma, *OM* = outer myometrium, *P* = parametrium.

***Fallopian Tubes.***—The fallopian tubes extend from the uterine cornua to the ovaries (39). Proximally, the intramural portion passes through the myometrium; distally, the infundibulum with fimbriae opens into the peritoneal cavity near the ovary. The fallopian tubes are surrounded by the mesosalpinx of the broad ligament (Fig 6). At MRI, they appear as T2-hypointense tubular structures between the ovaries and uterus.

## Uterus

***Uterine Corpus and Cervical Anatomy.***—The uterus consists of the uterine corpus and cervix, with the inferior cervix, or portio, protruding into the upper vagina (Figs 2,3) (24,25,43). At T2-weighted imaging, the premenopausal uterus demonstrates distinct zonal anatomy in both the corpus (endometrium, junctional zone, and outer myometrium) and cervix (cervical canal, inner cervical stroma, and outer cervical stroma). The zonal anatomy becomes indistinct after menopause or radiation therapy (24,25,43) The endometrial cavity, lined by uniformly T2-hyperintense endometrium, extends into the similarly T2-hyperintense cervical canal (38). Endometrial thickness, measured in the midsagittal plane along the long axis of the uterus, varies with menopausal status and menstrual phase (Table S3) (38,44–49). In patients with postmenopausal bleeding, an endometrial thickness of 5 mm or more is abnormal; thresholds for asymptomatic patients are less clear (50). The junctional zone (inner myometrium) is T2-hypointense, continuing caudally as the T2-hypointense inner fibrous cervical stroma. The outer myometrium is T2-intermediate and transitions into the T2-intermediate outer interstitial cervical stroma. Normal junctional zone thickness is 8 mm or less, or up to 11 mm if microcysts are absent (45).

The isthmus, the transition between the uterine corpus and cervix, is marked by the focal narrowing at sagittal T2-weighted imaging and the entry of uterine vessels at axial oblique T2-weighted imaging (Figs 2,3) (24,25). The internal os and external os represent the upper and lower openings of the cervical canal. The cervix, surrounding the canal, includes an epithelial lining and cervical stroma (43). The upper cervix is lined by glandular columnar epithelium; the lower cervix (including portio), by squamous epithelium. The squamocolumnar junction, where these meet, is dynamic during reproductive years and the origin of most cervical precancer and cancer. The parametria, formed by the cardinal and uterosacral ligaments, extend from the lateral cervix to the pelvic sidewalls, enclosing the uterine vessels, nerves, and ureters (Figs 2,3). Table S3 and Figures 11–13 outline MRI features of common benign uterine corpus and cervical observations (38,44–49).

***Cervical Version and Uterine Corpus Flexion.***—The position of the uterus in the pelvis varies based on bladder filling and pelvic scarring. *Version* refers to the angle between the cervix and vagina: *anteversion* is the anterior tilt and *retroversion* is the posterior tilt (Fig 14) (38). *Flexion* describes the angle between the uterine corpus and cervix: *anteflexion* is a forward tilt and *retroflexion* is a backward tilt (38).

## Vagina

The vagina is a fibromuscular structure, separated from the bladder by the vesicovaginal septum and from the rectum by the rectovaginal septum (Fig 4) (51). At axial T2-weighted imaging, the premenopausal vagina is typically collapsed in an H- or W-shape, with hyperintense mucosal rugal folds and

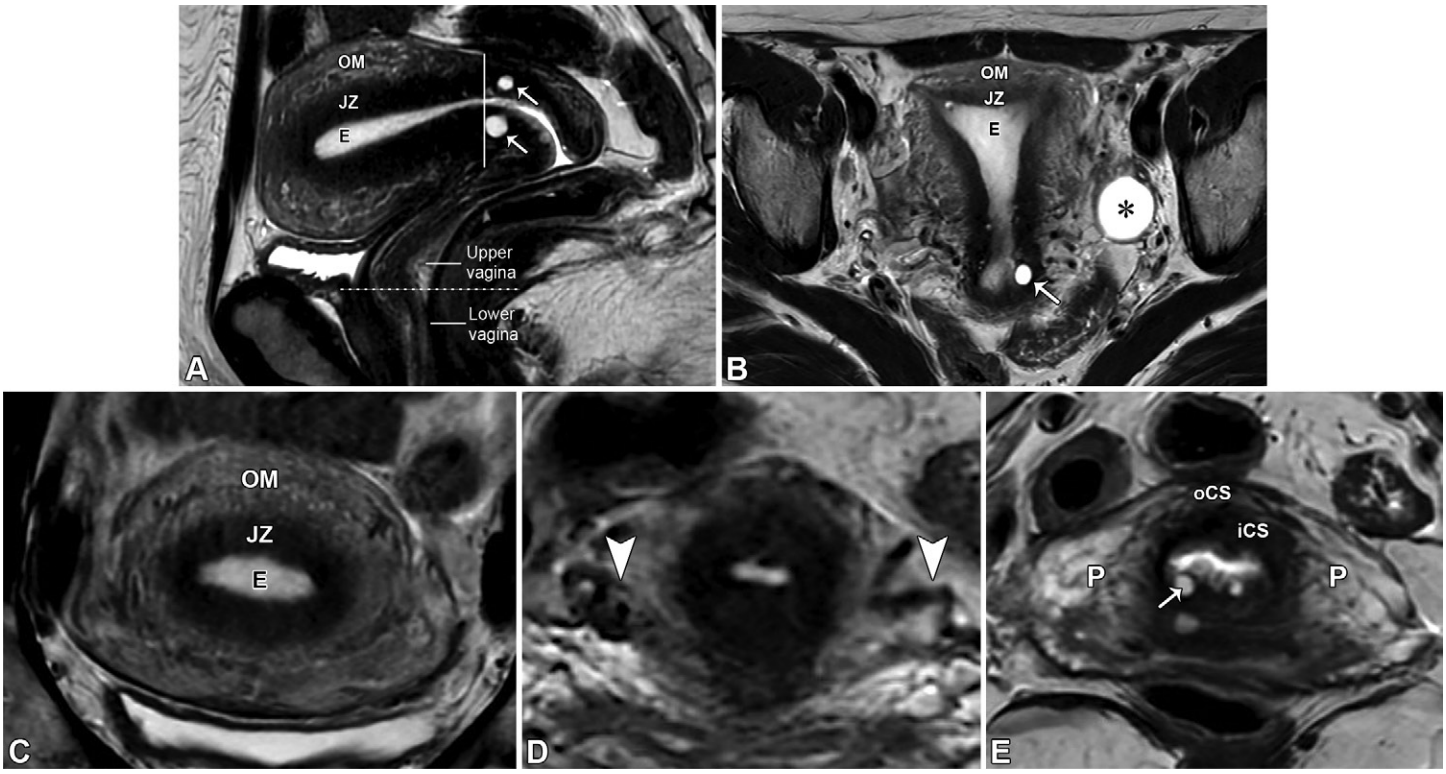


**Figure 3.** Normal appearance of the uterine corpus and cervix on T2-weighted images in a 46-year-old female patient. Sagittal **(A)**, coronal oblique **(B)**, uterine axial oblique **(C)**, axial oblique at the isthmus **(D)**, and cervical axial oblique **(E)** images show the normal zonal anatomy of the uterus and cervix. The centrally located hyperintense endometrium *(E)* is surrounded by the hypointense junctional zone (*JZ*, or inner myometrium) and the intermediate-signal-intensity outer myometrium *(OM)*, as shown in **A–C**. The isthmus marks the uterocervical junction and the location of the internal os and is indicated by narrowing of the outer uterine contour and funneling of the cervical canal before it expands into the endometrial cavity **(A)**, as well as by the entry of the uterine vessels (arrowheads in **D**). The dotted line placed horizontally at the bladder neck on the sagittal T2-weighted image **(A)** differentiates the upper two-thirds from the lower one-third of the vagina, a distinction relevant for cervical cancer staging. Note the small nabothian cysts in the cervix (arrows in **A**, **B**, and **E**), and a T2-hyperintense follicle in the left ovary (∗ in **B**). *iCS* = inner cervical stroma, *oCS* = outer cervical stroma, *P* = parametrium.

a hypointense wall. After menopause, the folds vanish, and vaginal wall thickness decreases. The superior vagina has fornices formed by the protruding cervix, and the inferior vagina opens via the introitus into the vulvar vestibule. Table S4 and Figure 15 detail the MRI features of common benign vaginal observations (51–53).

### Vulva

The vulva comprises the female external genitalia (Fig 16) (53). The mons pubis, anterior to the pubic symphysis, consists of adipose tissue. The labia majora are thick skin folds inferior to and contiguous with the mons pubis. The labia minora are thinner folds between the labia majora, converging anteriorly at the clitoral glans. The vestibule, between the labia minora, contains the external urethral meatus (urethral opening) and the introitus (vaginal opening).

## Step-by-Step Approach to Interpretation

A systematic approach to assess lesion origin, its tissue composition, and solid tissue morphology at female pelvic MRI is crucial for diagnosis. Radiologic reports should follow a structured format, outlining the differential diagnosis, and, when possible, providing a definitive diagnosis.

### Step 1: Clinical Context

Before interpretation, radiologists should review the clinical information, including patient age and indications for MRI. Key clinical details include symptoms such as pelvic pain, amenorrhea, abnormal bleeding or discharge, virilization, or precocious puberty; duration of symptoms; and signs of infection. For reproductive-age patients, knowledge of pregnancy status is critical. Relevant medical history may include congenital anomalies, benign conditions (eg, endometriosis, leiomyomas), infections (eg, pelvic inflammatory disease), previous cancers and treatments, and genetic mutations or syndromes associated with increased gynecologic cancer risk (Table 1) (54). The surgical history is also crucial to avoid diagnostic errors (eg, mistaking transposed ovaries for peritoneal implants). Laboratory information also helps focus the interpretation (Table 2) (55). Elevated levels of serum tumor markers may suggest specific tumors in the appropriate clinical context. However, normal values do not rule out these conditions.

### Step 2: Lesion Origin

Characterizing a lesion begins with identifying normal structures and the likely origin, guided by the clinical history. Start by locating the ovaries and uterus. Clues to ovarian origin include the absence of a normal ipsilateral ovary ("phantom

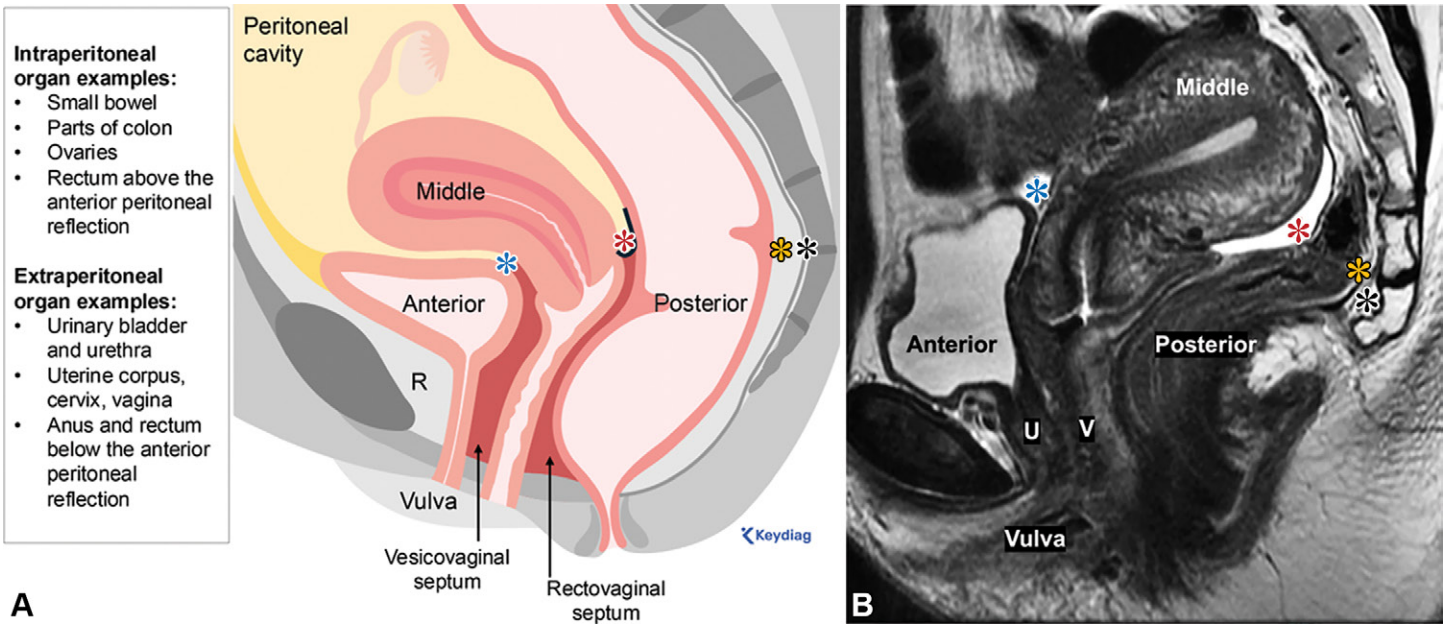


**Figure 4.** Midsagittal illustration **(A)** and midsagittal T2-weighted image **(B)** show the peritoneal cavity and extraperitoneal compartments of the female pelvis. The pelvis is divided into the peritoneal cavity, lined by the peritoneum, and the subperitoneal space. The vesicouterine pouch (anterior cul-de-sac, blue ∗) and rectouterine pouch (posterior cul-de-sac or pouch of Douglas, red ∗) are the two main pelvic peritoneal recesses. The posterior border of the rectouterine pouch is formed by the anterior peritoneal reflection, which separates the intra- and extraperitoneal rectum and appears as a thin T2-hypointense line (black line in **A**). The subperitoneal space contains extraperitoneal organs organized into anterior, middle, and posterior compartments, as well as the bilateral pelvic sidewalls. The anterior compartment includes the urinary bladder, urethra, perivesical space (immediately surrounding the bladder), and prevesical space, including the retropubic space of Retzius *(R* in **A**), located just posterior to the pubic symphysis. The middle compartment contains the uterus and vagina, with the vagina separated from the urinary bladder by the vesicovaginal septum and from the rectum by the rectovaginal septum. The posterior compartment includes the rectum, anus, mesorectal fat (yellow ∗), which is enclosed by the mesorectal fascia, and the presacral space (black ∗). *U* = urethra, *V* = vagina.

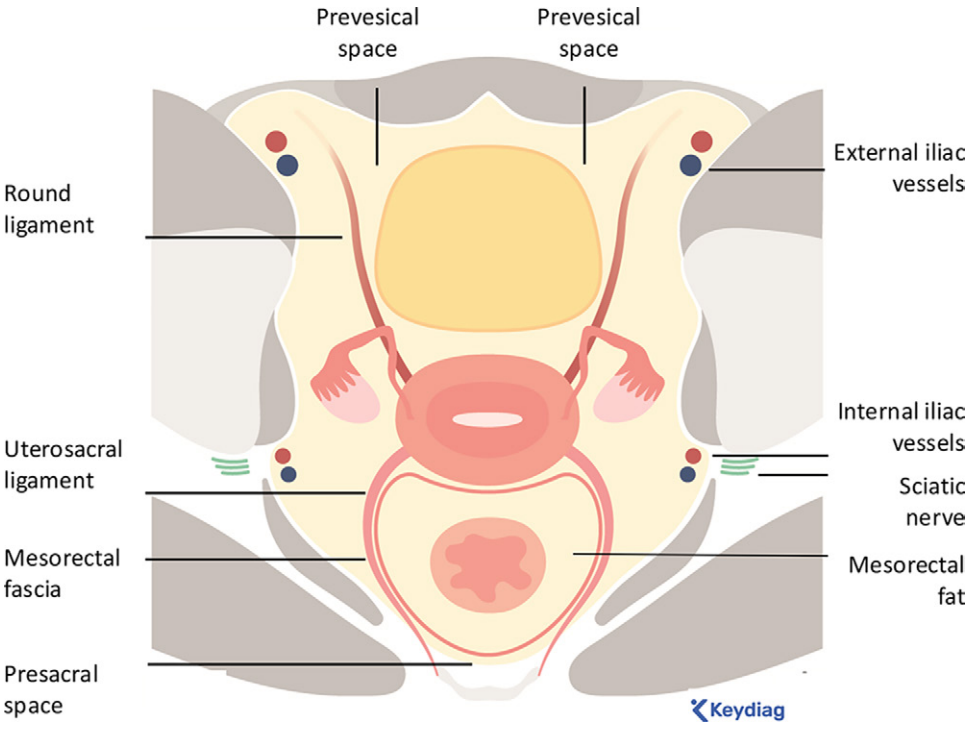


**Figure 5.** Axial illustration depicts the pelvis at the uterocervical junction.

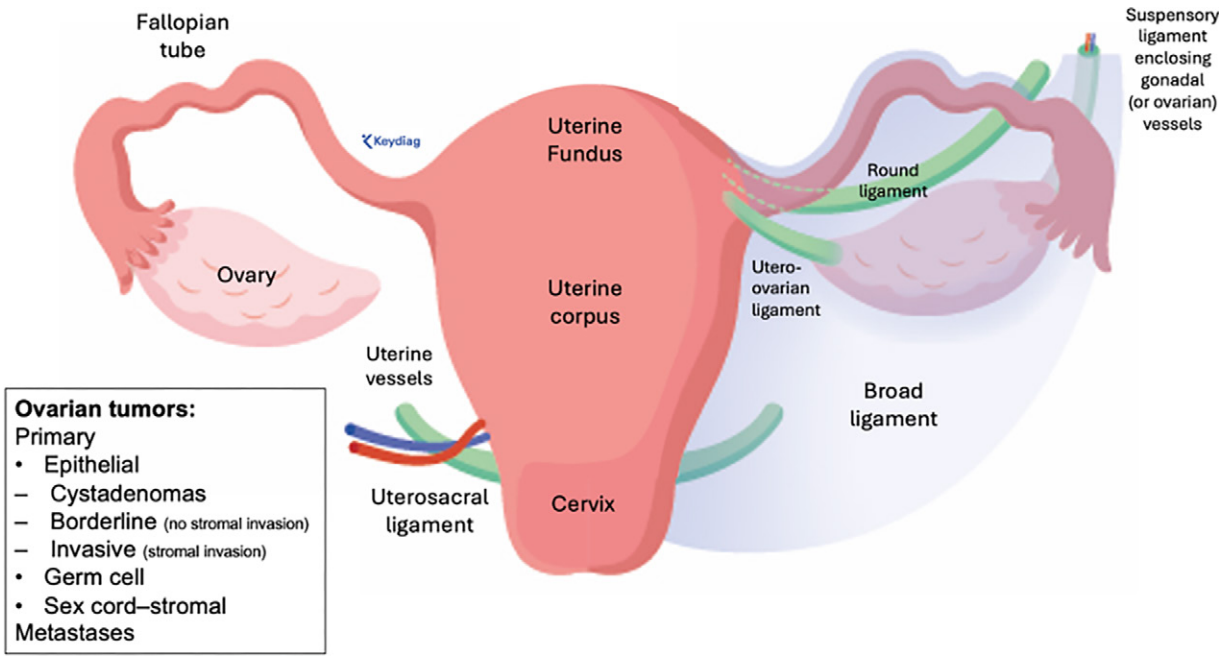


**Figure 6.** Coronal illustration depicts the uterus, ovaries, fallopian tubes, and supporting connective tissues. The uterus is supported by the broad ligaments—paired, wing-shaped, double-layered peritoneal folds that extend to the pelvic sidewalls and pelvic floor. The ovaries are supported by the ovarian ligament, mesovarium (which anchors the ovary to the broad ligament, not shown), and suspensory ligament (which connects the ovary to the pelvic sidewall and encloses the ovarian vessels). The broad ligament contains the fallopian tubes, round ligaments, and ovarian ligaments, as well as the uterine and ovarian vessels. The uterosacral ligaments attach the torus uterinus (posterolateral uterocervical junction) to the pelvic sidewalls and are the most common site of deep endometriosis. The uterine vessels approach the uterus at the isthmus, the transition between the uterine corpus and cervix. The inset box describes the most common types of ovarian tumors.

organ" sign); ovarian tissue draping around the mass with sharp angles at its lateral edges ("beak" sign); a deformed crescent-shaped ovary abutting the mass ("embedded organ" sign); and gonadal vascular supply ("ovarian vascular pedicle" sign) (Fig 17) (56,57). The ovarian vascular pedicle sign is best seen in the ovarian axis or coronal oblique plane acquired parallel to the uterine corpus (Figs 2,3). Tubular morphology suggests fallopian tube origin.

Clues to uterine origin include uterine tissue wrapping around and forming acute angles on either side of the mass ("claw" sign) or, for a pedunculated mass, a stalk of tissue and/or vessels extending from the uterus to the mass ("bridging tissue/vessels" sign) (Fig 18) (56,57). The claw and beak signs (described above) both suggest that a lesion arises from, rather than simply abuts, an organ, based on deformation of the organ's margins into sharp angles—typically more pronounced in the claw sign. Although they represent similar imaging features, the term *beak sign* is used to refer an ovarian origin, while the term *claw sign* is used to indicate a uterine origin (57,58).

Additional clues include the displacement of adjacent structures (28). Intraperitoneal origin is suggested by posterior or lateral displacement of the uterus and rectosigmoid colon or anterior displacement of the uterus and posterior displacement of the rectum. Extraperitoneal origin is indicated by anterior or central displacement of the extraperitoneal organs. Pelvic sidewall origin is suggested by central displacement of the ureters and iliac vessels, while perineal origin is indicated by superior displacement of the levator ani muscles.

## Step 3: Lesion Tissue Composition and Solid Tissue Morphology

Once the likely lesion origin is identified, assessing the tissue composition and solid tissue morphology provides valuable insights (59). A systematic review of in- and opposed-phase and fat-saturated T1-weighted images to assess for lipid versus blood content, followed by review of T2-weighted and contrast-enhanced images to distinguish cysts from cystic and solid lesions based on the presence of solid tissue in the latter two, along with evaluation of diffusion-weighted images and the ADC map, enables categorization of lesions into five groups: *(a)* T1-hyperintense lipid-containing lesions, *(b)* T1-hyperintense blood-containing lesions without solid tissue, *(c)* cysts (simple or proteinaceous fluid) without solid tissue, *(d)* cystic or solid lesions with dark T2/dark DWI solid tissue, and *(e)* cystic or solid lesions with non-dark T2/non-dark DWI solid tissue.

T1 signal intensity is hypointense if similar to that of urine or cerebrospinal fluid (CSF), intermediate if between that of skeletal muscle and adipose tissue, and hyperintense if the same or higher than that of adipose tissue. T2 signal intensity is hypointense or dark if the same as or lower than that of skeletal muscle, intermediate if between that of skeletal muscle and urine, and hyperintense if the same as or higher than that of urine or CSF. For adnexal lesions, high *b*-value diffusion-weighted signal intensity is hypointense or dark if similar to that of urine or CSF and hyperintense if higher (19). For uterine lesions, high *b*-value diffusion-weighted signal

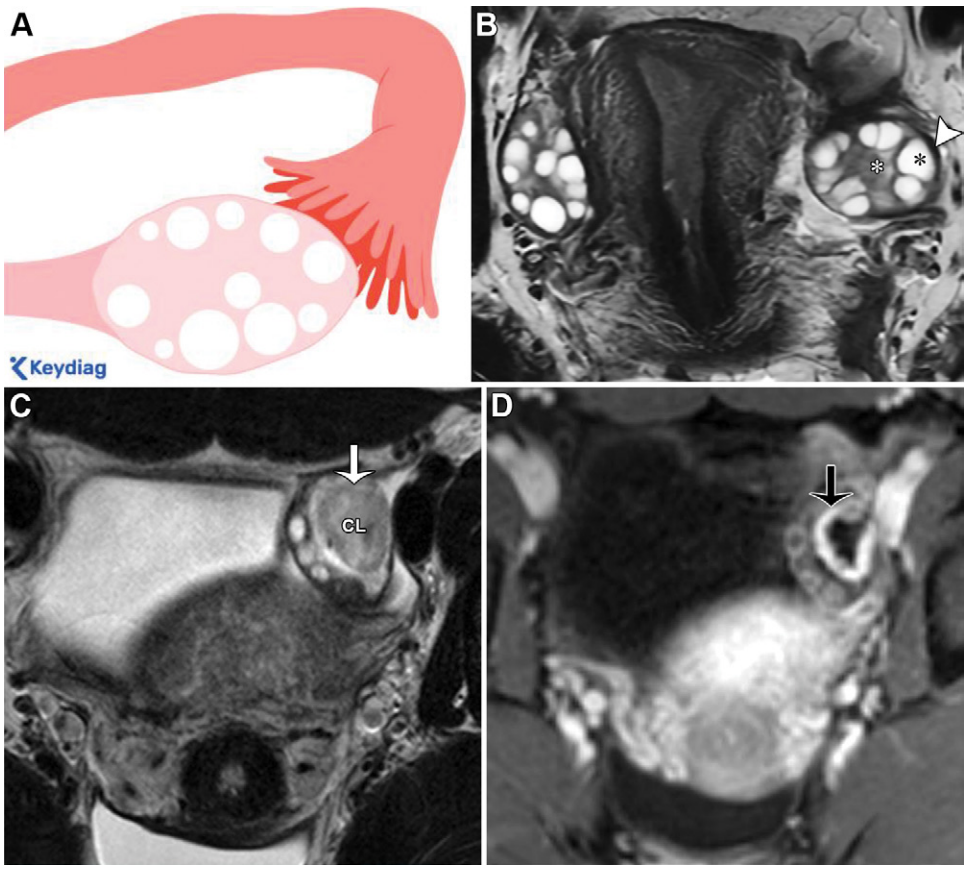


**Figure 7.** Normal premenopausal ovaries in two different patients, with physiologic observations highlighted. **(A)** Schematic illustration shows a premenopausal ovary with follicles. **(B)** Axial T2-weighted image in a 27-year-old female patient shows an oval-shaped ovary with a T2-hypointense cortex (arrowhead), T2-intermediate medulla (white ∗), and multiple T2-hyperintense follicles (black ∗). **(C, D)** Axial T2-weighted **(C)** and contrast-enhanced fat-saturated T1-weighted **(D)** images in a 30-year-old female patient show a corpus luteum *(CL)*, a common physiologic finding in premenopausal women. The imaging appearance varies with the developmental phase. A typical corpus luteum manifests as a cystic structure with a hyperintense center and a thick crenulated wall of intermediate signal intensity at T2-weighted imaging (arrow in **C**), which enhances avidly following intravenous contrast material administration (arrow in **D**).

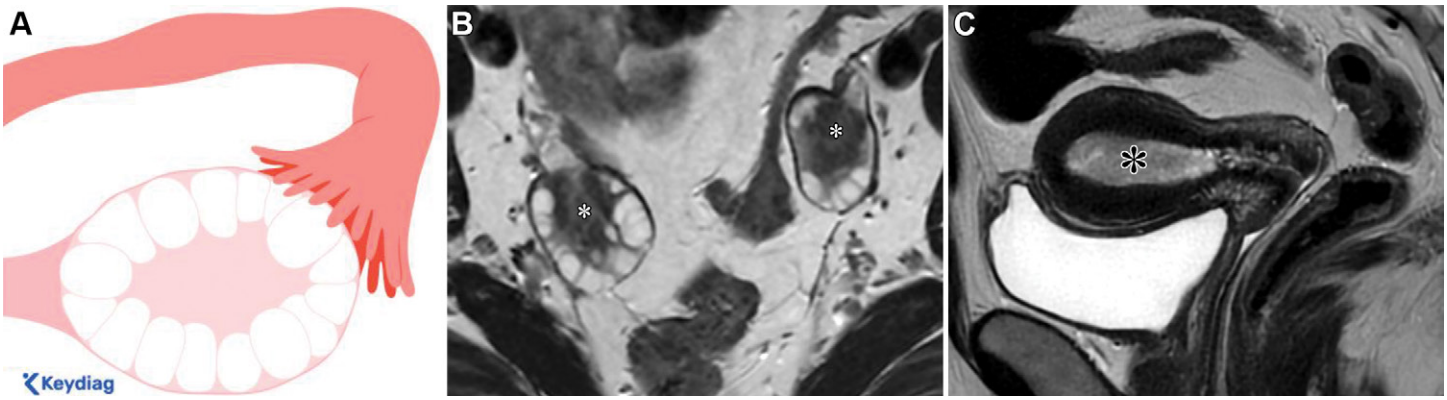


**Figure 8.** Polycystic ovarian syndrome and secondary atypical endometrial hyperplasia in a 34-year-old female patient who presented with amenorrhea. **(A)** Schematic illustration depicts a polycystic ovary, a common endocrine disorder affecting up to 10% of women of reproductive age. The diagnosis of polycystic ovarian syndrome is based on the Rotterdam criteria, which require that at least two of the following three criteria are met: polycystic ovaries, oligomenorrhea or anovulation, and hyperandrogenism. Polycystic ovaries are defined as either an ovarian volume of 10 mL or more or the presence of 20 or more follicles per ovary in at least one ovary (see Table S2 for reference). **(B)** Axial T2-weighted image shows bilateral polycystic ovarian enlargement, with centrally located T2-intermediate stroma (small ∗) and multiple peripherally arranged T2-hyperintense follicles. **(C)** Sagittal T2-weighted image shows heterogeneous T2-intermediate signal intensity within the endometrial cavity (large ∗), corresponding to biopsy-proven atypical endometrial hyperplasia. Atypical endometrial hyperplasia demonstrates less enhancement than the myometrium on images from all postcontrast sequences, including delayed images (not shown), similar to the enhancement pattern seen in endometrial cancer.

intensity is hypointense or dark if lower than that of the myometrium, intermediate if the same as or higher than that of the myometrium but lower than that of the endometrium or LN, and hyperintense if the same as or higher than that of the endometrium or LN (22).

Solid lesions have 80% or more solid tissue; cystic lesions contain either no solid tissue (cysts) or less than 80% solid tissue (cystic with solid tissue). *Solid tissue* is defined as a solid component that demonstrates enhancement. It may manifest as papillary projections (branching architecture), mural nodules (nodules ≥3 mm), irregular septations or walls (uneven thickness), or a larger solid portion. Fluid can be either simple or nonsimple. Nonsimple fluid may include blood (eg, endometriotic, hemorrhagic) or proteinaceous fluid (eg, mucin) (19).

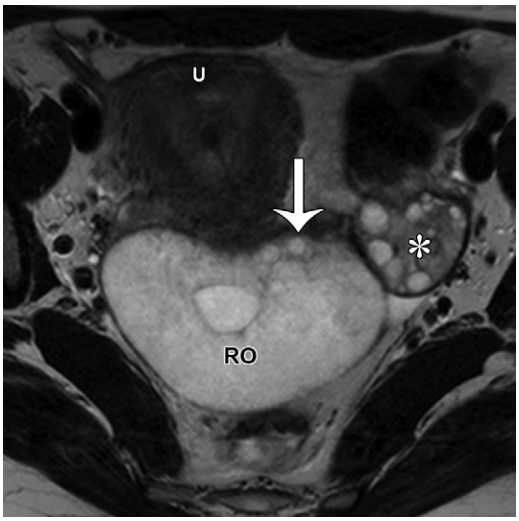


**Figure 9.** Right ovarian torsion in a 27-year-old female patient who presented with acute pelvic pain. Axial T2-weighted image shows an enlarged and edematous right ovary *(RO)* with peripheral follicles (arrow). The right ovary is abnormally positioned centrally and posterior to the uterus *(U)*, in contrast to the normal left ovary (∗). Additional findings in ovarian torsion (not shown) may include a twisted vascular pedicle and variable enhancement, depending on the degree of ischemia or the presence of infarction.

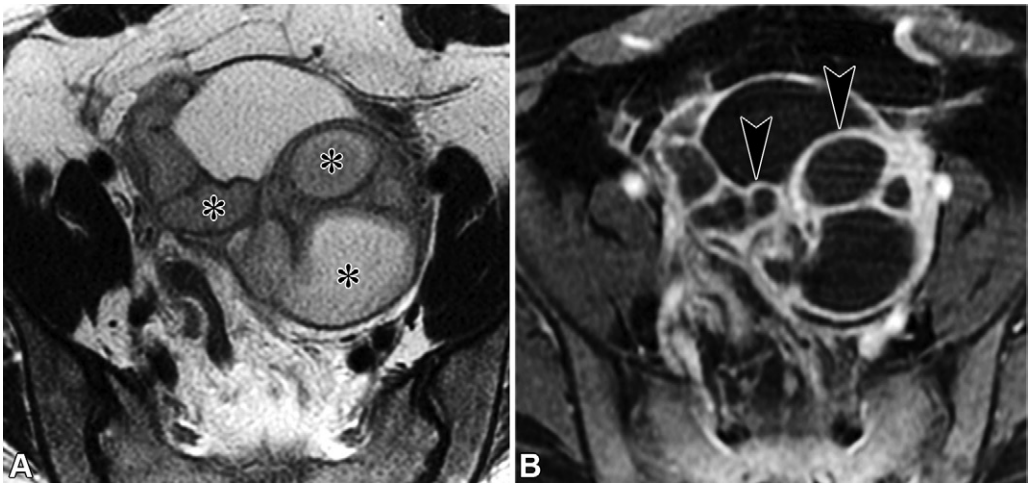


**Figure 10.** Tubo-ovarian abscess in a 43-year-old female patient who presented with nausea, vomiting, and pelvic pain after an endometrial biopsy. Axial T2-weighted **(A)** and contrast-enhanced fat-saturated T1-weighted **(B)** images show a multilocular cystic mass in the left adnexa. The mass contains purulent fluid, indicated by variable T2 signal intensity (∗ in **A**) and has a thick enhancing wall, as well as multiple enhancing septations (arrowheads in **B**). The high *b*-value diffusion-weighted images and ADC map (not shown) showed restricted diffusion consistent with the presence of pus. Bacterial culture obtained after percutaneous drainage was positive for *Escherichia coli*.

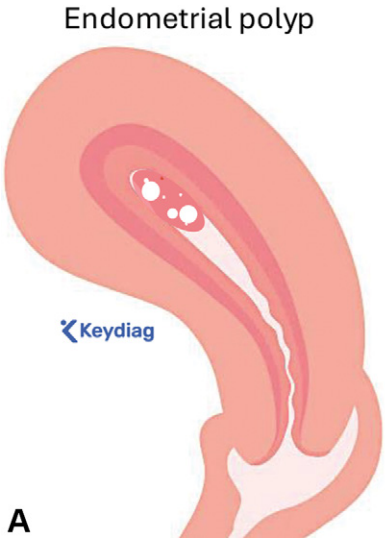


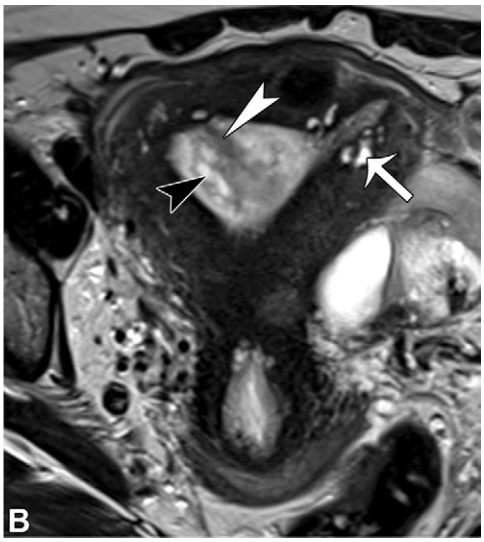


**Figure 11.** Endometrial polyp in a 50-year-old female patient undergoing tamoxifen therapy following breast cancer resection. **(A)** Sagittal illustration through the uterus shows a polypoid endometrial lesion with cystic foci due to dilated endometrial glands. **(B)** Coronal oblique T2-weighted image shows a pedunculated lesion in the endometrium with a T2-hypointense fibrovascular core (white arrowhead) and T2-hyperintense foci (black arrowhead) representing dilated endometrial glands, findings suggestive of an endometrial polyp. Avid postcontrast enhancement, similar to that of the myometrium, is typically observed (not shown). Definitive diagnosis requires hysteroscopic resection, as endometrial polyps, hyperplasia, and neoplasia may coexist and overlap in their imaging features. Incidentally noted is adenomyosis, indicated by the presence of microcysts in the junctional zone (arrow).

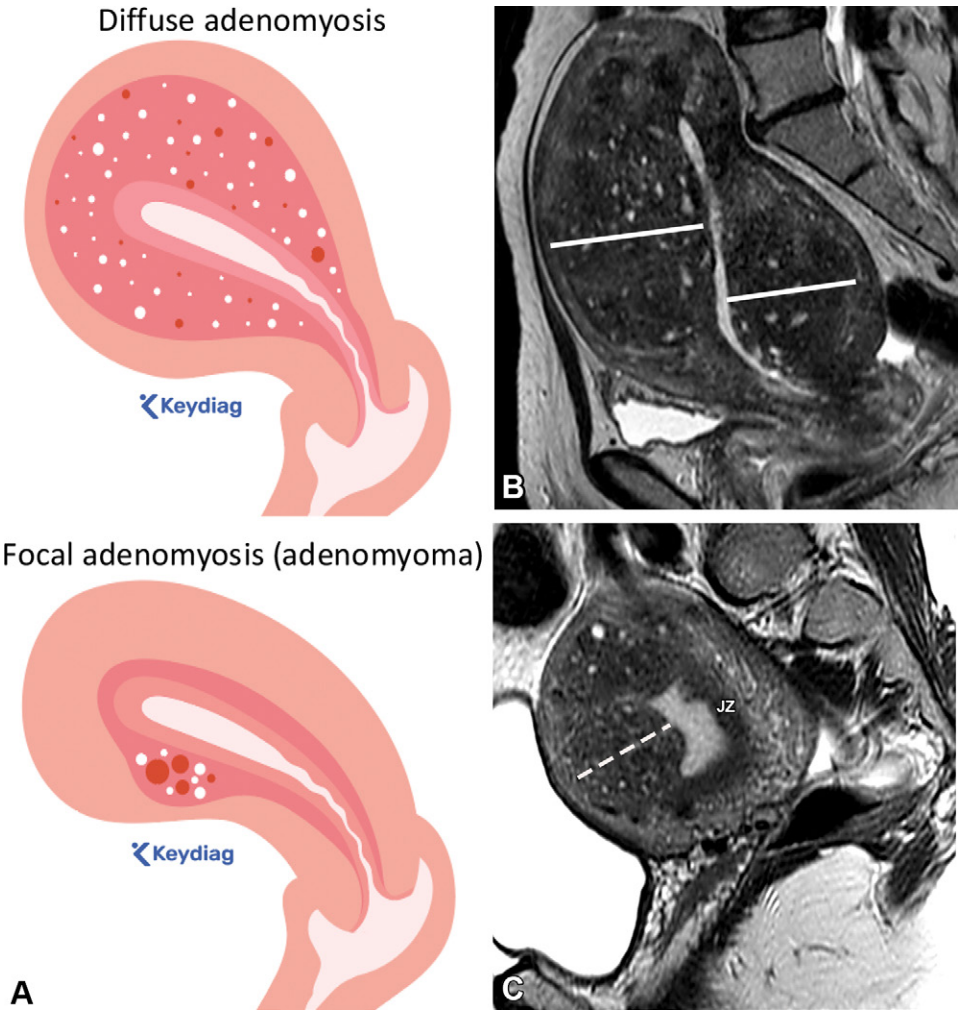


**Figure 12.** Diffuse and focal adenomyosis (or adenomyoma). **(A)** Illustrations in the midsagittal plane through the uterus show diffuse adenomyosis (top image) versus focal adenomyosis or adenomyoma (bottom image). **(B, C)** Sagittal T2-weighted images in two different patients with menorrhagia show a diffusely thickened T2-hypointense junctional zone *(JZ)* with scattered T2-hyperintense microcysts (solid lines in **B**) and focal masslike asymmetric thickening of the anterior junctional zone with microcysts (dashed line in **C**). These findings are due to ectopic endometrial glands and stroma within the inner myometrium (microcysts) and reactive smooth muscle proliferation (thickened junctional zone).

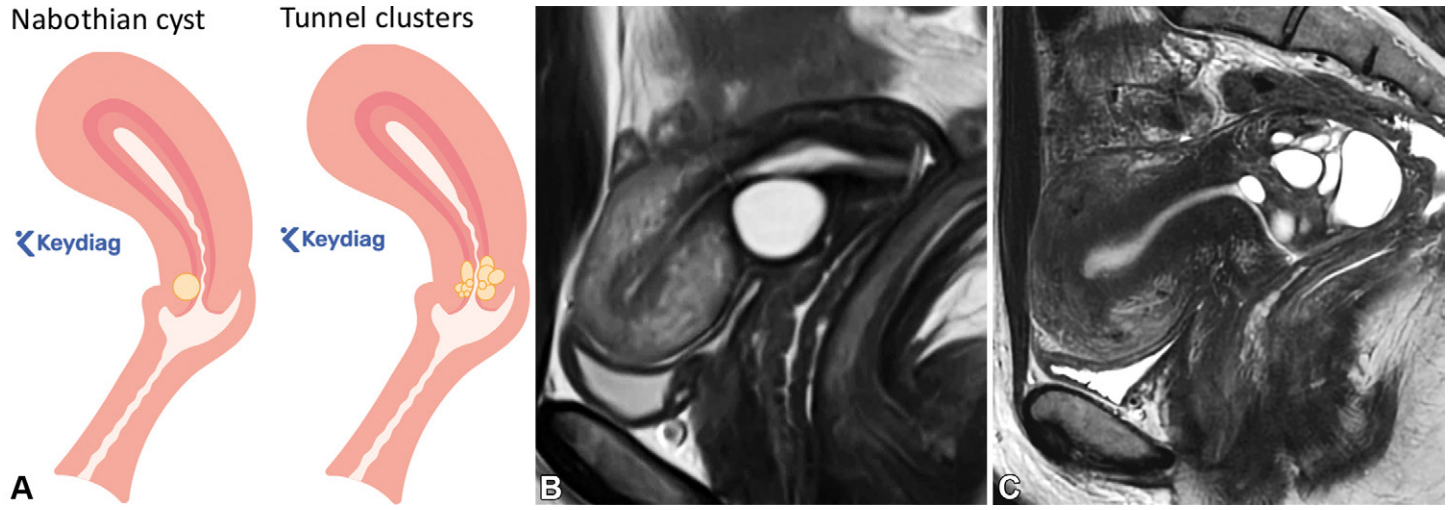


**Figure 13.** Nabothian cysts and tunnel clusters. Illustrations **(A)** and T2-weighted images in two different patients **(B, C)** in the midsagittal plane through the uterus show a unilocular cyst in the superficial cervical stroma, typical of a nabothian cyst (left image in **A**; **B**), and a multilocular cyst extending deep into the cervical stroma, characteristic of tunnel clusters (right image in **A**; **C**). It is essential to exclude the presence of enhancing solid tissue on contrast-enhanced images (not shown), as its presence in a multilocular cervical lesion raises suspicion for gastric-type adenocarcinoma of the cervix. A cone biopsy may be necessary to establish diagnosis.

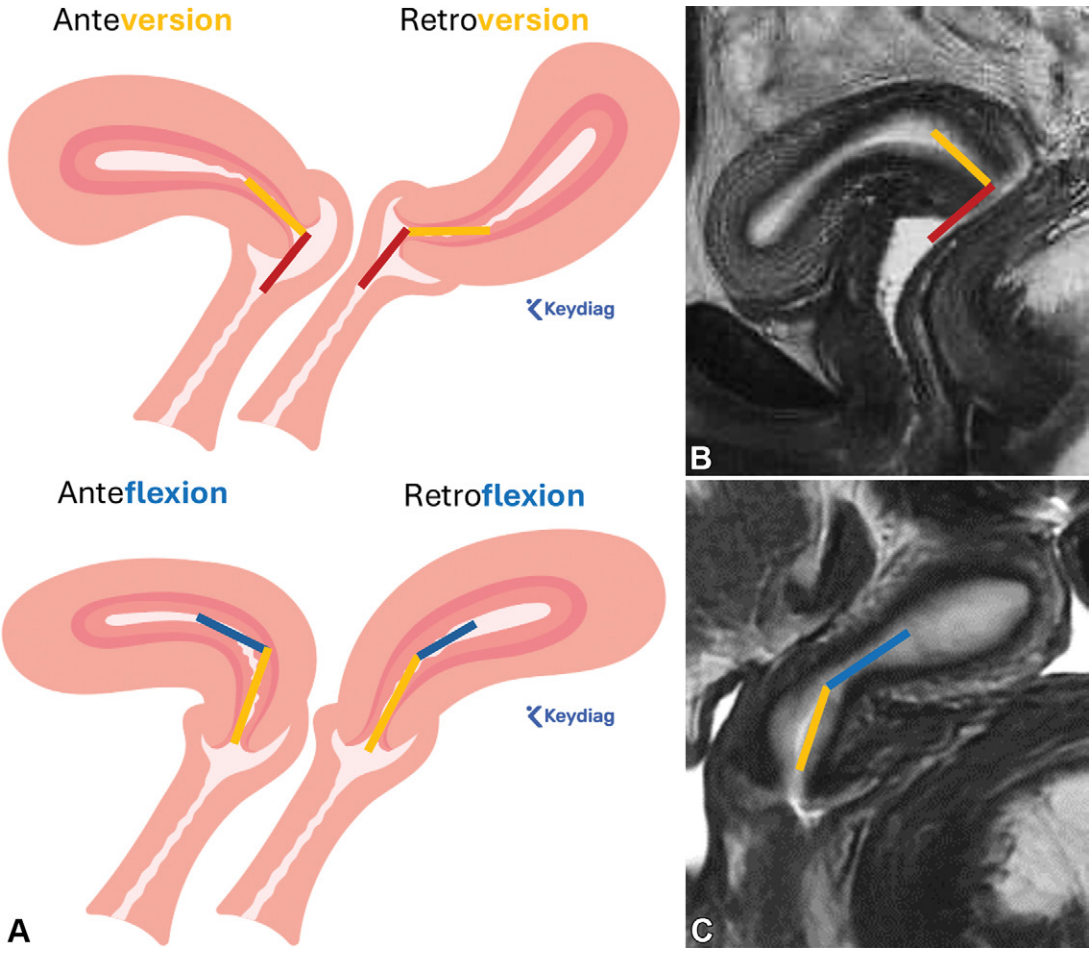


**Figure 14.** Illustrations **(A)** and MR images **(B, C)** show various uterine positions within the female pelvis. *Version* refers to the angle between the cervix and vagina: the top set of illustrations in **A** show the angle as the tilt of the yellow line relative to the red line. *Anteversion* indicates an anterior tilt, and *retroversion* indicates a posterior tilt. *Flexion* describes the angle between the uterine corpus and cervix: the bottom set of illustrations in **A** show the angle as the tilt of the blue line relative to the yellow line. *Anteflexion* refers to a forward tilt, and *retroflexion* refers to a backward tilt. Sagittal T2-weighted images **(B, C)** in two patients show an anteverted anteflexed uterus in **B** and a retroverted retroflexed uterus in **C**.

### T1-Hyperintense Lipid-containing Lesions

In-phase, out-of-phase, and fat-saturated T1-weighted imaging helps assess for the presence of lipid, which can be macroscopic, microscopic, or both (59). Macroscopic lipids appear as a loss of T1 hyperintensity following fat saturation or as an India ink artifact at the fat-water interface on out-of-phase images; microscopic lipid causes signal loss on out-of-phase versus in-phase images (Figs 19, 20). Table S5 details the MRI features of the most common gynecologic T1-hyperintense lipid-containing lesions, organized by their origin (19,57,60–64).

***Adnexal Lesions.***—For lesions with an ovarian origin, the most common diagnosis is a mature teratoma (dermoid), a benign ovarian germ cell tumor (62). Often asymptomatic, mature teratomas may cause torsion-related pain. They typically appear as a cyst with predominant macroscopic lipid, occasional microscopic lipid, hair, dermal elements, and toothlike calcifications (T1 and T2 hypointense). They may restrict diffusion and contain an enhancing Rokitansky nodule, neither of which are signs of malignancy (Fig 19) (19,57,60,61). Rarely, lipid-containing lesions can be malignant. In older patients, mature teratomas can undergo malignant transformation (≤2%), typically into squamous cell carcinoma; a key imaging feature is larger solid tissue, often with transmural extension (19,62). Women under 30 years of age can present with an immature teratoma, a malignant ovarian germ cell tumor, associated with elevated serum α-fetoprotein and lactate dehydrogenase levels. Immature teratomas appear as a large unilateral cystic lesion with solid tissue, dispersed small lipid foci, and irregular small calcifications, which may be difficult to detect at MRI (Fig 19) (62,63).

***Nonadnexal Lesions.***—For lesions with a uterine origin, lipoleiomyoma, a type of leiomyoma seen in postmenopausal women, is a likely diagnosis. Lipoleiomyoma is a benign lesion containing adipose tissue and smooth muscle, with adipose tissue originating from smooth muscle metaplasia (64). At MRI, lipoleiomyomas appear as well-circumscribed tumors with macroscopic lipid mixed with smooth muscle. They lack diffusion restriction and show enhancement of T2-hypointense smooth muscle (Fig 20).

For lesions with a nongynecologic origin, the differential diagnosis includes omental infarct, benign and malignant primary lipomatous tumor (eg, liposarcoma, lipoma, hibernoma), extra-adrenal myelolipoma, extramedullary hematopoiesis, and sacrococcygeal teratoma (63).

### T1-Hyperintense Blood-containing Lesions without Solid Tissue

If T1 hyperintensity persists at fat-saturated T1-weighted imaging with no lipid at in-phase and out-of-phase T1-weighted imaging, then the lesion contains blood or proteinaceous fluid (59). Blood signal intensity varies depending on the time since the hemorrhagic event (Table S6) (19).

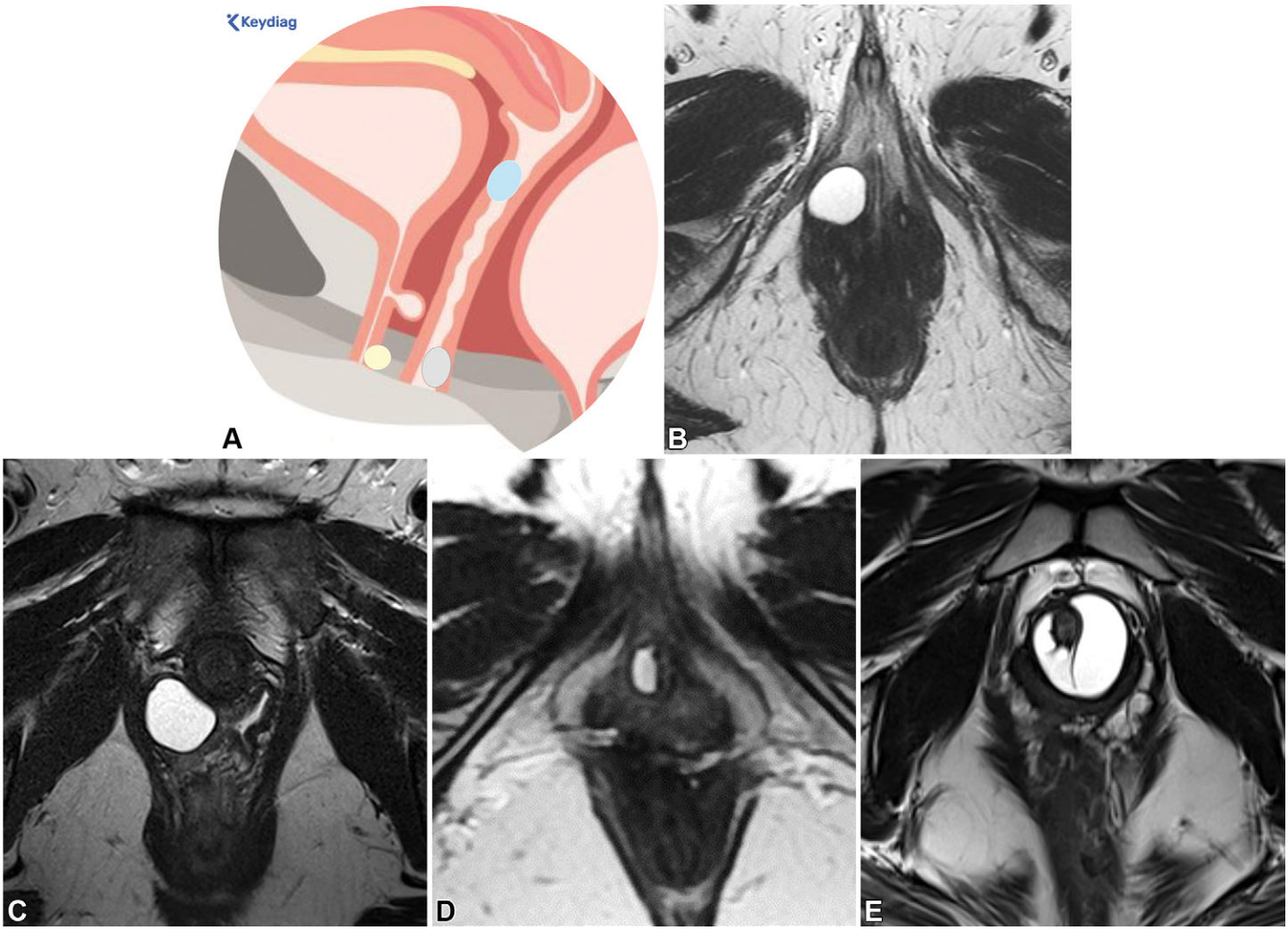


**Figure 15.** Midsagittal schematic illustration **(A)** and axial T2-weighted images **(B–E)** in four different patients show vaginal and Skene duct cysts, as well as a urethral diverticulum. Bartholin duct cyst: A unilocular cyst located in the posterolateral vaginal wall at or below the pubic symphysis (gray oval in **A** , T2-hyperintense cystic lesion in **B**). Gartner duct cyst: A unilocular cyst located in the anterolateral vaginal wall at or above the pubic symphysis (blue oval in **A**, T2-hyperintense cystic lesion in **C**). Skene duct cysts: Unilateral or bilateral small unilocular cysts located inferior to the pubic symphysis, anterior to the vagina, and lateral to the lower urethra (light yellow oval in **A**, T2-hyperintense cystic lesion in **D**). Urethral diverticulum: A round, oval, or U-shaped T2-hyperintense fluid-filled outpouching of the posterolateral mid to distal urethra near the pubic symphysis (urethral outpouching in **A**). In rare cases, the urethral diverticulum may encircle the urethra entirely (T2-hyperintense circumferential cystic lesion in **E**).

***Adnexal Lesions.***—Table S7 lists the most common gynecologic T1-hyperintense blood-containing lesions without solid tissue, organized by their origin (10,19,39,44,64–68).

For lesions with an ovarian origin, endometriomas and hemorrhagic cysts are likely diagnoses. Endometriomas are a common sign of endometriosis, which affects 10% of reproductive-age women and is linked to chronic pain and infertility (10). Endometriosis is characterized by endometrial glands and stroma outside the endometrium, causing inflammation, fibrosis, and architectural distortion. Imaging may show endometriomas and deep endometriosis. Endometriomas appear as ovarian cysts, are often multifocal and bilateral, and have diffuse marked T1 hyperintensity and T2 shading (darkening) due to cyclical hemorrhage (Fig 21). A thick T2-hypointense rim from fibrosis and hemosiderin, T2-dark spots from blood clots, and persistence over time increase the diagnostic specificity for endometrioma (65,66).

Contrast-enhanced imaging with subtraction is essential to evaluate for solid tissue, which could indicate an endometriosis-associated malignancy—most commonly endometrioid or clear cell carcinomas—or, in pregnancy, a decidualized endometrioma caused by hormonal stimulation and hypertrophy of ectopic endometrium (10). Unlike endometriomas, hemorrhagic cysts are single unilateral cysts with variable T1 and T2 signal intensity, based on blood age (19). Hemorrhagic cysts lack the thick T2-hypointense rim and T2-dark spots and resolve overtime. They are considered a physiologic observation when 3 cm or less in premenopausal patients. Corpus luteal cysts may also contain hemorrhage and have a typical “crenulated” thick wall with avid enhancement (Fig 7) (38).

For lesions with a paraovarian origin, hematosalpinx is a likely diagnosis. Hematosalpinges appear as a dilated T1-hyperintense blood-filled fallopian tube (39). They can be

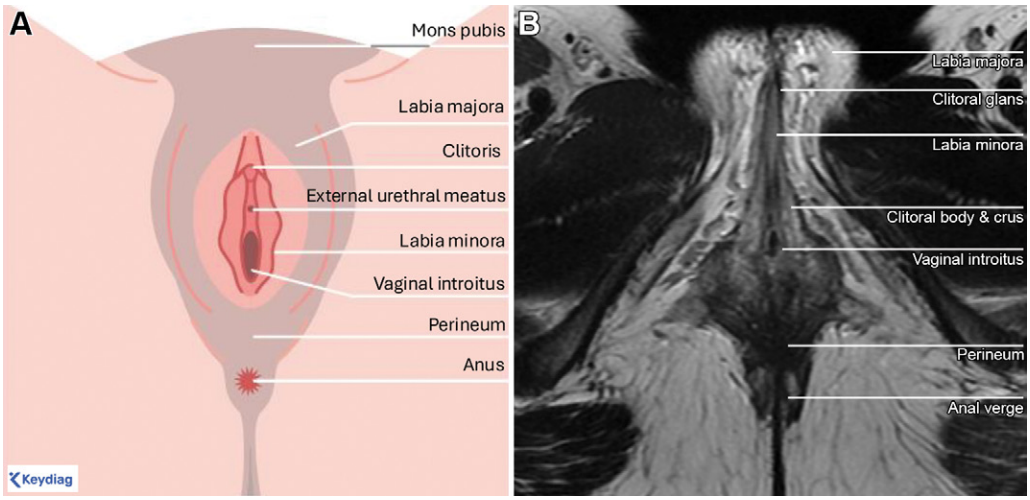


**Figure 16.** Illustration **(A)** and axial T2-weighted image **(B)** show the vulvar region or external female genitalia. The mons pubis, anterior to the pubic symphysis, consists of adipose tissue. The labia majora are thick skin folds inferior to and contiguous with the mons pubis. The labia minora are thinner folds between the labia majora, converging anteriorly at the clitoral glans. The vestibule, between the labia minora, contains the external urethral meatus (urethral opening) anteriorly and the introitus (vaginal opening) posteriorly.

**Table 1: Most Common Hereditary Syndromes and Genetic Mutations Associated with Increased Risk of Gynecologic Cancers**

| Hereditary Syndrome and Genetic Mutations | Most Common Tumors |
|---|---|
| Hereditary breast and ovarian cancer syndrome<br>DNA repair genes (*BRCA1*, *BRCA2*, other)<br>10× more common in those of Ashkenazi Jewish descent vs the general U.S. population | Gynecologic cancers: ovarian, fallopian, and primary peritoneal cancers (high-grade serous) with a lifetime risk of 35%–70% *(BRCA1)* and 10%–30% *(BRCA2)* by age 70 years (vs 2% in the general population)<br>Nongynecologic cancers: breast, prostate, pancreatic, melanoma |
| Lynch syndrome (or hereditary nonpolyposis colorectal cancer)<br>DNA mismatch repair genes:<br>*MLH1* (most common)<br>*MSH2* (second most common)<br>*MSH6* (10%)<br>*PMS2* and other (rare) | Gynecologic cancers: endometrial (up to 60% lifetime risk, vs 3% in the general population), ovarian cancer (up to 24% lifetime risk; mostly epithelial [eg, clear cell and endometrioid carcinomas])<br>Nongynecologic cancers: colon (up to 80% lifetime risk), gastric, urothelial |
| Peutz–Jeghers syndrome (rare)<br>*STK11 (LKB1)* | Gynecologic cancers: cervical gastric-type adenocarcinoma, sex cord tumor with annular tubules<br>Nongynecologic cancers: breast (up to 50% lifetime risk), colon, pancreatic, gastric, small bowel<br>Other (benign): gastrointestinal hamartomas, mucocutaneous hyperpigmentation |
| Cowden syndrome (rare)<br>*PTEN* | Gynecologic cancers: endometrial (5%–10% lifetime risk)<br>Nongynecologic cancers: breast (25%–50% lifetime risk), colon (9% lifetime risk), thyroid (most likely, follicular)<br>Other (benign): mucocutaneous lesions, gastrointestinal hamartomas, macrocephaly |
| Hereditary leiomyomatosis and renal cell carcinoma syndrome<br>*FH* | Gynecologic cancers: uterine leiomyomas (100% lifetime risk by age 30 years)<br>Nongynecologic cancers: skin leiomyomas, a variety of high-grade renal cell carcinomas (eg, papillary renal cell carcinoma type 2, collecting duct carcinoma, unclassified; unilateral, solitary, often manifests with high-stage disease) |

Source.—Reference 54.

associated with endometriosis, obstructive congenital conditions, pelvic inflammatory disease, or ectopic pregnancy (39).

***Nonadnexal Lesions.***—For lesions with a uterine origin, a lesion within the myometrium may indicate a leiomyoma with red degeneration from a hemorrhagic infarction(64). Leiomyomas, incidental or painful, show diffuse or rimlike T1 hyperintensity and T2 hypointensity, reflecting vascular thrombosis (Fig 22). The absence of contrast enhancement confirms the diagnosis (64).

Blood accumulation in the endometrial cavity, endocervical canal, or vagina can mimic a T1-hyperintense blood-containing lesion. Hematometra (uterine blood) and hematocolpos (vaginal blood) are often secondary to congenital müllerian duct anomalies, an imperforated hymen, scarring-related stenosis, or an obstructing tumor (44). Accessory cavitated uterine mass is a rare congenital müllerian anomaly that manifests with chronic pelvic pain, dysmenorrhea, and infertility in women under 30 years of age, requiring surgical excision (67). It consists of a noncommunicating accessory cavity lined by a functional endometrium, filled with blood from cyclical bleeding, and surrounded by smooth muscles, giving it a uterus-like morphology. It is located in the uterus beneath the round ligament insertion site (67,68).

**Table 2: Most Common Serum Tumor Markers Relevant to Interpretation of Female Pelvic MRI**

| Serum Tumor Marker | Most Common Gynecologic Cancers | Most Common Other Conditions |
|---|---|---|
| CA-125* | Epithelial ovarian cancer†<br>Nonendometrioid endometrial cancers (eg, serous, clear cell, carcinosarcoma)<br>Ovarian metastases | Endometriosis<br>Pelvic inflammatory disease<br>Ovarian hyperstimulation<br>Cirrhosis, other liver diseases<br>Peritonitis |
| CEA* | Mucinous ovarian cancer†<br>Fibroma and fibrothecoma<br>Ovarian metastases | Colorectal cancer |
| CA19-9 | Mucinous ovarian cancer† (benign to invasive) | Pancreaticobiliary cancer |
| HE-4 | Epithelial ovarian cancer (particularly, serous and endometrioid) | Pregnancy<br>Estrogen-progesterone oral contraceptive use<br>Renal failure |
| AFP | Virtually diagnostic of a malignant ovarian germ cell tumor,† particularly a yolk sac tumor | Fetal anomalies |
| β-hCG | Virtually diagnostic of a malignant ovarian germ cell tumor, particularly choriocarcinoma<br>Gestational trophoblastic disease | Pregnancy |
| LDH | Dysgerminoma | Endometriosis<br>Leiomyomas |
| Inhibin (especially β subunit) | Granulosa cell tumor†<br>Sertoli–Leydig cell tumor | Physiologically elevated before menopause; thus, it is primarily a useful serum tumor marker after menopause |
| Estradiol | Granulosa cell tumor | Varies physiologically based on the phase of the menstrual cycle and menopausal status |

Source.—Reference 55.
Note.—AFP = α-fetoprotein, β-hCG = β-human chorionic gonadotropin, CA-125 = cancer antigen 125, CA19-9 = carbohydrate antigen 19-9, CEA = carcinoembryogenic antigen, HE-4 = human epididymis protein 4, LDH = lactate dehydrogenase.
* A CA-125/CEA ratio greater than 25 favors a diagnosis of primary mucinous ovarian malignancy, whereas a ratio of 25 or less suggests the need for a gastrointestinal workup, including upper and lower endoscopy, to rule out mucinous ovarian metastases originating from a gastrointestinal primary tumor.
† Most common cancer types.

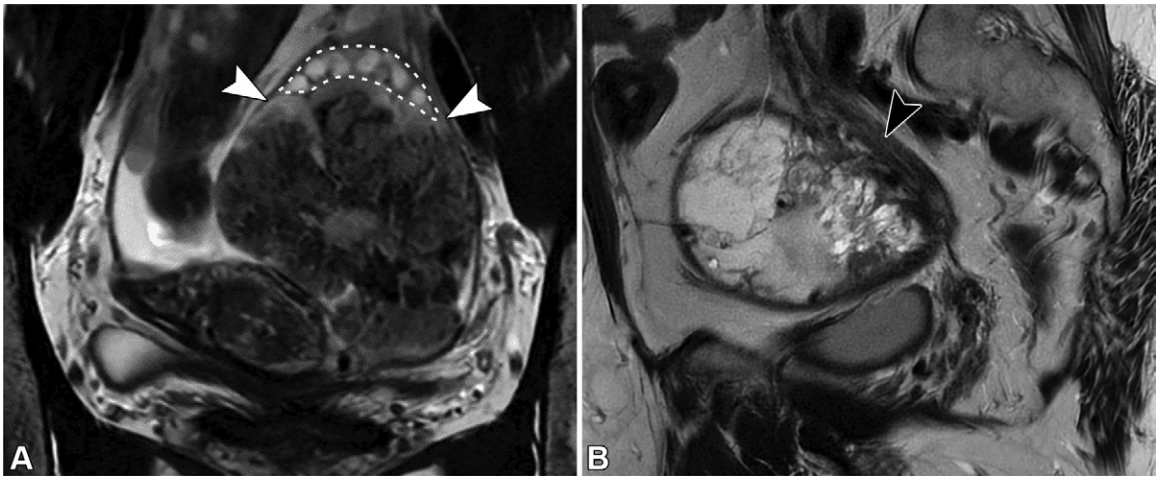


**Figure 17.** Imaging clues suggestive of ovarian origin of a lesion. **(A)** Coronal T2-weighted image in a 31-year-old female patient with polycystic ovarian syndrome, endometrial adenocarcinoma (not shown), and left ovarian metastasis shows a deformed crescent-shaped ovary (dotted white outline) abutting the lesion (embedded organ sign). Note the sharp angles formed at the lateral margins of the ovarian tissue where it contacts the lesion, consistent with the beak sign (arrowheads). **(B)** Sagittal T2-weighted image in a 69-year-old female patient with ovarian metastasis from colon adenocarcinoma shows the absence of the normal ipsilateral ovary (phantom organ sign) and the presence of gonadal vascular supply (ovarian vascular pedicle sign, arrowhead). The ovarian vascular pedicle sign is best visualized on the ovarian axis or coronal oblique images (not shown) acquired parallel to the uterine corpus.

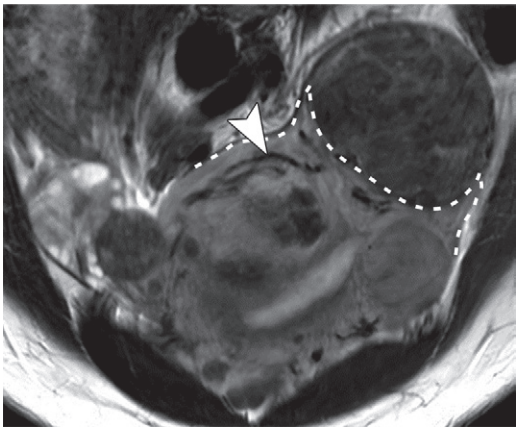

**Figure 18.** Imaging clues suggestive of uterine origin of a lesion. Axial oblique T2-weighted image in a 37-year-old female patient shows uterine tissue surrounding the mass (leiomyoma) with acute lateral margins (claw sign, dotted line) and vessels extending from the uterus to the mass (bridging vessels sign, arrowhead).

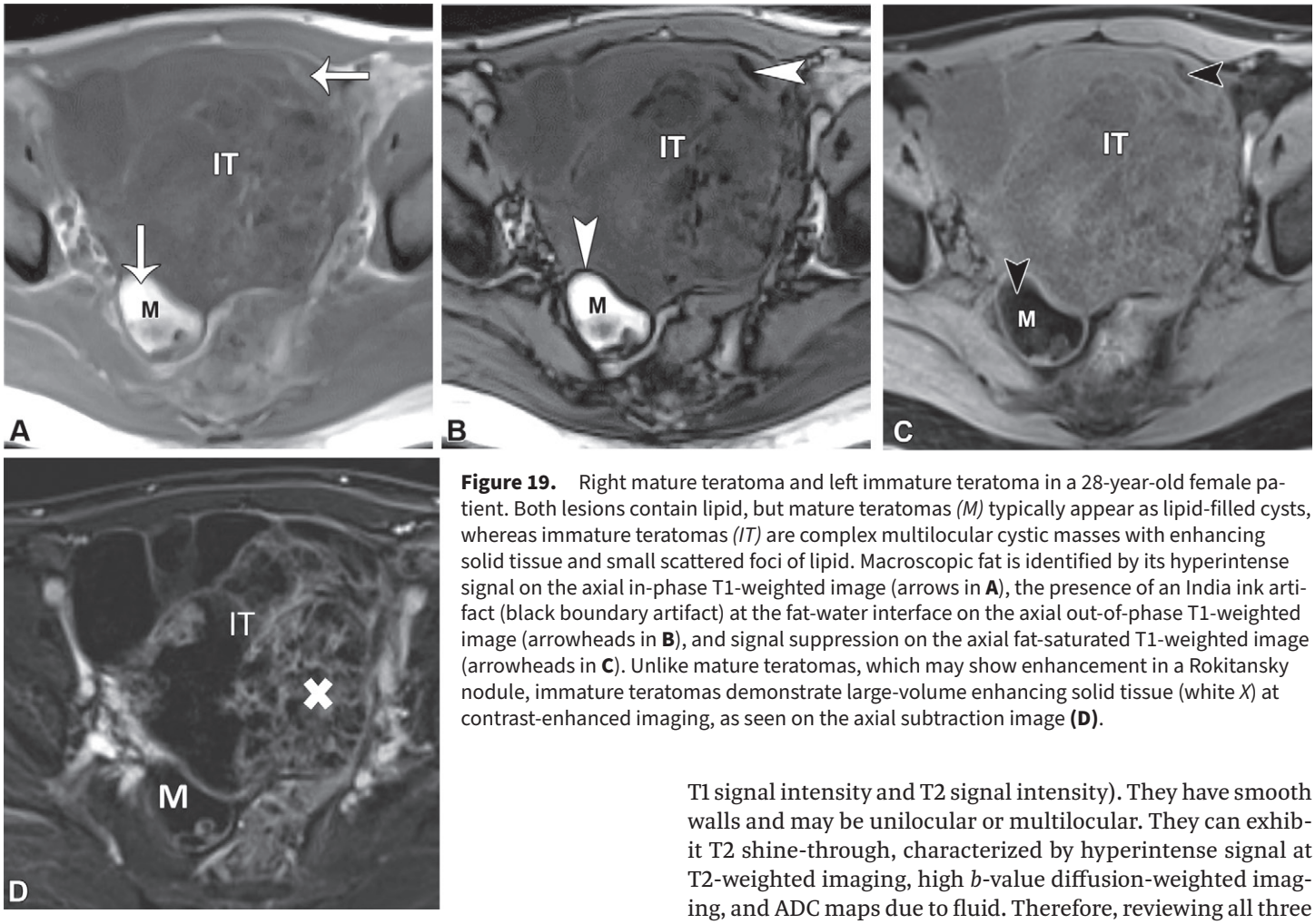


**Figure 19.** Right mature teratoma and left immature teratoma in a 28-year-old female patient. Both lesions contain lipid, but mature teratomas *(M)* typically appear as lipid-filled cysts, whereas immature teratomas *(IT)* are complex multilocular cystic masses with enhancing solid tissue and small scattered foci of lipid. Macroscopic fat is identified by its hyperintense signal on the axial in-phase T1-weighted image (arrows in **A**), the presence of an India ink artifact (black boundary artifact) at the fat-water interface on the axial out-of-phase T1-weighted image (arrowheads in **B**), and signal suppression on the axial fat-saturated T1-weighted image (arrowheads in **C**). Unlike mature teratomas, which may show enhancement in a Rokitansky nodule, immature teratomas demonstrate large-volume enhancing solid tissue (white *X*) at contrast-enhanced imaging, as seen on the axial subtraction image **(D)**.

For lesions with a nongynecologic origin, the differential diagnosis includes hematoma or hemoperitoneum from trauma, procedure, and other causes (eg, ruptured ovarian cyst).

**Cysts (Simple or Proteinaceous Fluid) without Solid Tissue**

Table S8 details the most common gynecologic conditions causing cysts without solid tissue, organized by their origin (36,39,69–71). These lesions are typically benign and contain either simple fluid (T1-hypointense and T2-hyperintense signal, like that of urine or CSF) or proteinaceous fluid (variable T1 signal intensity and T2 signal intensity). They have smooth walls and may be unilocular or multilocular. They can exhibit T2 shine-through, characterized by hyperintense signal at T2-weighted imaging, high *b*-value diffusion-weighted imaging, and ADC maps due to fluid. Therefore, reviewing all three sequences is crucial to avoid misinterpretation.

***Adnexal Lesions.*—**For lesions with an ovarian origin, the differential diagnosis includes functional cysts, postmenopausal cysts, and benign epithelial tumors such as serous or mucinous cystadenomas (Fig 23). Serous cystadenomas are typically unilocular, occasionally bilateral, and are filled with simple fluid, resembling postmenopausal ovarian cysts (36). Mucinous cystadenomas are unilateral and multilocular and exhibit locules with variable T1 signal intensity and T2 signal intensity due to mucin, creating a “stained glass” appearance

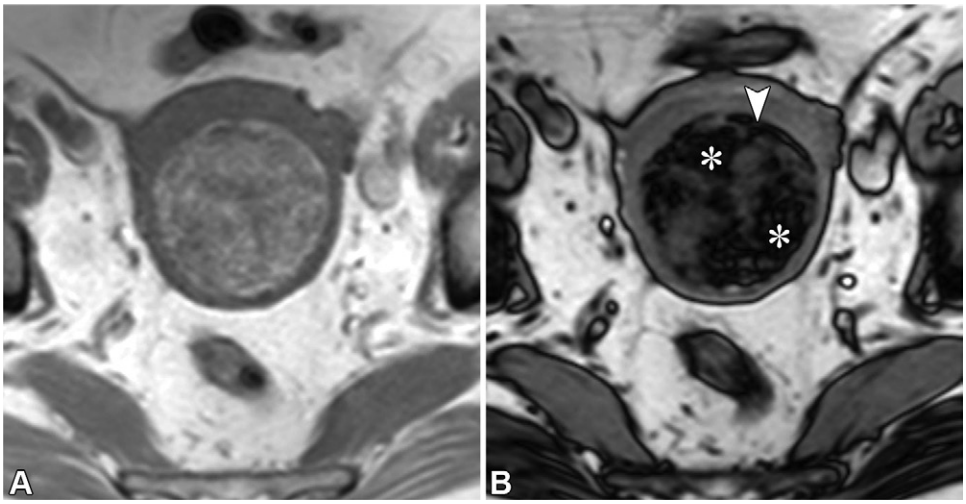


**Figure 20.** Lipoleiomyoma in a 65-year-old female patient. **(A)** Axial in-phase T1-weighted image shows a well-circumscribed hyperintense mass within the myometrium. **(B)** Axial opposed-phase T1-weighted image shows an India ink artifact (black boundary artifact, arrowhead) and signal drop within the lesion (∗), confirming the presence of macroscopic and microscopic fat.


**Figure 21.** Bilateral endometriomas in a 20-year-old female patient with dysmenorrhea. **(A, B)** Axial fat-saturated T1-weighted **(A)** and T2-weighted **(B)** images show classic features of endometriomas, such as bilateral T1-hyperintense lesions (∗ in **A**) with T2 shading (∗ in **B**), T2-hypointense walls, and intralesional T2-dark spots (arrowheads in **B**), all indicative of chronic repetitive hemorrhage. **(C)** Contrast-enhanced fat-saturated T1-weighted image with subtraction confirms the absence of enhancing solid tissue.

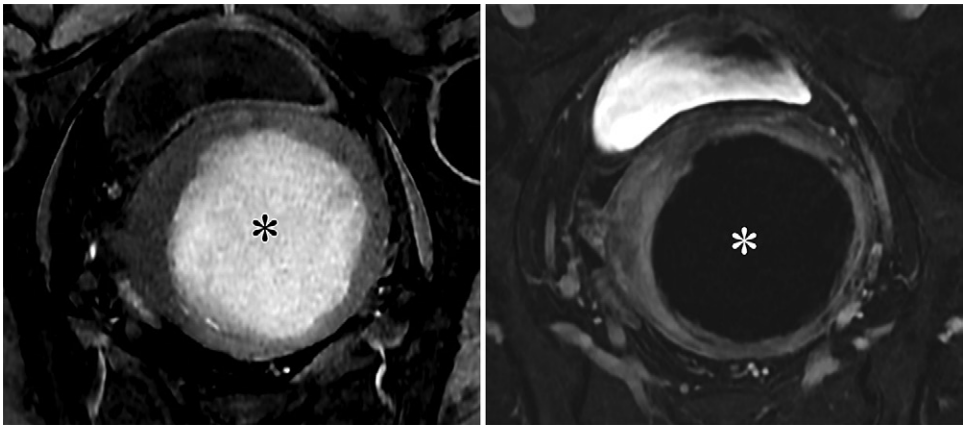

**Figure 22.** Hemorrhagic myometrial lesion in a 40-year-old female patient with menorrhagia, consistent with red (cavernous) degeneration of a leiomyoma. **(A)** Axial oblique fat-saturated T1-weighted image shows diffusely a T1-hyperintense uterine mass (∗), indicating hemorrhage. **(B)** Axial oblique subtracted image shows lack of contrast enhancement in this uterine mass (∗), confirming hemorrhagic infarction within a leiomyoma. If enhancing solid tissue is present on subtracted images, careful differentiation from leiomyosarcoma is essential.

(69). Bilateral mucinous cystadenoma-like lesions should raise suspicion for metastases.

For lesions with a paraovarian origin, the differential diagnosis includes paraovarian cyst, hydrosalpinx, and peritoneal inclusion cyst (Fig 23). Paraovarian cysts are round or oblong unilocular cysts in the broad ligament between the uterus and ovary (70). Hydrosalpinx is a C- or U-shaped, fluid-filled, obstructed fallopian tube near the ovary, with characteristic incomplete septa or endosalpingeal folds. Hydrosalpinges are commonly caused by scarring from pelvic inflammatory disease and less often from endometriosis or surgery (39). Peritoneal inclusion cysts, typically seen in premenopausal women

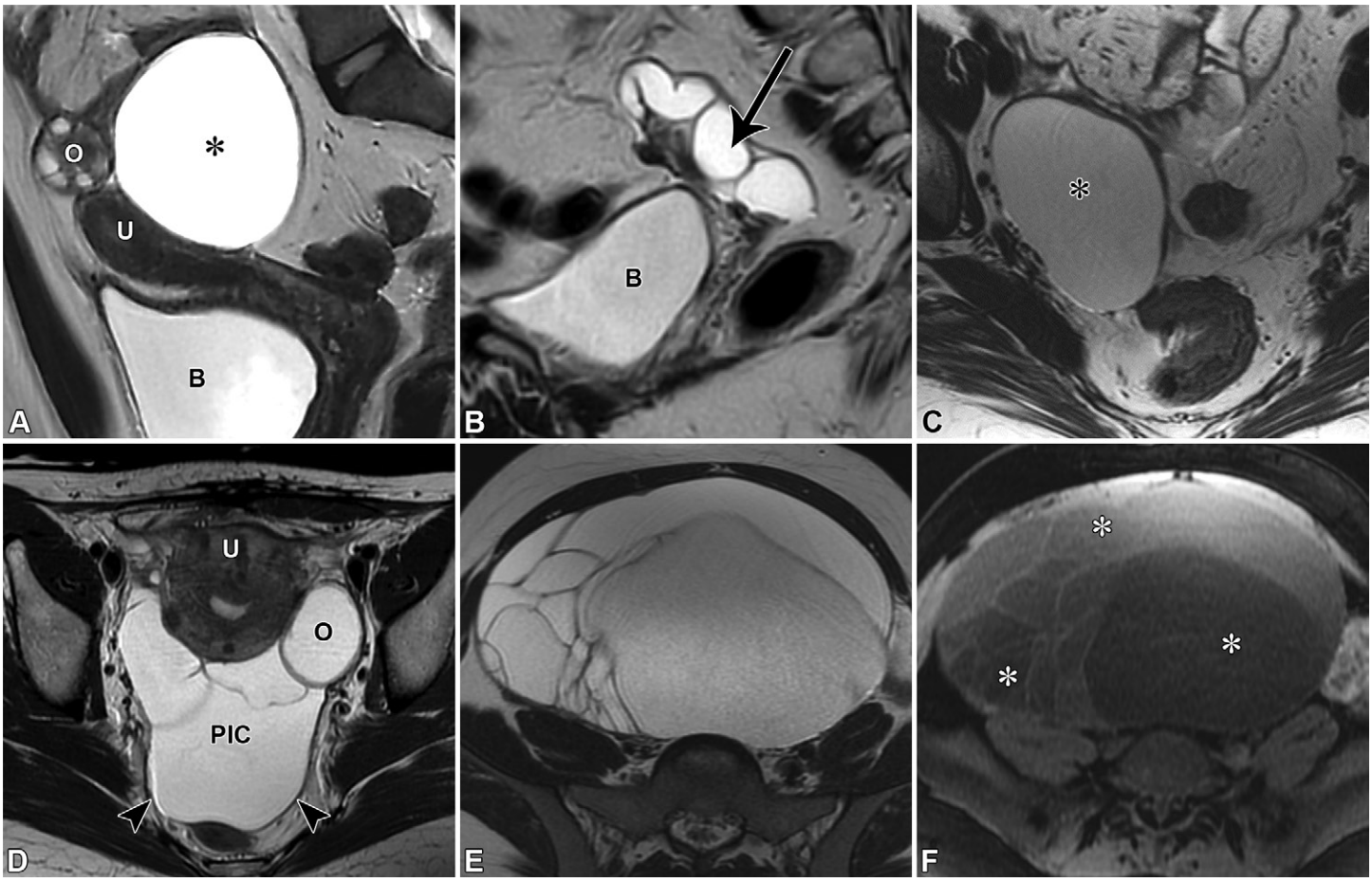


**Figure 23.** MRI of various gynecologic cystic lesions without enhancing solid tissue in different patients. **(A)** Sagittal T2-weighted image shows a paraovarian cyst, a unilocular simple cyst (∗) located adjacent to but separate from the uterus *(U)* and ovary *(O)*. *B* = urinary bladder. **(B)** Sagittal T2-weighted image shows a hydrosalpinx, a dilated, fluid-filled tubular structure (arrow) with a smooth wall and endosalpingeal folds, separate from the uterus and ovaries (not shown). *B* = urinary bladder. **(C)** Axial T2-weighted image shows a serous cystadenoma (∗), a unilocular cyst that persists over time. An ovary is not visualized as separate from this lesion. **(D)** Axial T2-weighted image in a 46-year-old female patient with prior bowel resection shows a peritoneal inclusion cyst *(PIC)*, a multilocular cystic lesion with thin septations caused by adhesions, conforming to the peritoneal cavity's shape (arrowheads), with the ovary *(O)* suspended at the margin. *U* = uterus. **(E, F)** Axial T2-weighted image **(E)** and fat-saturated T1-weighted image **(F)** show a mucinous cystadenoma, a large unilateral multilocular cystic mass with locules of variable signal intensity (∗; most apparent in **F**; ∗), resembling stained glass.

with functional ovaries and prior pelvic insult (eg, surgery, trauma, endometriosis), are multilocular thin-walled lesions that conform to the peritoneal cavity and surround the ovary, creating a "spider in the web" appearance (70).

***Nonadnexal Lesions.***—For lesions with a uterine origin, the differential diagnosis includes the rare purely cystic leiomyoma due to cystic degeneration, nabothian cysts or tunnel clusters for cervical lesions, and vaginal cysts for vaginal lesions (Tables S3, S4; Figs 13,15).

For lesions with a nongynecologic origin, consider urethral diverticulum, Skene duct cyst (lateral to the external urethral meatus), appendiceal mucocele, enteric duplication cyst, mesenteric cyst, lymphangioma, retrorectal cyst, postsurgical seroma, or a lymphocele after LN dissection (Fig 15).

**Cystic or Solid Lesions with Dark-T2/Dark-DWI Solid Tissue**

Table S9 details the most common gynecologic conditions with dark-T2/dark-DWI solid tissue, organized by their origin (10,36,64,72–74). Most are benign lesions containing fibrotic or fibromuscular tissue. Dark-T2 is defined as T2-SI equal to or lower than skeletal muscle (19,22). For ovarian lesions and fibrotic plaques, the dark SI at high *b*-value DWI (≥1000 sec/mm$^2$) is defined as DWI signal intensity equal to or lower than that of urine or CSF, while for uterine lesions, the dark signal intensity at high *b*-value DWI is defined as DWI signal intensity lower than that of the myometrium (19,22). Dark-T2/dark-DWI solid tissue is also typically accompanied by dark signal intensity on the ADC map, known as the "T2-blackout" pattern (57).

***Adnexal Lesions.***—For lesions with an ovarian origin, fibroma and fibrothecoma are primary considerations for solid lesions with dark-T2/dark-DWI solid tissue, whereas cystadenofibroma is considered for cystic lesions with dark T2/dark DWI solid tissue (36). Ovarian fibromas and fibrothecomas are benign, often asymptomatic sex-cord stromal tumors typically affecting middle-aged women. They contain fibrous tissue and theca cells. While usually unilateral, bilateral fibromas may

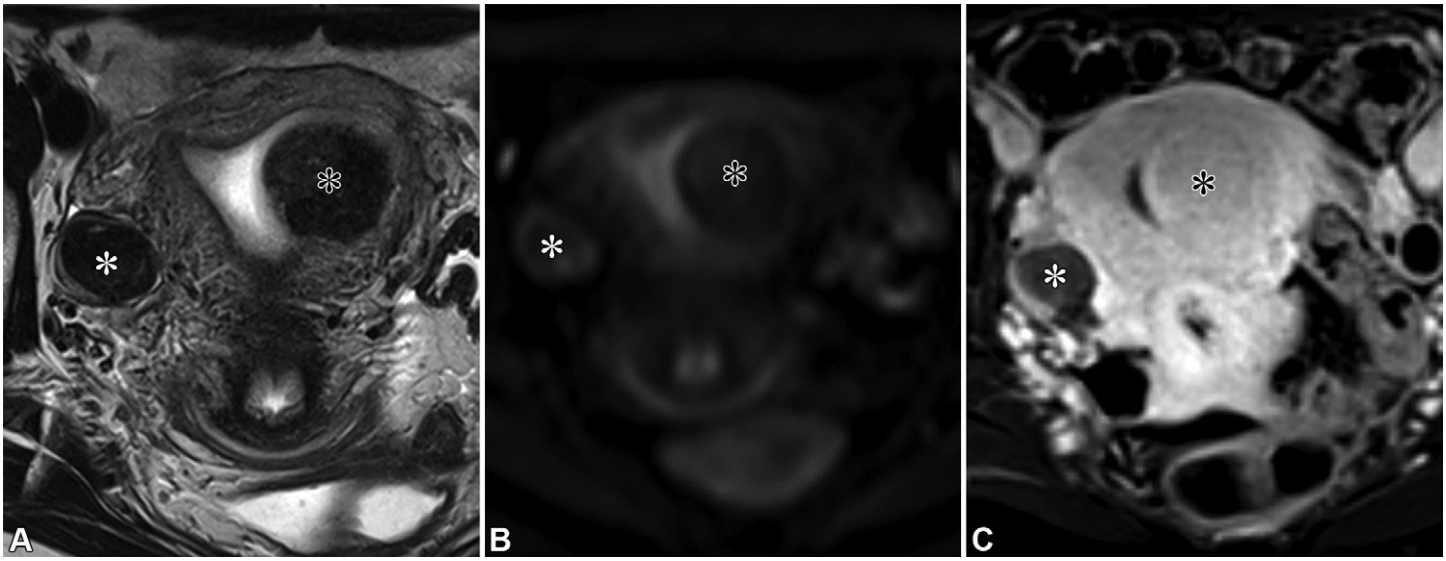


**Figure 24.** Right ovarian fibroma and left intramural leiomyoma with a submucosal component in a 37-year-old female patient with dysmenorrhea. **(A, B)** Axial T2-weighted **(A)** and high *b*-value diffusion-weighted **(B)** images show a dark T2/dark DWI right ovarian fibroma (white ∗) and left uterine leiomyoma (black ∗). **(C)** Axial contrast-enhanced fat-saturated T1-weighted image with subtraction shows mild enhancement in the fibroma (white ∗) compared with the avid enhancement in the leiomyoma (black ∗).

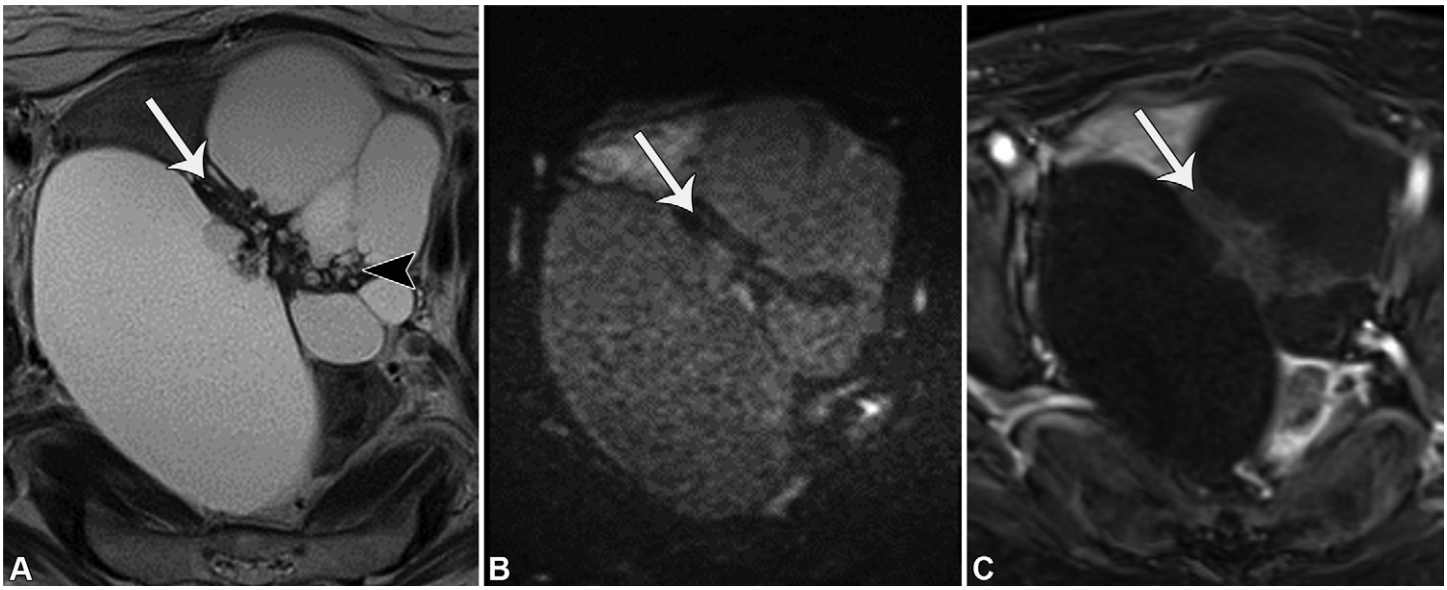


**Figure 25.** Cystadenofibroma in a 72-year-old female patient with abdominal pain and a palpable pelvic mass. **(A, B)** Axial T2-weighted **(A)** and high *b*-value diffusion-weighted **(B)** images show a multilocular right ovarian lesion with cystic components and solid tissue (arrow) that is dark T2/dark DWI. Note the cystic foci interspersed between solid tissue, known as "black sponge" (arrowhead in **A**), a nonspecific finding that may also be seen in other less common ovarian tumors. **(C)** Axial contrast-enhanced fat-saturated T1-weighted image with subtraction shows mild enhancement within the solid tissue (arrow).

occur in Gorlin (basal cell nevus) syndrome. Meigs syndrome (pleural effusion, ascites, and an ovarian mass) is rare but is more common with ovarian fibromas than with other ovarian tumors. Ovarian fibromas and fibrothecomas typically show dark-T2/dark-DWI solid tissue, with T2-blackout pattern and minimal delayed enhancement (Fig 24). Brenner tumors, rare epithelial-stromal neoplasms, can be difficult to differentiate from fibromas and fibrothecomas but are typically smaller (36). Cystadenofibroma, a benign epithelial tumor, is the most probable diagnosis for a cystic lesion with dark-T2/dark-DWI solid tissue (Fig 25). Occasionally, solid tissue can contain interspersed cystic foci, referred to as "black sponge" (36,72). The "black sponge" sign is a nonspecific feature that may also be seen in other less common entities.

***Nonadnexal Lesions.*—**For lesions of uterine origin, leiomyoma is the primary consideration (64). Leiomyomas are benign hormonally driven tumors with a lifetime prevalence of up to 70%, enlarging before menopause and regressing afterward. They may be asymptomatic or cause pelvic pain, pressure, abnormal uterine bleeding, and subfertility. Leiomyomas can undergo various types of degeneration, with hyaline degeneration—

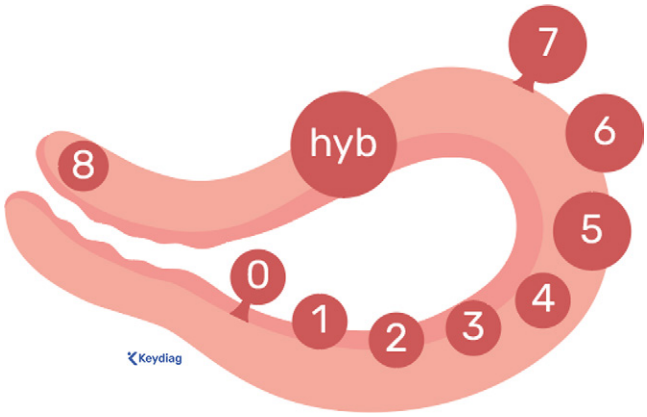


**Figure 26.** The FIGO classification of uterine leiomyomas aids in precisely communicating the location of the leiomyomas. Submucosal leiomyomas: type 0 = pedunculated intracavitary; type 1 = less than 50% intramural; type 2 = 50% or more intramural. Other leiomyomas: type 3 = 100% intramural with endometrial contact; type 4 = 100% intramural without endometrial or serosal contact; type 5 = subserosal 50% or more intramural; type 6 = subserosal less than 50% intramural; type 7 = pedunculated subserosal; type 8 = located outside the myometrium (cervix, broad ligament, etc). Hybrid: types 2–5 = the first number indicates the submucosal portion, and the second number indicates the subserosal portion.

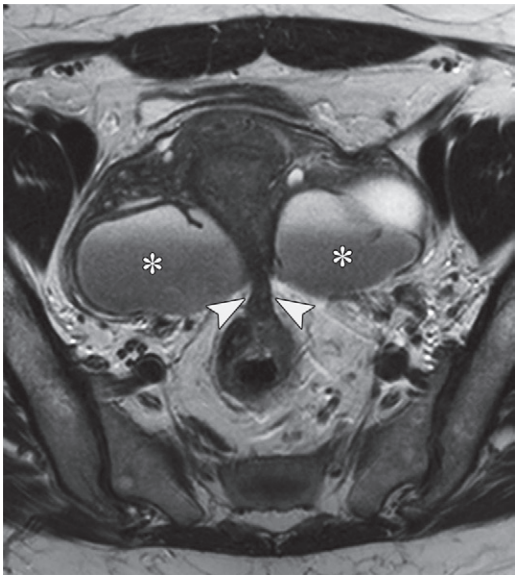

**Figure 27.** Bilateral endometriomas and deep pelvic endometriosis in a 46-year-old female patient with pelvic pain. Axial T2-weighted image shows bilateral endometriomas (∗) with T2 shading. T2-hypointense scarring, caused by deep endometriosis, is seen between the uterus, ovaries, and rectosigmoid colon (arrowheads). This scarring tethers the colon and displaces the ovaries posteriorly to the uterus, known as the kissing ovaries sign.

replacement of smooth muscle with collagen—being the most common. Both conventional and hyalinized leiomyomas typically demonstrate homogeneous dark-T2/dark-DWI solid tissue, enabling a confident benign diagnosis (Fig 24). Unlike ovarian fibromas, conventional leiomyomas show early avid enhancement like the myometrium, whereas hyalinized leiomyomas enhance less. Leiomyomas can be subserosal, intramural, or submucosal, with precise classification using the International Federation of Gynecology and Obstetrics (FIGO) system (Fig 26). Rare broad ligament leiomyomas share imaging features of their uterine counterparts but are located within the broad ligament and lack the connection to either the uterus or the ipsilateral ovary (73,74). When degeneration in a leiomyoma leads to non-dark T2/non-dark DWI solid tissue, differentiating it from malignancy, particularly leiomyosarcoma, is critical and is discussed in the next section.

For lesions with a parauterine/paraovarian origin, deep endometriosis is the primary consideration (10). Deep endometriosis is a severe form, manifesting as fibrotic lesions with subperitoneal extension. It is typically multifocal and mainly affects the pelvis, particularly the uterosacral ligaments at their attachment to the torus uterinus. Other commonly involved sites include the rectosigmoid colon ("mushroom cap" sign), posterior cul-de-sac, vagina, round ligaments, urinary bladder, and ovarian surfaces. In advanced cases, the ovaries may be displaced posterior to the uterus, leading to the "kissing ovaries" sign (Fig 27). Deep endometriosis appears as dark-T2/dark-DWI thickening, smooth or spiculated nodules, and infiltration that may tether adjacent structures and cause architectural distortion (eg, uterine retroflexion, uterine deviation, "kissing ovaries," and bowel angulation). Deep endometriosis may occasionally contain hyperintense foci on T2-and fat-saturated T1-weighted imaging due to blood in the ectopic endometrial glands.

For lesions with a nongynecologic origin, the differential diagnosis includes leiomyoma or fibroma arising from other organs and fibrosis from a previous procedure, trauma, or infection.

### Cystic or Solid Lesions with Non-Dark T2/Non-Dark DWI Solid Tissue

Table S10 (10,36,62,69,72,75–78) and Table S11 (8,9,20–25,79–82) describe the most common gynecologic conditions with non-dark T2/non-dark DWI solid tissue, organized by their origin. Non-dark T2 is defined as T2 signal intensity higher than that of skeletal muscle (19,22). For adnexal lesions, non-dark DWI is defined as DWI signal intensity higher than that of urine or CSF (19), while for uterine lesions, non-dark DWI is defined as DWI signal intensity equal to or higher than that of the myometrium (22). Solid tissue restricts diffusion if it increases in signal intensity at high *b*-value DWI compared with at low *b*-value DWI and is hypointense on the ADC map (57).

***Adnexal Lesions.***—For lesions of ovarian origin, primary ovarian tumors or metastases should be considered (Table S10, Fig 6). Among primary tumors, the differential diagnosis includes borderline epithelial tumors (serous, mucinous, seromucinous, and others), invasive epithelial tumors (high- and low-grade serous, mucinous, endometrioid, clear cell, and others), malignant germ cell tumors (dysgerminoma, yolk sac tumor, embryonal carcinoma, and choriocarcinoma), and several sex cord-stromal tumors (granulosa cell tumor, Sertoli-Leydig cell tumors, and others) (36).

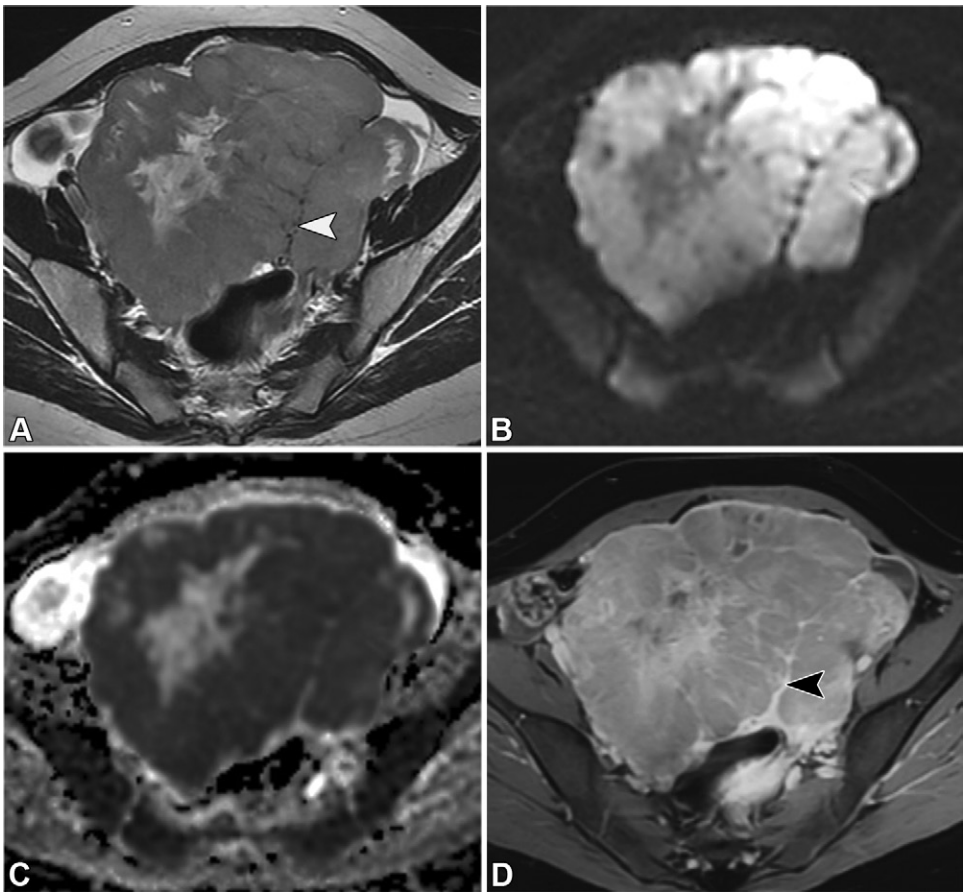


**Figure 28.** Left ovarian dysgerminoma in a 20-year-old female patient with an elevated LDH level. Axial T2-weighted **(A)**, high *b*-value diffusion-weighted **(B)**, ADC **(C)**, and contrast-enhanced fat-saturated T1-weighted **(D)** images show a T2-intermediate solid ovarian lesion with diffusion restriction (hyperintense signal in **B** and hypointense signal in **C**) and enhancement. This lesion is divided into lobules by fibrovascular septa that show characteristic intermediate-to-hypointense signal (arrowhead in **A**) on T2-weighted images and avid enhancement (arrowhead in **D**) on contrast-enhanced images.

Patient age, malignancy history, symptoms, serum tumor markers, and MRI features can provide important diagnostic clues. The Ovarian-Adnexal Reporting and Data System (O-RADS) MRI algorithm refines the assessment of malignancy risk by evaluating the enhancement kinetics of the most avidly enhancing solid tissue versus the outer myometrium (19). Further details are beyond the scope of this article and are available in the referenced source. Additionally, the morphology of solid tissue—such as papillary projections, mural nodules, irregular septations or walls, or a larger solid portion—can provide further insights.

In women under 30 years of age with a unilateral solid ovarian lesion and elevated lactate dehydrogenase, dysgerminoma is the most likely diagnosis (36,62). Dysgerminoma, a malignant germ cell tumor and the ovarian counterpart of testicular seminoma, manifests as a unilateral non-dark T2/non-dark DWI solid lesion that is divided into lobules by T2-hypointense avidly enhancing fibrovascular septa (Fig 28) (62). Conversely, in women under 30 years of age, elevated α-fetoprotein is virtually diagnostic of yolk sac tumors, while elevated β-human chorionic gonadotropin is virtually diagnostic of choriocarcinoma (36,62).

In young women with virilization, oligo- or amenorrhea, and a unilateral solid ovarian lesion, a Sertoli-Leydig cell tumor is the most likely diagnosis (36,75). This sex-cord stromal tumor, the most common ovarian tumor associated with elevated testosterone levels, can have indolent or aggressive behavior. It typically appears as a heterogeneous non-dark T2/non-dark DWI solid lesion with small scattered cystic foci (36,75).

In older women with elevated inhibin B levels, granulosa cell tumor should be considered (36,55). It is a rare malignant sex-cord stromal tumor that occurs primarily in postmenopausal women (adult type) and less frequently in women under 30 (juvenile form) (36). These tumors are the most common cause of elevated estrogen levels, leading to abnormal uterine bleeding, endometrial polyps, hyperplasia, or carcinoma (Fig 29).

Borderline epithelial tumors typically manifest at a younger age and are distinguished from invasive epithelial tumors by the absence of stromal invasion (72). Serous borderline tumors, the most common type, occur in premenopausal women and may be unilateral or bilateral, with the latter occurring in one-third of cases. They may also manifest with peritoneal implants. When solid tissue shows papillary morphology with T2-hyperintense architecture and T2-hypointense internal branching, it is virtually diagnostic of a serous borderline tumor (Fig 30) (36,72). Large papillary projections may resemble a sea anemone (76). Mucinous borderline tumors, the second most common type, typically manifest as large unilateral multilocular masses with honeycomb-like locules. If mural nodules and irregular septations are present, they are indistinguishable from mucinous carcinoma (36,69,72). Bilateral mucinous lesions should raise the suspicion for metastases.

High-grade serous ovarian cancer (HGSOC) is the most common invasive epithelial tumor and the most prevalent ovarian carcinoma overall (36). It typically occurs in postmenopausal women and is associated with elevated CA-125 levels. A risk factor for HGSOC is hereditary breast and ovarian cancer syndrome, primarily caused by germline *BRCA1/2*

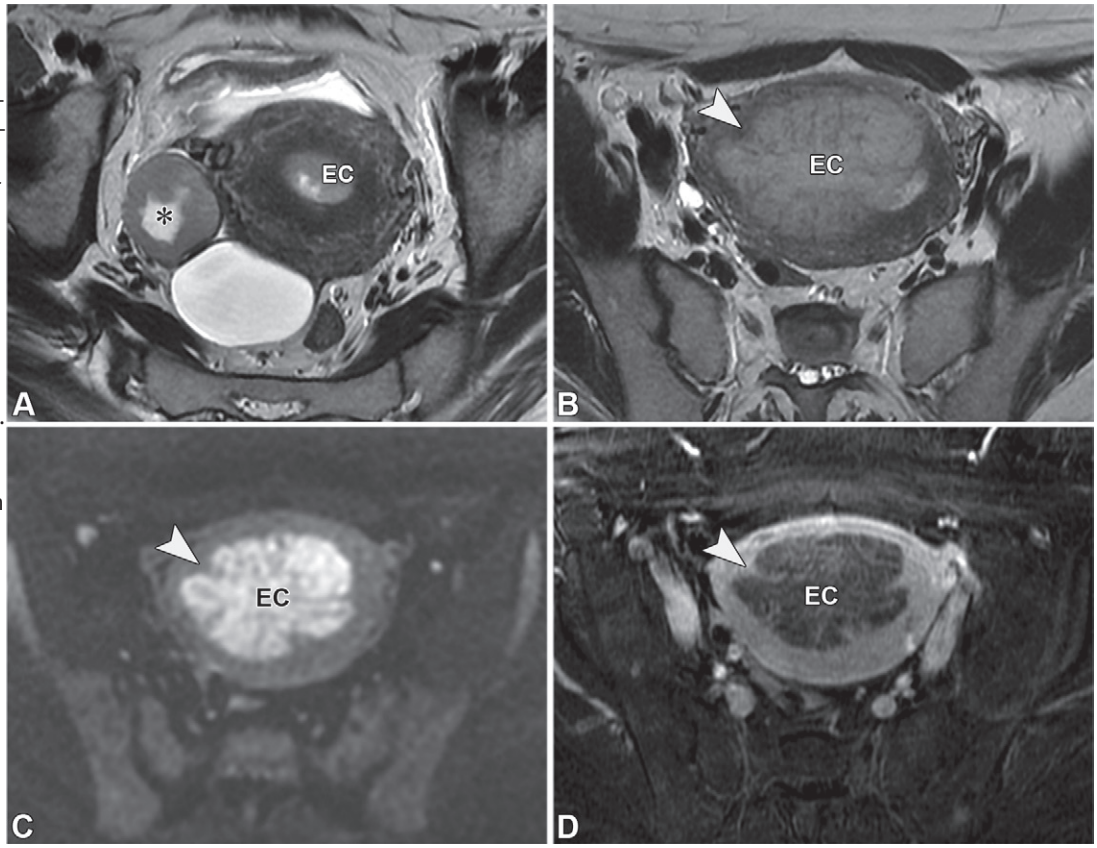


**Figure 29.** Granulosa cell tumor and secondary endometrioid adenocarcinoma in a 31-year-old female patient with abnormal vaginal bleeding. *EC* = endometrial cancer. **(A, B)** Axial oblique T2-weighted images, acquired perpendicular to the uterine corpus for endometrial cancer staging, show a right ovarian mass (∗ in **A**) with non-dark T2/non-dark DWI solid tissue, corresponding to a pathologically confirmed granulosa cell tumor (diffusion-weighted and contrast-enhanced images not shown). A T2-intermediate (non-dark T2) endometrial mass expands the endometrial cavity, consistent with known endometrioid adenocarcinoma. **(C)** Axial oblique high b-value diffusion-weighted image **(C)**, obtained using the same plane, field of view, and section thickness as the T2-weighted images, shows high-signal-intensity endometrial cancer with corresponding low signal intensity on the ADC map (not shown), indicative of restricted diffusion. **(D)** Axial oblique contrast-enhanced fat-saturated T1-weighted image with subtraction shows endometrial cancer enhancement less than that of the myometrium. An irregular tumor-myometrium interface (arrowhead in **B-D**) is noted on the T2-weighted, high *b*-value diffusion-weighted, and subtraction images **(B–D)**, consistent with myometrial invasion.

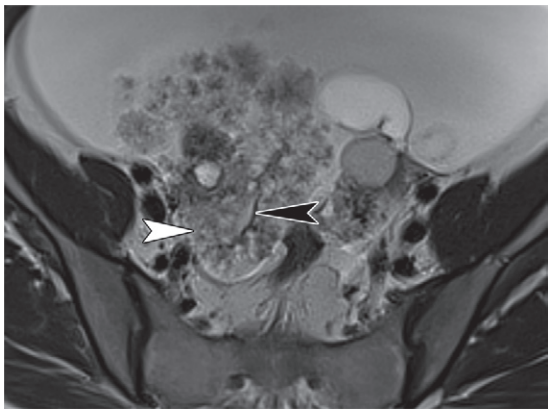

**Figure 30.** Bilateral serous borderline tumors in a 41-year-old female patient presenting with pelvic pain, bloating, and elevated serum CA-125 levels. Axial T2-weighted image shows bilateral ovarian lesions with a predominant exophytic surface growth pattern of the visualized papillary projections. The papillary projections show a characteristic T2-hyperintense architecture (white arrowhead) with T2-hypointense internal branching (black arrowhead). This distinctive sea anemone–like appearance is diagnostic of serous borderline tumors.

mutations, which leads to an earlier onset (54). HGSOC often manifests as bilateral solid or cystic lesions with large-volume non-dark T2/non-dark DWI solid tissue, peritoneal implants, ascites, and sometimes lymphadenopathy, reflecting its typically advanced stage at presentation due to absent early symptoms and rapid peritoneal spread (Fig 31) (36).

Endometriosis-associated malignancy occurs in about 1% of patients with long-standing endometriosis, primarily arising in endometriomas (75%) (10,77). The most common subtypes are endometrioid and clear cell carcinomas, as well as several borderline tumors (seromucinous, endometrioid, clear cell). Malignancy is suspected when T2-shading is absent or lost due to hemorrhage dilution by tumor cell secretions, and non-dark T2/non-dark DWI solid tissue is seen on subtracted images (Fig 32). Endometrioid and clear cell carcinomas may also be associated with Lynch syndrome, often with synchronous endometrial carcinoma.

Ovarian metastases should be considered in the presence of a known primary malignancy but may also represent the first manifestation of an occult primary malignancy (36). The most common sources include colonic or endometrial adenocarcinoma, followed by gastric, breast, appendiceal, and pancreatobiliary adenocarcinoma. Patients with ovarian metastases are typically younger than those with primary invasive epithelial ovarian tumors, and the lesions are usually bilateral and rapidly growing. Krukenberg tumors, a subtype of ovarian metastases, account for about 50% of cases and originate from adenocarcinoma with mucin-secreting signet ring cells (78). They often originate from the stomach but may also arise from other sites, including the colon, appendix, and breast (83). Ovarian metastases typically present as bilateral rapidly enlarging solid

**Figure 31.** High-grade serous ovarian carcinoma in a 52-year-old female patient with abdominal pain, bloating, and elevated serum CA-125 levels. Axial T2-weighted **(A)**, high *b*-value diffusion-weighted **(B)**, and contrast-enhanced fat-saturated T1-weighted **(C)** images show bilateral adnexal cystic lesions with solid tissue (*) exhibiting intermediate signal intensity on the T2-weighted image **(A)**, high signal intensity on the high *b*-value diffusion-weighted image **(B)**, and contrast enhancement **(C)**. Additionally, a peritoneal implant in the posterior cul-de-sac (black arrowhead), ascites, and right pelvic lymphadenopathy (white arrowhead) are noted.

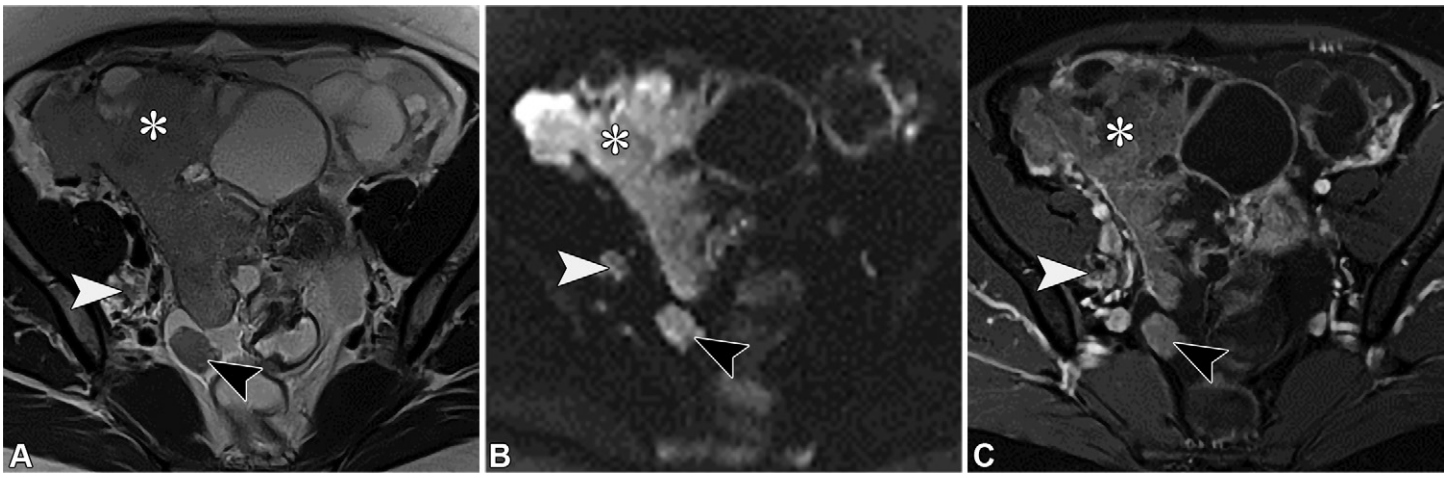


**Figure 32.** Left ovarian endometrioid borderline tumor arising from an endometrioma in a 58-year-old female patient with endometriosis. Axial T2-weighted **(A)**, fat-saturated T1-weighted **(B)**, contrast-enhanced T1-weighted fat-saturated image with subtraction **(C)**, high *b*-value diffusion-weighted **(D)**, and ADC **(E)** images show a left endometrioma (*) with enhancing solid tissue (arrowhead) with high signal intensity on the T2-weighted **(A)**, diffusion-weighted **(D)**, and ADC **(E)** images. High signal intensity on the diffusion-weighted image and relatively high signal intensity on the ADC map in the enhancing solid tissue are suggestive of a borderline tumor. The underlying left endometrioma exhibits T2 shading **(A)** and high T1 signal intensity **(B)**.

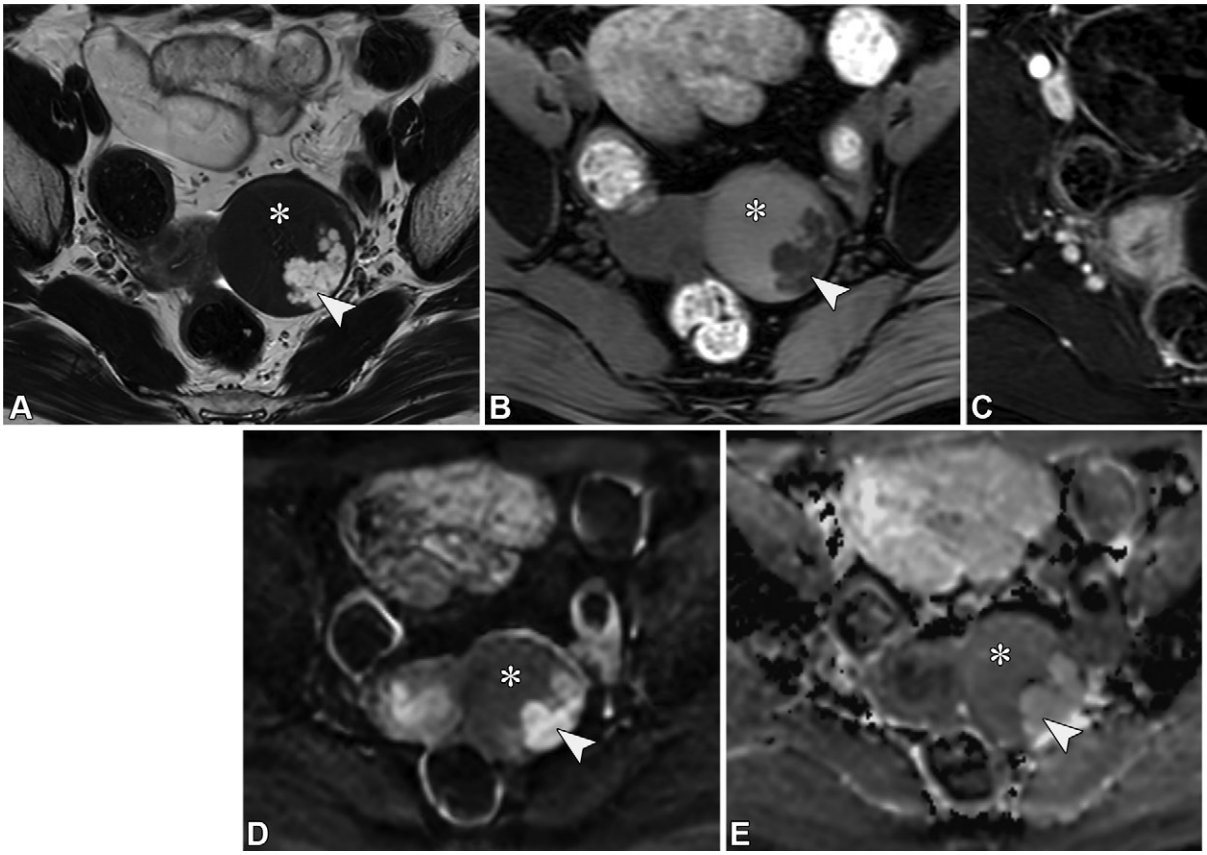


or cystic lesions with non-dark T2/non-dark DWI solid tissue. In Krukenberg tumors, the cystic component represents mucin secreted by the tumor cells (Fig 33) (36,78).

***Nonadnexal Lesions.***—If the lesion is of uterine origin and centered in the myometrium, it is critical to distinguish common benign leiomyomas from malignancies, such as rare

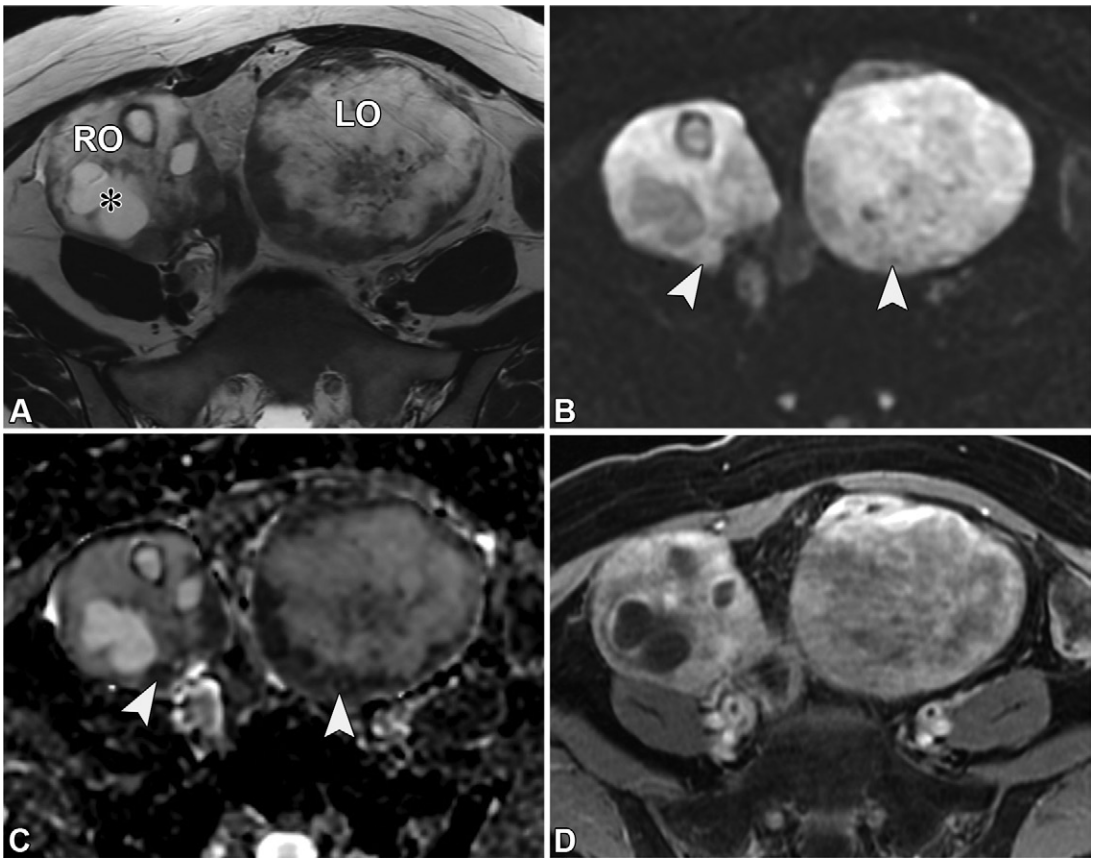


**Figure 33.** Bilateral ovarian metastases (Krukenberg tumors) from signet ring gastric adenocarcinoma in a 44-year-old female patient. **(A)** Axial T2-weighted image shows a cystic lesion with heterogeneous solid tissue replacing the right ovary *(RO)* and a heterogeneous solid lesion replacing the left ovary *(LO)*. The T2-hyperintense cystic portion in the right mass (*) is due to mucin secreted by tumor cells. **(B, C)** Axial high *b*-value diffusion-weighted image **(B)** shows high signal intensity with corresponding low signal intensity on the axial ADC map **(C)**, consistent with diffusion restriction (arrowheads) in both masses. **(D)** Axial contrast-enhanced fat-saturated T1-weighted image shows enhancing solid tissue in both ovarian masses.

but aggressive uterine sarcomas—most commonly leiomyosarcomas. Leiomyomas may deviate from the classic dark-T2/dark-DWI solid tissue, resulting in an atypical appearance due to histologic variants like cellular leiomyoma or degeneration (64). A recently published algorithmic approach using T2- and DWI signal intensity of solid tissue provides a structured framework for assessing malignancy risk in a myometrial mass (Fig 34) (22). After excluding enlarged LNs or peritoneal implants, compare the T2 signal intensity of the solid tissue to that of skeletal muscle. If it is greater, evaluate the solid tissue at high *b*-value DWI. If the DWI signal intensity is equal to or higher than that of the endometrium or LNs, determine the ADC value by placing a small region of interest on the solid tissue with the lowest ADC signal intensity. Malignancy is suspected if the ADC value is $0.905 \times 10^{-3}$ $mm^2/sec$ or less, valid only when DWI with a *b* value of 1000 $sec/mm^2$ is performed. Exclude hemorrhagic and necrotic areas to prevent errors. Additional MRI features suggesting malignancy include irregular margins, hemorrhage, and necrosis. Growth of a myometrial mass after menopause, in the absence of hormonal therapy, is another strong indicator of malignancy (22).

Enhancing lesions with non-dark T2/non-dark DWI solid tissue in the endometrium, cervix, or vulva encompass a broad range of conditions, including but not limited to endometrial, cervical, or vulvar cancer (Table S11) (8,9,20–25,79–82). MRI is valuable for assessing locoregional tumor extent and guiding treatment planning. Critical MRI findings for endometrial cancer include the presence and depth of myometrial invasion, cervical stromal invasion, extrauterine extension, and pelvic/para-aortic LN metastases (Fig 29) (23). For cervical cancers, critical findings include tumor size (for lesions confined to the cervix or upper vagina), parametrial invasion, vaginal involvement (upper two-thirds vs lower one-third), bladder or rectal mucosal invasion, and pelvic/para-aortic LN metastases (Fig 35) (24). For vulvar cancers, MRI evaluation focuses on identifying adjacent organ involvement (urethra, vagina, anus) and inguino-femoral LN metastases(81). Further details are available in the above referenced sources.

For cystic lesions with non-dark T2/non-dark DWI solid tissue of cervical origin, minimal deviation adenocarcinoma (adenoma malignum), a rare well-differentiated gastric-type adenocarcinoma, should be a key consideration (79). Gastric-type adenocarcinoma accounts for 10% of cervical adenocarcinomas. It is an aggressive mucinous tumor with early peritoneal spread and is associated with the Peutz-Jeghers syndrome in 10% of cases (84). MRI features can range from solid lesions with cystic foci to multilocular cystic lesions with solid tissue (as seen with adenoma malignum), extending deeply into the cervical stroma (49). Unlike nabothian cysts, tunnel clusters, or endocervical glandular hyperplasia, which are asymptomatic, adenoma malignum presents with watery discharge and abnormal bleeding. MRI findings alone may be inconclusive for differentiating these conditions, requiring a cone biopsy for diagnosis(49,79).

For non-dark T2/non-dark DWI lesions with a non-gynecologic origin, various lesions from other pelvic organs should be considered, though these are beyond the scope of this review (28).

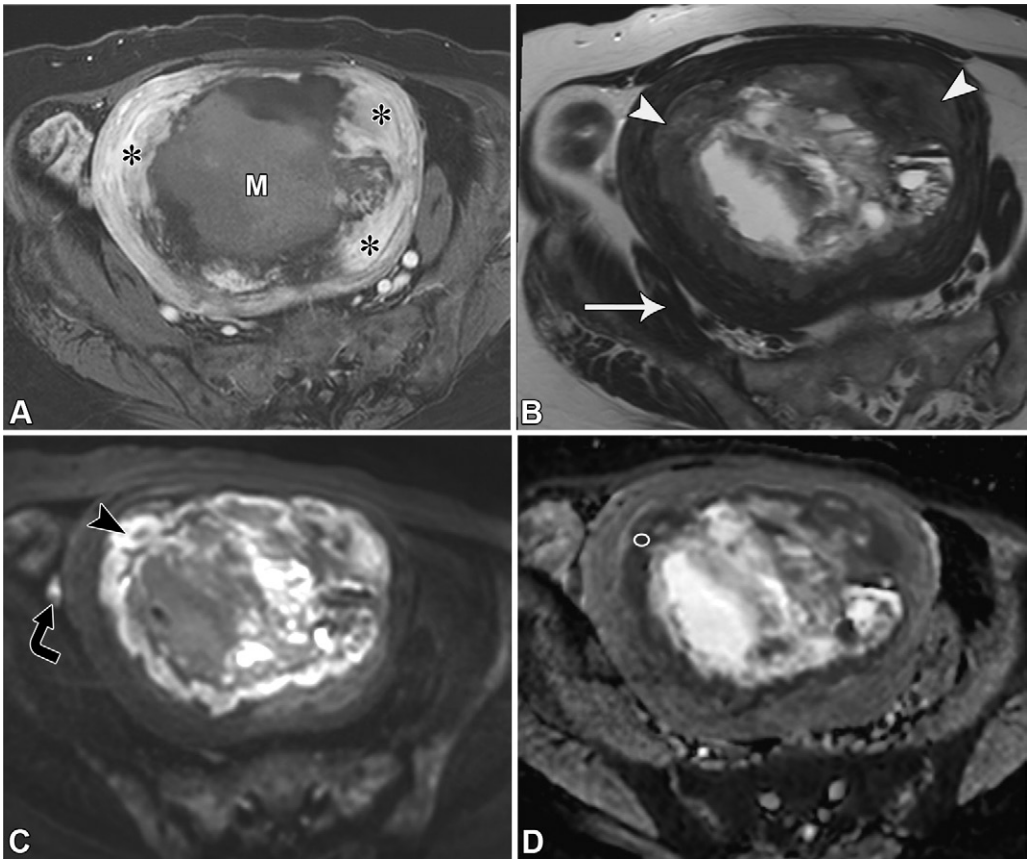


**Figure 34.** Uterine leiomyosarcoma in a 58-year-old female patient with postmenopausal bleeding. **(A)** Axial contrast-enhanced fat-saturated T1-weighted image shows enhancing solid tissue (∗) at the periphery of a centrally necrotic and hemorrhagic myometrial mass *(M)* (subtraction image is not shown). **(B)** Axial T2-weighted image shows that the T2 signal intensity of the enhancing solid tissue (arrowheads) exceeds that of the iliopsoas muscle (arrow). **(C)** Axial high *b*-value diffusion-weighted image shows that the signal intensity of the enhancing solid tissue at DWI (arrowhead) is equal to or greater than that of an LN (curved arrow). **(D)** Axial ADC map shows restricted diffusion (circle) with an ADC value of 0.905 × $10^{-3}$ $mm^2$/sec or less. Hemorrhagic and necrotic areas are carefully excluded during the evaluation of these features.

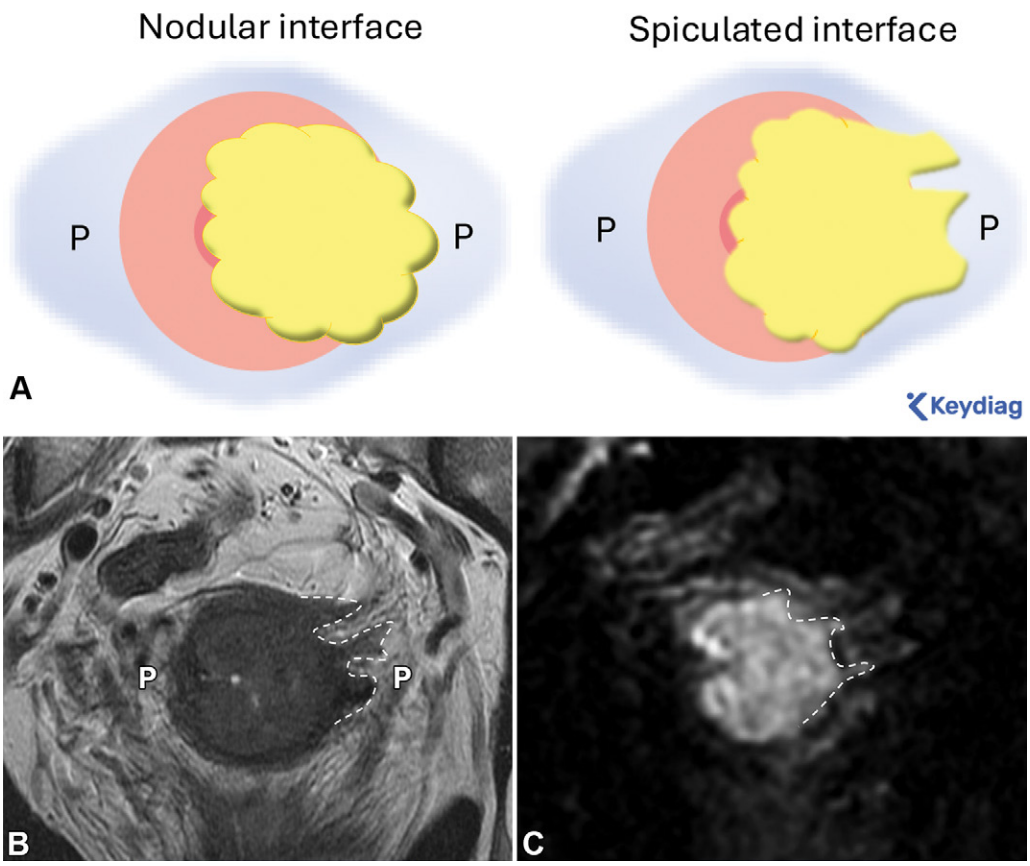


**Figure 35.** Squamous cell carcinoma of the uterine cervix in a 39-year-old female patient, with accompanying schematic illustration showing the diagnostic criteria for parametrial invasion. **(A)** Schematic illustration of parametrial invasion, indicated by a nodular or spiculated interface between the tumor and the parametrium. This may occasionally be accompanied by encasement of parametrial vessels. *P* = parametrium. **(B)** Axial oblique T2-weighted image, obtained perpendicular to the short axis of the cervix, shows a T2-intermediate cervical tumor with full-thickness infiltration of the normally T2-hypointense cervical stroma. A spiculated and/or nodular interface between the tumor and the parametrial region (dashed outline in **B** and **C**) indicates parametrial invasion. *P* = parametrium. **(C)** Axial oblique high *b*-value diffusion-weighted image, acquired using the same plane, field of view, and section thickness as the T2-weighted image, confirms the findings in **B**. The addition of DWI enhances the accuracy of detecting parametrial invasion by better delineating tumor margins and differentiating tumor from edema or fibrosis.

### Step 4: Structured Reporting

Disease-specific structured reporting enables clear, comprehensive, and relevant communication that facilitates clinical decision making and supports research for future improvements. Examples of disease-specific structured reporting templates are available from the European Society of Urogenital Radiology, the Society of Abdominal Radiology, and the American College of Radiology (9,10,20,24,25,85).

## Conclusion

The interpretation of gynecologic pelvic MRI benefits from tailored MRI protocols, knowledge of normal female pelvic anatomy, and a step-by-step approach focusing on lesion origin, lesion tissue composition, and solid tissue morphology, with findings then presented in a structured report.

**Author affiliations:**

[1]Department of Radiology, Mayo Clinic, Jacksonville, Fla

[2]Department of Radiology, Montpellier Cancer Institute, Montpellier France; PINKCC Laboratory, Montpellier Cancer Research Institute, Montpellier France

[3]Department of Radiology, Vanderbilt University Medical Center, Nashville, Tenn

[4]Department of Abdominal Imaging, MD Anderson Cancer Center, Houston, Tex

[5]Department of Radiology, Mayo Clinic, Rochester, Minn

[6]Imaging Institute, Cleveland Clinic, Cleveland, Ohio

[7]Department of Radiology, Memorial Sloan Kettering Cancer Center, 1275 York Ave, New York, NY 10065

[8]Department of Radiology, University of Washington, Seattle, Wash

[9]Division of Abdominal Radiology, SUNY Upstate Medical University, Syracuse, NY

[10]Departments of Radiology and Obstetrics and Gynecology, University of Wisconsin School of Medicine and Public Health, Madison, Wis

[11]Department of Radiology, Weill Cornell Medical College, New York, NY

Received March 3, 2025; revision requested March 27 received May 14; accepted May 19.

**Address correspondence to:** Y.L. (email: LakhmanY@mskcc.org).

**Supplemental material:** Supplemental material is available at *RadioGraphics* online.

**Funding:** Supported in part by the NIH/NCI Cancer Center Support Grant (P30 CA008748). S.N. supported by a European Research Council (ERC) Starting Grant (MROMICS).

**Acknowledgments:** Joanne Chin, MFA, ELS, for manuscript preparation, and Frédérique Réty, MD, President of Keymaging, for creating the illustrations.

**Disclosures of conflicts of interest:** Please see ICMJE form(s) for author conflicts of interest. These have been provided as supplemental materials.

## References

1. Bazot M, Bharwani N, Huchon C, et al. European society of urogenital radiology (ESUR) guidelines: MR imaging of pelvic endometriosis. Eur Radiol 2017;27(7):2765–2775.
2. Kubik-Huch RA, Weston M, Nougaret S, et al. European Society of Urogenital Radiology (ESUR) Guidelines: MR Imaging of Leiomyomas. Eur Radiol 2018;28(8):3125–3137.
3. Maciel C, Bharwani N, Kubik-Huch RA, et al. MRI of female genital tract congenital anomalies: european Society of Urogenital Radiology (ESUR) guidelines. Eur Radiol 2020;30(8):4272–4283.
4. Tong A, VanBuren WM, Chamié L, et al. Recommendations for MRI technique in the evaluation of pelvic endometriosis: consensus statement from the Society of Abdominal Radiology endometriosis disease-focused panel. Abdom Radiol (NY) 2020;45(6):1569–1586.
5. Sheikh-Sarraf M, Nougaret S, Forstner R, Kubik-Huch RA. Patient preparation and image quality in female pelvic MRI: recommendations revisited. Eur Radiol 2020;30(10):5374–5383.
6. Ciggaar IA, Henneman ODF, Oei SA, Vanhooymissen IJSML, Blikkendaal MD, Bipat S. Bowel preparation in MRI for detection of endometriosis: comparison of the effect of an enema, no additional medication and intravenous butylscopolamine on image quality. Eur J Radiol 2022;149:110222.
7. Jayaprakasam VS, Javed-Tayyab S, Gangai N, et al. Does microenema administration improve the quality of DWI sequences in rectal MRI? Abdom Radiol (NY) 2021;46(3):858–866.
8. Manganaro L, Lakhman Y, Bharwani N, et al. Staging, recurrence and follow-up of uterine cervical cancer using MRI: updated Guidelines of the European Society of Urogenital Radiology after revised FIGO staging 2018. Eur Radiol 2021;31(10):7802–7816.
9. Nikolić O, Sousa FAE, Cunha TM, et al; ESUR Female Pelvic Imaging Working Group. Vulvar cancer staging: guidelines of the European Society of Urogenital Radiology (ESUR). Insights Imaging 2021;12(1):131.
10. VanBuren W, Feldman M, Shenoy-Bhangle AS, et al. Radiology State-of-the-art Review: endometriosis Imaging Interpretation and Reporting. Radiology 2024;312(3):e233482.
11. Unlu E, Virarkar M, Rao S, Sun J, Bhosale P. Assessment of the Effectiveness of the Vaginal Contrast Media in Magnetic Resonance Imaging for Detection of Pelvic Pathologies: a Meta-analysis. J Comput Assist Tomogr 2020;44(3):436–442.
12. Sakala MD, Shampain KL, Wasnik AP. Advances in MR Imaging of the Female Pelvis. Magn Reson Imaging Clin N Am 2020;28(3):415–431.
13. Rockall AG, Jalaguier-Coudray A, Thomassin-Naggara I. MR imaging of the Adnexa: technique and Imaging Acquisition. Magn Reson Imaging Clin N Am 2023;31(1):149–161.
14. Ueda T, Ohno Y, Yamamoto K, et al. Compressed sensing and deep learning reconstruction for women's pelvic MRI denoising: utility for improving image quality and examination time in routine clinical practice. Eur J Radiol 2021;134:109430.
15. Lee EJ, Hwang J, Park S, et al. Utility of accelerated T2-weighted turbo spin-echo imaging with deep learning reconstruction in female pelvic MRI: a multi-reader study. Eur Radiol 2023;33(11):7697–7706.
16. Ueda T, Yamamoto K, Yazawa N, et al. Efficacy of compressed sensing and deep learning reconstruction for adult female pelvic MRI at 1.5 T. Eur Radiol Exp 2024;8(1):103.
17. Chen NK, Guidon A, Chang HC, Song AW. A robust multi-shot scan strategy for high-resolution diffusion weighted MRI enabled by multiplexed sensitivity-encoding (MUSE). Neuroimage 2013;72:41–47.
18. Lawrence EM, Zhang Y, Starekova J, et al. Reduced field-of-view and multi-shot DWI acquisition techniques: prospective evaluation of image quality and distortion reduction in prostate cancer imaging. Magn Reson Imaging 2022;93:108–114.
19. Sadowski EA, Thomassin-Naggara I, Rockall A, et al. O-RADS MRI Risk Stratification System: guide for Assessing Adnexal Lesions from the ACR O-RADS Committee. Radiology 2022;303(1):35–47.
20. Nougaret S, Horta M, Sala E, et al. Endometrial Cancer MRI staging: updated Guidelines of the European Society of Urogenital Radiology. Eur Radiol 2019;29(2):792–805.
21. Maheshwari E, Nougaret S, Stein EB, et al. Update on MRI in Evaluation and Treatment of Endometrial Cancer. RadioGraphics 2022;42(7):2112–2130.
22. Hindman N, Kang S, Fournier L, et al. MRI Evaluation of Uterine Masses for Risk of Leiomyosarcoma: a Consensus Statement. Radiology 2023;306(2):e211658.
23. Avesani G, Bonatti M, Venkatesan AM, Nougaret S, Sala E. RadioGraphics Update: 2023 FIGO Staging System for Endometrial Cancer. RadioGraphics 2024;44(7):e240084.
24. Lakhman Y, Aherne EA, Jayaprakasam VS, Nougaret S, Reinhold C. Staging of Cervical Cancer: a Practical Approach Using MRI and FDG PET. AJR Am J Roentgenol 2023;221(5):633–648.
25. Lee M, Andrieu PIC, Nougaret S, et al. Role of MRI in Assessing the Feasibility of Fertility-Sparing Treatments for Early-Stage Endometrial and Cervical Cancers. AJR Am J Roentgenol 2025;224(3):e2432157.
26. Meyers MA, Charnsangavej C, Oliant M. Meyers' Dynamic Radiology of the Abdomen: Normal and Pathologic Anatomy, 6th ed. New York, NY: Springer New York, 2011.
27. Pannu HK, Oliant M. The subperitoneal space and peritoneal cavity: basic concepts. Abdom Imaging 2015;40(7):2710–2722.
28. Nougaret S, Nikolovski I, Paroder V, et al. MRI of Tumors and Tumor Mimics in the Female Pelvis: anatomic Pelvic Space-based Approach. RadioGraphics 2019;39(4):1205–1229.
29. Kaniewska M, Gołofit P, Heubner M, Maake C, Kubik-Huch RA. Suspensory Ligaments of the Female Genital Organs: MRI Evaluation with Intraoperative Correlation. RadioGraphics 2018;38(7):2195–2211.
30. Gollub MJ, Maas M, Weiser M, et al. Recognition of the anterior peritoneal reflection at rectal MRI. AJR Am J Roentgenol 2013;200(1):97–101.
31. Tielbeek JAW, Stoker J. Magnetic Resonance Imaging: Methodology and Normal Pelvic Floor Anatomy. In: Santoro GA, Wieczorek AP, Sultan AH, eds. Pelvic Floor Disorders. Cham: Springer International Publishing, 2021; 171-177.

32. Kim SW, Kim HC, Yang DM, Min GE. The prevesical space: anatomical review and pathological conditions. Clin Radiol 2013;68(7):733–740.
33. Montanarella M, Gonzalez Baerga CI, Menendez Santos MJ, et al. Retroperitoneal anatomy with the aid of pathologic fluid: an imaging pictorial review. J Clin Imaging Sci 2023;13:36.
34. Pontes Fernandez CFR, Oliveira BC, Franco IP, et al. Imaging anatomy of the lateral pelvic compartment applied to endometriosis. Abdom Radiol (NY) 2025;50(2):936–952.
35. Kostov S, Selçuk I, Watrowski R, et al. Pelvic Sidewall Anatomy in Gynecologic Oncology-New Insights into a Potential Avascular Space. Diagnostics (Basel) 2022;12(2):519.
36. Taylor EC, Irshaid L, Mathur M. Multimodality Imaging Approach to Ovarian Neoplasms with Pathologic Correlation. RadioGraphics 2021;41(1):289–315.
37. Bookwalter CA, VanBuren WM, Neisen MJ, Bjarnason H. Imaging Appearance and Nonsurgical Management of Pelvic Venous Congestion Syndrome. RadioGraphics 2019;39(2):596–608.
38. Langer JE, Oliver ER, Lev-Toaff AS, Coleman BG. Imaging of the female pelvis through the life cycle. RadioGraphics 2012;32(6):1575–1597.
39. Revzin MV, Moshiri M, Katz DS, Pellerito JS, Mankowski Gettle L, Menias CO. Imaging Evaluation of Fallopian Tubes and Related Disease: a Primer for Radiologists. RadioGraphics 2020;40(5):1473–1501.
40. Dawood MT, Naik M, Bharwani N, Sudderuddin SA, Rockall AG, Stewart VR. Adnexal Torsion: review of Radiologic Appearances. RadioGraphics 2021;41(2):609–624.
41. Huddleston HG, Dokras A. Diagnosis and Treatment of Polycystic Ovary Syndrome. JAMA 2022;327(3):274–275.
42. Smith KA, Parvinian A, Ainsworth AJ, Shenoy CC, Packard AT. Normal and Abnormal Appearances of the Ovaries during Assisted Reproduction: multimodality Imaging Review. RadioGraphics 2023;43(11):e230089.
43. Mansoori B, Khatri G, Rivera-Colón G, Albuquerque K, Lea J, Pinho DF. Multimodality Imaging of Uterine Cervical Malignancies. AJR Am J Roentgenol 2020;215(2):292–304.
44. Gupta A, Desai A, Bhatt S. Imaging of the Endometrium: Physiologic Changes and Diseases: women's Imaging. RadioGraphics 2017;37(7):2206–2207.
45. Novellas S, Chassang M, Delotte J, et al. MRI characteristics of the uterine junctional zone: from normal to the diagnosis of adenomyosis. AJR Am J Roentgenol 2011;196(5):1206–1213.
46. Grasel RP, Outwater EK, Siegelman ES, Capuzzi D, Parker L, Hussain SM. Endometrial polyps: MR imaging features and distinction from endometrial carcinoma. Radiology 2000;214(1):47–52.
47. Nougaret S, Cunha TM, Benadla N, Neron M, Robbins JB. Benign Uterine Disease: the Added Role of Imaging. Obstet Gynecol Clin North Am 2021;48(1):193–214.
48. Takeuchi M, Matsuzaki K. Adenomyosis: usual and unusual imaging manifestations, pitfalls, and problem-solving MR imaging techniques. RadioGraphics 2011;31(1):99–115.
49. Bin Park S, Lee JH, Lee YH, Song MJ, Choi HJ. Multilocular cystic lesions in the uterine cervix: broad spectrum of imaging features and pathologic correlation. AJR Am J Roentgenol 2010;195(2):517–523.
50. Goldstein RB, Bree RL, Benson CB, et al. Evaluation of the woman with postmenopausal bleeding: society of Radiologists in Ultrasound-Sponsored Consensus Conference statement. J Ultrasound Med 2001;20(10):1025–1036.
51. Zulfiqar M, Shetty A, Yano M, et al. Imaging of the Vagina: spectrum of Disease with Emphasis on MRI Appearance. RadioGraphics 2021;41(5):1549–1568.
52. Sekhar A, Eberhardt L, Lee KS. Imaging of the female urethra. Abdom Radiol (NY) 2019;44(12):3950–3961.
53. Hosseinzadeh K, Heller MT, Houshmand G. Imaging of the female perineum in adults. RadioGraphics 2012;32(4):E129–E168.
54. Hereditary Cancer Syndromes and Risk Assessment: ACOG COMMITTEE OPINION, Number 793. Obstet Gynecol 2019;134(6):e143–e149.
55. Rao S, Smith DA, Guler E, et al. Past, Present, and Future of Serum Tumor Markers in Management of Ovarian Cancer: a Guide for the Radiologist. RadioGraphics 2021;41(6):1839–1856.
56. Elsherif SB, Agely A, Gopireddy DR, et al. Mimics and Pitfalls of Primary Ovarian Malignancy Imaging. Tomography 2022;8(1):100–119.
57. Forstner R, Thomassin-Naggara I, Cunha TM, et al. ESUR recommendations for MR imaging of the sonographically indeterminate adnexal mass: an update. Eur Radiol 2017;27(6):2248–2257.
58. Castiglione D, Delfa GL, Tiralongo F, Inì C, Basile A. The "claw" sign. Abdom Radiol (NY) 2024;49(7):2554–2558.
59. Allen BC, Hosseinzadeh K, Qasem SA, Varner A, Leyendecker JR. Practical approach to MRI of female pelvic masses. AJR Am J Roentgenol 2014;202(6):1366–1375.
60. Fujii S, Kakite S, Nishihara K, et al. Diagnostic accuracy of diffusion-weighted imaging in differentiating benign from malignant ovarian lesions. J Magn Reson Imaging 2008;28(5):1149–1156.
61. Nougaret S, Tirumani SH, Addley H, Pandey H, Sala E, Reinhold C. Pearls and pitfalls in MRI of gynecologic malignancy with diffusion-weighted technique. AJR Am J Roentgenol 2013;200(2):261–276.
62. Shaaban AM, Rezvani M, Elsayes KM, et al. Ovarian malignant germ cell tumors: cellular classification and clinical and imaging features. RadioGraphics 2014;34(3):777–801.
63. Fattahi N, Moeini A, Morani AC, et al. Fat-containing pelvic lesions in females. Abdom Radiol (NY) 2022;47(1):362–377.
64. Tu W, Yano M, Schieda N, et al. Smooth Muscle Tumors of the Uterus at MRI: focus on Leiomyomas and FIGO Classification. RadioGraphics 2023;43(6):e220161.
65. Siegelman ES, Outwater EK. Tissue characterization in the female pelvis by means of MR imaging. Radiology 1999;212(1):5–18.
66. Corwin MT, Gerscovich EO, Lamba R, Wilson M, McGahan JP. Differentiation of ovarian endometriomas from hemorrhagic cysts at MR imaging: utility of the T2 dark spot sign. Radiology 2014;271(1):126–132.
67. Gupta S, Manchanda S, Vyas S, Malhotra N, Mathur SR, Kulshrestha V. Imaging features of accessory cavitated uterine mass (ACUM): a peculiar yet correctable cause of dysmenorrhea. Abdom Radiol (NY) 2023;48(3):1100–1106.
68. Peyron N, Jacquemier E, Charlot M, et al. Accessory cavitated uterine mass: MRI features and surgical correlations of a rare but under-recognised entity. Eur Radiol 2019;29(3):1144–1152.
69. Marko J, Marko KI, Pachigolla SL, Crothers BA, Mattu R, Wolfman DJ. Mucinous Neoplasms of the Ovary: radiologic-Pathologic Correlation. RadioGraphics 2019;39(4):982–997.
70. Moyle PL, Kataoka MY, Nakai A, Takahata A, Reinhold C, Sala E. Nonovarian cystic lesions of the pelvis. RadioGraphics 2010;30(4):921–938.
71. Bharwani N, Crofton ME. Peritoneal pseudocysts: aetiology, imaging appearances, and natural history. Clin Radiol 2013;68(8):828–836.
72. Tsuboyama T, Sato K, Ota T, et al. MRI of Borderline Epithelial Ovarian Tumors: pathologic Correlation and Diagnostic Challenges. RadioGraphics 2022;42(7):2095–2111.
73. Fasih N, Prasad Shanbhogue AK, Macdonald DB, et al. Leiomyomas beyond the uterus: unusual locations, rare manifestations. RadioGraphics 2008;28(7):1931–1948.
74. Spencer JA, Ghattamaneni S. MR imaging of the sonographically indeterminate adnexal mass. Radiology 2010;256(3):677–694.
75. Javadi S, Ganeshan DM, Jensen CT, Iyer RB, Bhosale PR. Comprehensive review of imaging features of sex cord-stromal tumors of the ovary. Abdom Radiol (NY) 2021;46(4):1519–1529.
76. Tanaka YO, Okada S, Satoh T, et al. Ovarian serous surface papillary borderline tumors form sea anemone-like masses. J Magn Reson Imaging 2011;33(3):633–640.
77. Radzynski L, Boyer L, Kossai M, Mouraire A, Montoriol P-F. Pictorial essay: MRI evaluation of endometriosis-associated neoplasms. Insights Imaging 2023;14(1):144.
78. Zulfiqar M, Koen J, Nougaret S, et al. Krukenberg Tumors: update on Imaging and Clinical Features. AJR Am J Roentgenol 2020;215(4):1020–1029.
79. Gordhandas SB, Kahn R, Sassine D, et al. Gastric-type adenocarcinoma of the cervix in patients with Peutz-Jeghers syndrome: a systematic review of the literature with proposed screening guidelines. Int J Gynecol Cancer 2022;32(1):79–88.
80. Lakhman Y, Vargas HA, Reinhold C, et al; Expert Panel on GYN and OB Imaging. ACR Appropriateness Criteria® Staging and Follow-up of Vulvar Cancer. J Am Coll Radiol 2021;18(5s):S212–Ss228.
81. Chow L, Tsui BQ, Bahrami S, et al. Gynecologic tumor board: a radiologist's guide to vulvar and vaginal malignancies. Abdom Radiol (NY) 2021;46(12):5669–5686.
82. Surabhi VR, Garg N, Frumovitz M, Bhosale P, Prasad SR, Meis JM. Aggressive angiomyxomas: a comprehensive imaging review with clinical and histopathologic correlation. AJR Am J Roentgenol 2014;202(6):1171–1178.
83. Wu F, Zhao X, Mi B, et al. Clinical characteristics and prognostic analysis of Krukenberg tumor. Mol Clin Oncol 2015;3(6):1323–1328.
84. Chung SH, Woldenberg N, Roth AR, et al. BRCA and Beyond: comprehensive Image-rich Review of Hereditary Breast and Gynecologic Cancer Syndromes. RadioGraphics 2020;40(2):306–325.
85. American College of Radiology: o-RADS™ MRI. https://www.acr.org/Clinical-Resources/Clinical-Tools-and-Reference/Reporting-and-Data-Systems/O-RADS/MRI. Published 2025. Accessed April 28, 2025.

**Table S1.** Female pelvic MRI protocol: sequence details, rationale, and interpretation tips.

**Patient Preparation**

- Either 1.5T or 3T systems are suitable, with the patient supine and a pelvic phased-array coil used to enhance SNR ratio
  - 3T imaging improves signal-to-noise ratio and spatial resolution, but is more susceptible to artifacts from magnetic field inhomogeneity, chemical shift, and dielectric effect
- Administration of an anti-peristaltic agent (e.g., glucagon 1 mg IM/IV), if not contraindicated, may reduce image blurring from peristalsis
- An enema or suppository may reduce rectal gas and minimize artifacts on DWI
- Partial bladder filling, achieved by emptying the bladder approximately one hour before the exam, can optimize uterine positioning
- Vaginal distention with ultrasound gel may aid in evaluating vaginal involvement in deep endometriosis, cervical cancer staging, and congenital Müllerian duct anomalies
- Placement of saturation bands over the subcutaneous fat of the anterior and posterior body walls may help reduce respiratory motion artifacts

**Protocol and rationale**

**Large field-of-view coronal or axial T2WI through the pelvis and kidneys**

Detects renal anomalies (e.g., congenital Müllerian duct anomalies), hydronephrosis, and para-aortic lymph node enlargement (e.g., for gynecologic cancer staging)

**Axial in- and out-of-phase T1WI through the pelvis**

- Longer TE is assigned to in-phase images; the Dixon method may also be used, with water-only images providing robust fat suppression
- Assesses bone lesions, lymph node enlargement, and enables tissue characterization (e.g., distinguishing lipid from blood)
- Detects susceptibility artifact from prior procedures, hemosiderin, or gas, appearing as blooming on longer TE in-phase images

| **Findings** | • India ink artifact at the water-fat interface on out-of-phase image indicates macroscopic fat<br>• A signal drop on out-of-phase image suggests microscopic fat | 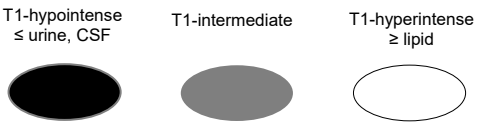 |
|---|---|---|

**High-resolution small field-of-view 2D T2WI without fat saturation, at least 2 orthogonal planes, slice thickness ≤4 mm***

- Provides detailed anatomic evaluation, tissue characterization, detection of enlarged lymph nodes
- 3D T2WI is not routinely used due to lower spatial resolution and higher susceptibility to motion artifacts from longer acquisition times

| **Findings** | 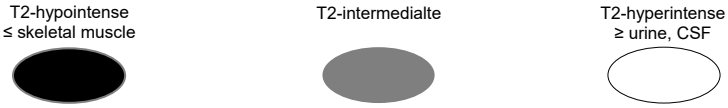 |
|---|---|

| Imaging Planes | **Axial** | **Sagittal** | **Coronal or as specified** |
|---|---|---|---|
| Endometriosis | + | + | Coronal or coronal oblique, parallel to the uterine corpus<br>Axial oblique, perpendicular to the cervix and along uterosacral ligament |
| Indeterminate adnexal mass | + | + | Coronal oblique, or 'ovarian axis' parallel to the uterine corpus, to visualize the gonadal vessels leading to the ovaries |
| Endometrial cancer | + | + | Axial oblique, perpendicular to the endometrium, to assess for the presence and depth of myometrial invasion |
| Cervical cancer | + | + | Axial oblique, perpendicular to cervix, to assess for parametrial invasion |
| LM, LMS | + | + | Axial oblique, perpendicular to the uterine corpus |
| Vulvar cancer | +<br>(include the perineum and groin regions) | + | Axial and coronal oblique, perpendicular and parallel to the urethra<br>Fat saturation may improve the delineation of local tumor extent |

**DWI with low and high b-values (0–50 mm²/s and 1000 mm²/s), slice thickness ≤4 mm, and a corresponding ADC map****

- DWI should be matched to one of the T2WI sequences in terms of imaging plane, FOV, and slice thickness

Back

<table>
<tr><td colspan="4">• DWI is optimized when urine appears dark signal intensity on high b-value images; additional high b-value images can be computed to preserve signal-to-noise ratio<br>• DWI facilitates tissue characterization and enhances the visibility of LNs and peritoneal implants (appearing as high signal intensity on high b-value DWI and low signal intensity on the ADC map)</td></tr>
<tr><td>Findings<br>Focusing on high b-value DWI images</td><td colspan="3">Adnexal lesion<br>Dark DWI<br>≤ urine, CSF<br>  <br>Non-dark DWI<br>> urine, CSF<br>  <br>Myometrial Lesion<br>Dark DWI<br>< outer myometrium<br>  <br>Non-dark DWI<br>≥ outer myometrium<br>  </td></tr>
<tr><td>Reviewing T2WI, low- and high-b-value DWI, and ADC side-by-side is essential for accurate interpretation</td><td>Diffusion Restriction<br>• High signal intensity on high b-value DWI and low signal intensity on the ADC map<br>• Observed with highly cellular tissue or complex fluid<br>  </td><td>T2-blackout<br>• Low signal intensity on T2WI, high b-value DWI, and the ADC map, indicating fibrotic and/or calcified tissue<br>  </td><td>T2-shine through<br>• High signal intensity on T2WI, high b-value DWI, and the ADC map, indicating a cyst with simple fluid<br>  </td></tr>
<tr><td>Imaging Planes</td><td>Axial</td><td colspan="2">Other</td></tr>
<tr><td>Endometriosis</td><td>Match orientation, field-of-view, and slice thickness of axial T2WI</td><td colspan="2"></td></tr>
<tr><td>Adnexal mass</td><td>Same as above</td><td colspan="2"></td></tr>
<tr><td>Endometrial cancer</td><td>-</td><td colspan="2">Match the orientation, field-of-view, and slice thickness of axial oblique T2WI (perpendicular to the uterine corpus) to aid in evaluating local tumor extent (e.g., myometrial invasion)</td></tr>
<tr><td>Cervical cancer</td><td>-</td><td colspan="2">Match the orientation, field-of-view, and slice thickness of axial oblique T2WI (perpendicular to the cervix) to aid in evaluating local tumor extent (e.g., parametrial invasion)</td></tr>
<tr><td>LM, LMS</td><td>-</td><td colspan="2">Match the orientation, field-of-view, and slice thickness of axial oblique T2WI (perpendicular to the uterine corpus)</td></tr>
<tr><td>Vulvar cancer</td><td>Match orientation, field-of-view, and slice thickness of axial T2WI to aid in evaluating tumor extent</td><td colspan="2"></td></tr>
<tr><td colspan="4">3D spoiled gradient-echo fat-saturated T1WI, pre- and postcontrast (with subtracted images), slice thickness ≤3 mm***<br>• Detects enhancing solid tissue, evaluates enhancement kinetics (e.g., O-RADS MRI system or tumor perfusion in a research setting)<br>• Subtraction images increase the conspicuity of enhancing solid tissue, particularly in the presence of hemorrhage</td></tr>
<tr><td>Imaging Planes</td><td>Axial</td><td colspan="2">Sagittal or other as specified</td></tr>
<tr><td>Endometriosis</td><td>May follow recommendations for adnexal masses</td><td colspan="2">Optional: additional or alternative planes</td></tr>
<tr><td>Adnexal Mass</td><td>• Axial dynamic imaging: starting 30 s prior to contrast injection, with a 3 min acquisition and a temporal resolution of ≤15 s<br>• Alternative: Axial pre- and post-contrast acquisition obtained 30–40 s after IV contrast injection</td><td colspan="2">Alternative: Coronal or sagittal plane may be used for large masses to ensure complete coverage</td></tr>
<tr><td>Endometrial cancer</td><td>Axial oblique (aligned to axial oblique T2WI) pre- and postcontrast with 3 min delay after IV contrast injection</td><td colspan="2">Sagittal pre- and post-contrast multiphase imaging at 40 s and 1.5 to 2 min after iV contrast injection</td></tr>
<tr><td>Cervical cancer</td><td>Optional (often used as a research tool)</td><td colspan="2">Optional (primarily used as a research tool)</td></tr>
<tr><td>LM, LMS</td><td>Axial pre- and post-contrast multiphase imaging including post-contrast acquisition at 30–40 s after IV contrast injection and up to 3 min delay</td><td colspan="2">If evaluating prior to uterine embolization, perform MR angiography</td></tr>
<tr><td>Vulvar cancer</td><td>Axial or axial oblique (aligned to axial oblique T2WI) pre- and post -contrast using multiphase approach</td><td colspan="2">Optional: delayed images in sagittal or coronal planes</td></tr>
<tr><td colspan="4">Abbreviations: ADC, apparent diffusion coefficient; DWI, diffusion-weighted imaging; IM, intramuscular; IV, intravenous; LM, leiomyoma; LMS, leiomyosarcoma; T1WI, T1-weighted imaging; T2WI, T2-weighted imaging; TE, time to echo<br>Note:<br>*Deep learning reconstruction produces faster and sharper turbo and fast spin-echo T2WI by accelerating acquisition and reducing echo train length to minimize blurring and noise. This enables shorter exam times or allows for thinner slices or reduced slice gaps within the same scan time as the original T2 sequence.</td></tr>
</table>

** Reduced distortion DWI techniques, such as reduced field-of-view DWI (rFOV-DWI) and multi-shot echo-planar-based DWI with multiplexed sensitivity encoding (MUSE-DWI), minimize susceptibility-related image distortion by reducing the phase-encoding direction with a maintained echo train length (rFOV-DWI) or shortening the echo train length with a maintained phase-encoding direction (MUSE-DWI). MUSE is an image reconstruction algorithm to reduce motion-related artifact in multi-shot echo-planar-based DWI.
*** Radial acquisition with oversampling of peripheral and central k-space can be added for high-resolution postcontrast imaging.
**References**: 1-25

**Table S2. Physiologic and other common benign observations of the ovaries at female pelvic MRI**

| OVARIES | | |
|---|---|---|
| **Premenopausal ovaries** | | |
| **Clinical information**<br>• Reproductive-age women | | **MRI features**<br>• **Oval-shaped structures with physiologic observations described below**<br>• **T1WI:** iso- to hypointense<br>• **T2WI:** hypointense cortex and intermediate SI stroma; multiple follicles described below<br>• **DWI:** mild to moderate diffusion restriction<br>• **CE:** mild enhancement less than myometrium |
| **PHYSIOLOGIC OBSERVATIONS** | **Follicle,** ≤3 cm | |
| | • Reproductive-age women | **MRI features**<br>• **Thin-walled cyst with simple fluid**<br>• **T1WI:** Iso- to hypointense<br>• **T2WI:** Hyperintense<br>• **DWI:** No diffusion restriction<br>• **CE:** No enhancement except for smooth enhancing wall |
| | **Corpus luteum,** ≤3 cm | |
| | • Reproductive-age women | **MRI features**<br>• **Variable appearance based on the developmental phase**<br>• **T1WI:** Hypo- to isointense<br>  ○ Hyperintense centrally, if hemorrhagic<br>• **T2WI:** Hyperintense centrally; surrounded by a thick, crenulated, intermediate-SI wall<br>• **DWI:** No diffusion restriction unless hemorrhagic<br>• **CE:** Avidly enhancing, thick, crenulated wall |
| | **Hemorrhagic cyst,** ≤3 cm | |
| | • Reproductive-age women | **MRI features**<br>• **Unifocal, in contrast to endometriomas which are typically multifocal**<br>• **Resolves overtime, typically 2–3 months**<br>• **T1WI:** Variable due to hemorrhage amount and age; less hyperintense than endometrioma<br>• **T2WI:** Variable due to hemorrhage amount and age; T2 shading but less than in endometrioma<br>• **DWI:** No diffusion restriction<br>• **CE:** No enhancement except for smooth enhancing wall |

Back page 3

Back page 8

| Postmenopausal ovaries | |
|---|---|
| • Postmenopause | **MRI features**<br>• **Small ovaries; may see subcentimeter residual follicles**<br>• **T1WI:** Hypo- to isointense<br>• **T2WI:** Intermediate-to-low signal intensity stroma; may see subcentimeter residual hyperintense follicles<br>• **DWI:** Mild diffusion restriction<br>• **CE:** Mild enhancement less than myometrium |
| **Common benign conditions, best recognized on T2WI** | |
| **Polycystic ovarian syndrome, PCOS** | |
| **Pertinent information**<br>• **Age**<br>  ○ Premenopause<br>• **Most common endocrine disorder of young women**<br>• **Chronic anovulation**<br>  ○ Increased LH-FSH ratio<br>  ○ Increased androgens and estrogen<br>  ○ Irregular menstrual cycle<br>• **Increased risk of endometrial cancer during reproductive years**<br>• Diagnosis is based on the Rotterdam Criteria, which require the presence of 2 out of 3 criteria<br>  ○ Polycystic ovaries<br>  ○ Oligomenorrhea or anovulation<br>  ○ Hyperandrogenism | **MRI features**<br>• **Enlarged bilateral ovaries with increased central stroma and numerous small peripheral follicles**<br>• **T1WI**<br>  ○ Iso- to hypointense<br>• **T2WI**<br>  ○ At least one enlarged ovary (≥10 ml) or ≥20 follicles in either ovary<br>  ○ "String of pearls" appearance: multiple hyperintense peripheral follicles with increased intermediate-to-hypointense central stroma<br>  ○ Careful assessment of the endometrium<br>• **DWI**<br>  ○ Similar to a normal premenopausal ovary<br>• **CE**<br>  ○ Similar to a normal premenopausal ovary |
| **Ovarian Stimulation and Ovarian Hyperstimulation Syndrome (OHSS)** | |
| **Pertinent information**<br>• **Age**<br>  ○ Premenopause<br>• **Observed in patients undergoing ART**<br>• OHSS is an exaggerated response to ovulation induction during ART, characterized by:<br>  ○ Third spacing of fluids, leading to ascites and pleural effusions<br>  ○ Range of severities | • **Enlarged multicystic ovaries with cysts that are larger and less numerous compared with PCOS, without increased central stroma; ± ascites**<br>• **T1WI**<br>  ○ Variable SI; hyperintense if hemorrhagic cysts are present<br>• **T2WI**<br>  ○ Enlarged ovaries with multiple hyperintense follicles; ± ascites<br>  ○ After oocyte retrieval, multiple hemorrhagic cysts with variable SI and hemorrhage in the posterior cul-de-sac<br>  ○ If OHSS, enlarged ovaries with cysts predominantly located at the periphery, creating a "spoke-wheel" appearance; ± ascites and pleural effusions |

| | |
|---|---|
| | • **DWI**<br>  ○ Similar to a normal premenopausal ovary<br>• **CE**<br>  ○ Similar to a normal premenopausal ovary |
| **Ovarian Torsion** | |
| **Pertinent Information**<br>• **Age**<br>  ○ Premenopause<br>• **Cause**<br>  ○ Often a lead mass<br>  ▪ Dominant follicle<br>  ▪ Corpus luteal cyst<br>  ▪ Mature cystic teratoma<br>  ○ **Presentation**<br>  ▪ Acute onset pain<br>  ▪ Nausea and vomiting | **MRI features**<br>• **Enlarged, edematous ovary displaced centrally, with the uterus deviated toward the side of torsion**<br>• **T1WI**<br>  ○ Variable; hyperintense if hemorrhagic infarction<br>• **T2WI**<br>  ○ Enlarged hyperintense (edematous) ovary<br>  ○ Small peripheral hyperintense follicles<br>  ○ ± twisted pedicle<br>• **DWI**<br>  ○ No diffusion restriction; appears hyperintense on both DWI and ADC due to edema<br>• **CE**<br>  ○ Variable enhancement depending on degree of ischemia or presence of infarction<br>  ○ ± Twisted pedicle |
| **Tubo-ovarian abscess, TOA** | |
| **Pertinent Information**<br>• **Age**<br>  ○ Premenopause<br>• **Caused by ascending infection**<br>  • STD*: Neisseria gonorrhoeae* and *Chlamydia trachomatis*<br>  • Bacterial vaginosis: Polymicrobial<br>  • IUD: *Actinomyces israelii*<br>• **Presentation**<br>  ○ Asymptomatic or fever, discharge, pelvic pain, pain with intercourse, leukocytosis<br>• **Disease Spectrum**<br>  ○ Salpingitis, pyosalpinx, TOA | **MRI features**<br>• **Cystic lesion filled with pus, with a thick wall and septations, inseparable from the ovary**<br>• **T1WI:** Iso- to hypointense<br>• **T2WI:** Hyperintense pus-filled fallopian tube and/or abscess with intermediate-to-hypointense thick wall<br>• **DWI:** Diffusion restriction due to pus<br>• **CE:** Avidly enhancing wall, folds, and septations |

**Note:--Abbreviations:** ART, assisted reproductive technology; CE, contrast-enhanced; DWI, diffusion-weighted imaging; FSH, follicle-stimulating hormone; IUD, intrauterine device; LH, luteinizing hormone; T1WI, T1-weighted imaging; T2WI, T2-weighted imaging; SI, signal intensity; TOA, tubo-ovarian abscess; STD, sexually transmitted disease

**References: 19, 38-42**

**Table S3. Physiologic and other common benign observations of the uterine corpus and cervix at female pelvic MRI**

| UTERINE CORPUS | |
|---|---|
| **Endometrium** | |
| **Pertinent information**<br>• **Two layers of the endometrium**<br>  ○ Basal layer<br>  ▪ Serves as the supporting layer and is adherent to the myometrium<br>  ▪ Responsible for regenerating the endometrium after each cycle<br>  ▪ Persists after menopause<br>  ○ Functional layer<br>  • Overlies the basal layer<br>  • Grows in response to hormones, preparing the endometrium for implantation<br>  • Sloughs off during the menstrual phase unless pregnancy occurs<br>  • Disappears after menopause | **MRI features**<br>• **Best measured on the mid-sagittal plane**<br>• **Normal thickness varies with menopausal status and the phase of menstrual cycle**<br>• **In symptomatic postmenopausal patients, smooth homogenous endometrial thickness up to 4 mm excludes significant abnormality and indicates atrophy**<br>• **T1WI:** T1-iso to hypointense<br>• **T2WI:** Uniformly T2-hyperintense due to mucin-rich endometrial glands<br>• **DWI:** No diffusion restriction<br>• **CE:** Initially enhances less than the myometrium and then similar to the myometrium |
| **Junctional zone** | |
| **Pertinent information**<br>• **Inner myometrium** with densely packed smooth muscles and low water content | **MRI features**<br>• **T2-hypointense subendometrial band**<br>• **Thickness is best measured on the mid-sagittal image along the long axis of the uterus**<br>• **May be unable to delineate after the menopause**<br>• **T1WI:**<br>  ○ T1-iso to hypointense<br>• **T2WI**<br>  ○ T2-hypointense subendometrial band<br>  ○ Normal thickness is up to 8 mm (or up to 11 mm if no microcysts are present)<br>• **DWI**<br>  ○ No diffusion restriction<br>• **CE**<br>  ○ Variable enhancement |
| **Common benign conditions, best recognized on T2WI** | |
| **Endometrial Hyperplasia** | |
| **Pertinent information** | **MRI features**<br>• **Endometrial thickening: >16 mm premenopause and >4 mm** |

Back

| | |
|---|---|
| • **Abnormal proliferation of endometrial glands with an excess of glands relative to stroma**<br>  ○ May be diffuse or focal<br>• **Two types**<br>  ○ Endometrial hyperplasia without cellular atypia<br>  • Very low risk of associated EC<br>  ○ Endometrial hyperplasia with cellular atypia<br>  ▪ Up to 25% risk of associated EC<br>• **Symptoms**<br>  ○ Abnormal uterine bleeding, postmenopausal bleeding<br>• **Etiology**<br>  ○ Hyper-estrogenic state<br>  ▪ Obesity<br>  ▪ Chronic anovulation<br>  ▪ Tamoxifen use<br>  ▪ Estrogen-secreting tumors<br>  ▪ Exogenous estrogen use | **postmenopause with abnormal uterine bleeding**<br>• **T1WI**<br>  ○ T1-iso to hypointense<br>• **T2WI**<br>  ○ Lower T2-SI than normal endometrium with a smooth endometrium-myometrium interface<br>  ○ ± T2-hyperintense cystic foci<br>• **DWI**<br>  ○ Varies depending on the degree of atypia<br>• **CE**<br>  ○ EH without atypia: Enhances similar to normal endometrium<br>  ○ EH with atypia: May show enhancement pattern similar to EC with hypo-enhancement relative to the myometrium across all post-contrast phases |
| **Endometrial polyp** | |
| **Pertinent information**<br>• **Hyperplastic growth of endometrial glands and stroma**<br>  ○ Can be pedunculated or sessile<br>• **Symptoms**<br>  ○ Asymptomatic or associated with abnormal uterine bleeding (pre- or postmenopause)<br>• **Etiology**<br>  ○ Hyper-estrogenic state<br>  ▪ Obesity<br>  ▪ Chronic anovulation<br>  ▪ Tamoxifen use<br>  ▪ Estrogen-secreting tumors<br>  ▪ Exogenous estrogen use | **MRI features**<br>• **Pedunculated or sessile focal often oval endometrial lesion**<br>• **Intracavitary LMs are often larger and more round with broader base of attachment and continuity with the myometrium**<br>• **May be indistinguishable from or co-exist with early endometrial cancer**<br>• **T1WI**<br>  ○ T1-iso to hypointense<br>• **T2WI**<br>  ○ Central T2-hypointense fibrovascular core<br>  ○ Peripheral T2-hyperintense foci from dilated endometrial glands<br>• **DWI**<br>  ○ No diffusion restriction<br>• **CE**<br>  ○ Avidly enhancing central fibrovascular core; ≥ myometrium<br>  ○ May see lace-like enhancement of dilated endometrial glands |
| **Adenomyosis and Adenomyoma** | |
| **Pertinent information** | **MRI features** |

| | |
|---|---|
| • **Ectopic endometrial glands and stroma within the inner myometrium, accompanied by reactive smooth muscle proliferation**<br>• **Risk factors**<br>  ○ More common in multiparous women.<br>• **Can be diffuse or focal**<br>  ○ Adenomyoma is a rare focal mass-like form<br>• **Symptoms**<br>  ○ Abnormal uterine bleeding, dysmenorrhea, pelvic pain | • **Thickened JZ**<br>• **T1WI**<br>  ○ ± T1-hyperintense foci from hemorrhage in the ectopic endometrial glands<br>• **T2WI**<br>  ○ JZ thickness ≤8 mm excludes adenomyosis<br>  ○ Direct signs of adenomyosis<br>  ▪ T2-hyperintense microcysts in the JZ represent dilated ectopic endometrial glands; in the presence of microcysts adenomyosis is diagnosed when JZ thickness is 9-11 mm<br>  ▪ Adenomyoma, a rare mass-like collection of endometrial glands in the myometrium<br>  ▪ Both LM and adenomyomas appear as T2-hypointense lesions<br>  ▪ Unlike LM, adenomyomas are less well-defined, contain T2-hyperintense microcysts, lack enlarged vessels along their periphery, and exert minimal mass-effect on the endometrium<br>  ○ Indirect sign of adenomyosis<br>  ▪ Thickening of the JZ ≥12 mm is considered diagnostic and is caused by the reactive smooth muscle proliferation<br>• **DWI**<br>  ○ No diffusion restriction with SI lower than endometrium on high b-value DWI<br>• **CE**<br>  ○ Variable heterogenous enhancement |
| **Transient myometrial contraction** | |
| **Pertinent information**<br>• **Transient physiologic phenomenon, usually observed in younger women** | **MRI features**<br>• **Transient ill-defined myometrial bulge, deforms endometrium more than outer myometrium**<br>• **T1WI**<br>  ○ T1-iso-to-hypointense<br>• **T2WI**<br>  ○ Transient, ill-defined T2-hypointense myometrial bulge that resolves during the same exam or on subsequent exams<br>  ○ Deforms the endometrium more than the outer uterine contour |

| | |
|---|---|
| | • **DWI**<br>  ○ No diffusion restriction<br>• **CE**<br>  ○ Enhances similar to the uninvolved myometrium |
| **CERVIX** | |
| **Common benign conditions, best recognized on T2WI** | |
| **Nabothian cysts and Tunnel Clusters** | |
| **Pertinent information**<br>• **Mucinous retention cyst resulting from obstruction of endocervical glands**<br>• **Tunnel clusters: a subtype of Nabothian cyst**<br>  ○ More commonly observed in multiparous women | **MRI features**<br>• **Nabothian cyst: Typically, a unilocular cyst in the superficial cervical stroma (inner half)**<br>• **Tunnel clusters: Often a multilocular cyst extending deep into the cervical stroma (outer half)**<br>• **T1WI**<br>  ○ ± T1-hyperintense due to mucin<br>• **T2WI**<br>  ○ Nabothian cyst: T2-hyperintense unilocular cyst in the superficial cervical stroma<br>  ○ Tunnel clusters: T2-hyperintense multi-locular cyst in the deep cervical stroma<br>• **DWI**<br>  ○ No diffusion restriction<br>• **CE**<br>  ○ No enhancing solid tissue |

**Note:--Abbreviations**: CE, contrast-enhanced; DWI, diffusion-weighted imaging; EC, endometrial cancer; EH, endometrial hyperplasia; JZ, junctional zone; LM, Leiomyoma; T1WI, T1-weighted imaging; T2WI, T2-weighted imaging
**References:** 38, 44-49

**Table S4. Physiologic and other common benign observations of the vagina, vulva, and urethra at female pelvic MRI**

| VAGINA, VULVA, URETHRA | |
|---|---|
| **Common benign conditions, best recognized on T2WI** | |
| **Gartner duct cyst** | |
| • **Incomplete involution of the Wolffian ducts**<br>• **Associated with renal anomalies**<br>  ○ Agenesis, dysplasia, or crossed-fused ectopia<br>• Often asymptomatic unless large or infected | **MRI features**<br>• **Unilocular cyst located in anterolateral vaginal wall at or above the pubic symphysis**<br>• **T1WI:** Hypointense unless hyperintense due to hemorrhage or proteinaceous content<br>• **T2WI:** Hyperintense due to simple fluid unless hemorrhagic or proteinaceous<br>• **DWI:** No diffusion restriction<br>  ○ Restricted diffusion possible if fluid is complex<br>• **CE:** Smooth enhancing wall unless infected |
| **Bartholin cyst** | |
| • **Obstruction of a Bartholin gland** resulting in the accumulation of mucinous secretions<br>• Often asymptomatic unless large or infected | **MRI features**<br>• **Unilocular cyst located in posterolateral vaginal wall at or below the pubic symphysis**<br>• **T1WI:** Hypointense unless hyperintense due to hemorrhage or proteinaceous content<br>• **T2WI:** Hyperintense due to simple fluid unless hemorrhagic or proteinaceous<br>• **DWI:** No diffusion restriction<br>  ○ Restricted diffusion possible if fluid is complex<br>• **CE:** Smooth enhancing wall unless infected |
| **Skene duct cyst** | |
| • **Obstruction of the Skene glands**<br>  ○ Small periurethral glands located on either side of the lower urethra | **MRI features**<br>• **Unilateral or bilateral small unilocular cysts located inferior to the pubic symphysis, anterior to the vagina, and lateral to the lower urethra**<br>• **T1WI:** Hypointense unless hyperintense due to hemorrhage or proteinaceous content<br>• **T2WI:** Hyperintense due to simple fluid unless hemorrhagic or proteinaceous<br>• **DWI:** No diffusion restriction<br>  ○ Restricted diffusion possible if fluid is complex<br>• **CE:** Smooth enhancing wall |
| **Urethral diverticulum** | |

Back

| | |
|---|---|
| • **Focal outpouching of the urethra**<br>• **Common symptoms**<br>  ○ Recurrent urinary tract infections, dysuria, and postvoid dribbling | **MRI features**<br>• **Typically presents as a unilocular cystic lesion with a saddlebag appearance wrapping around the urethra, often with a neck connecting to the mid to distal urethra**<br>• **T1WI:** Hypointense<br>• **T2WI:** Hyperintense due to simple fluid; may show thin septations or occasional hypointense stones<br>• **DWI:** No diffusion restriction<br>• **CE:** Smooth enhancing wall unless infected<br>  ○ Enhancing solid tissue raises concern for adenocarcinoma arising in a diverticulum |

**Note:--Abbreviations**: CE, contrast-enhanced; DWI, diffusion-weighted imaging; T1WI, T1-weighted imaging; T2WI, T2-weighted imaging

**References**: 51-53

**Table S5. Most common gynecologic conditions presenting as T1-hyperintense lipid-containing lesions at female pelvic MRI, organized by their origin.**

| | | |
|---|---|---|
| **O V A R I A N** | **Mature Teratoma (Dermoid)** | |
| | **Pertinent Information**<br>● **Age**<br>○ Premenopause<br>● **Benign**<br>● **Most common OGCT**<br>● 10% bilateral<br>● **0.2–2% risk of malignant degeneration**<br>○ Older women<br>○ Squamous cell carcinoma >80% | **MRI features**<br>● **Lipid-containing cystic lesion (bilateral in ~10% of cases)**<br>● **T1WI**<br>○ Macroscopic fat<br>▪ T1-hyperintense with signal loss on fat-saturated images<br>▪ India ink artifact on out-of-phase images<br>○ Microscopic fat<br>▪ Signal loss on out-of-phase images<br>○ May contain T1-hypointense areas due to tooth-like calcifications, hair, or fibrous tissue<br>● **T2WI**<br>○ Variable appearance<br>● **DWI**<br>○ May show diffusion restriction due to complex contents<br>▪ Does not indicate malignancy unless there is enhancing solid tissue that exceeds the expected amount for a Rokitansky nodule<br>● **CE**<br>○ May show small solid tissue (Rokitansky nodule)<br>▪ Does not indicate malignancy<br>○ Increased risk of malignancy after menopause<br>▪ Enhancing solid tissue, often with transmural extension |
| | **Immature Teratoma** | |
| | **Pertinent Information**<br>● **Age**<br>○ Women <30 years<br>● **Malignant**<br>● **2nd most common malignant OGCT after dysgerminoma**<br>● **Tumor markers**<br>○ ± AFP (50%)<br>○ ± LDH<br>● **Associations**<br>○ Uni- or contralateral dermoid | **MRI features**<br>● **Large cystic lesion with enhancing solid tissue and small, dispersed foci of lipid**<br>● **T1WI**<br>○ Small, dispersed foci of lipid (smaller than in mature teratoma)<br>▪ T1-hyperintense with signal loss on fat-saturated images<br>▪ India ink artifact on out-of-phase images<br>● **T2WI**<br>○ Cystic component: Simple fluid<br>○ Solid component: T2-intermediate<br>● **DWI**<br>○ Diffusion restriction in enhancing solid tissue<br>● **CE** |

Back

| | | |
|---|---|---|
| | | ○ Enhancing solid tissue |
| **U T E R I N E** | **Lipoleiomyoma** | |
| | **Pertinent Information**<br>● **Age**<br>○ Postmenopause<br>● **Benign**<br>● **A subtype of LM**<br>● Adipose tissue arises from smooth muscle metaplasia | **MRI features**<br>● **Well-circumscribed myometrial lesion with adipose tissue and smooth muscle**<br>● **T1WI**<br>○ Fat component<br>▪ T1-hyperintense with signal loss after fat saturation<br>▪ India ink artifact on out-of-phase images<br>○ Smooth muscle component: T1-hypointense<br>● **T2WI**<br>○ Fat component: T2-hyperintense<br>○ Smooth muscle component: T2-hypointense<br>● **DWI**<br>○ No diffusion restriction<br>● **CE**<br>○ Enhancing smooth muscle component |

**Note:--Abbreviations:** AFP, alpha-fetoprotein; CE, contrast-enhanced; DWI, diffusion-weighted imaging; LDH, lactate dehydrogenase; LM, leiomyoma; OGCT, ovarian germ cell tumor; SI, signal intensity; T1WI, T1-weighted imaging; T2WI, T2-weighted imaging
**References**: 19, 57, 60-64

**Table S6. T1 and T2 signal intensity of blood products as a function of their age.**

| Time interval | Composition | T1 signal intensity | T2 signal intensity |
|---|---|---|---|
| Acute | Deoxyhemoglobin | Iso or hypointense 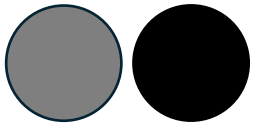 | Hypointense  |
| Early subacute | Intracellular methemoglobin | Hyperintense 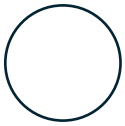 | Hyperintense 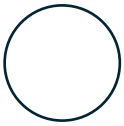 |
| Late subacute | Extracellular methemoglobin | Hyperintense 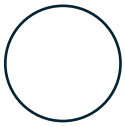 | Hypointense  |
| Chronic | Hemosiderin | Hypointense  | Hypointense  |

**Reference**: 19

Back

**Table S7. Most common gynecologic conditions presenting as T1-hyperintense blood-containing lesions without solid tissue at female pelvic MRI, organized by their origin.**

| | | |
|---|---|---|
| **OVARIAN** | **Endometrioma** | |
| | **Pertinent Information**<br>● **Age**<br>○ Premenopause<br>● **Common manifestation of endometriosis**<br>● **Blood products of varying ages resulting from repeated cyclical bleeding episodes**<br>● Can coexist with other features of endometriosis, including:<br>○ Deep endometriosis<br>○ Hematosalpinx | **MRI features**<br>● **Multifocal, often bilateral unilocular or multilocular cysts with chronic blood products; persist over time; associated with other features of endometriosis**<br>● **T1WI**<br>○ Homogenous and markedly T1-hyperintense signal that persists after fat saturation<br>● **T2WI**<br>○ Graded or diffuse T2-hypointense (T2 shading)<br>○ T2-hypointense wall due to fibrosis and hemosiderin (high specificity)<br>○ May show intralesional T2-dark spots due to chronic blood clots (high specificity)<br>● **DWI**<br>○ May show diffusion restriction due to endometriotic fluid<br>▪ Does not indicate malignancy unless enhancing solid tissue is present<br>● **CE**<br>○ Subtraction postcontrast images are essential to evaluate for solid tissue<br>▪ If present, can indicate malignant transformation<br>○ Smooth wall enhancement |
| | **Hemorrhagic cyst** | |
| | **Pertinent Information**<br>● **Age**<br>○ Premenopause<br>● **Blood products from a single bleeding episode** | **MRI features**<br>● **Unilateral, unilocular cyst with heterogenous variable signal on T1WI and T2WI, depending on the age of hemorrhage; usually decreases or resolves within 2–3 months**<br>○ If ≤3 cm, physiologic observation<br>● **T1WI**<br>○ Variable and heterogenous signal dependent on the age of hemorrhage<br>● **T2WI**<br>○ Variable and heterogenous signal dependent on the age of hemorrhage<br>● **DWI**<br>○ May show diffusion restriction due to hemorrhagic fluid |

Back

| | | |
|---|---|---|
| | | • **CE**<br>○ Subtraction postcontrast images show no solid tissue<br>○ Smooth wall enhancement |
| **PARA-OVARIAN** | **Hematosalpinx** | |
| | **Pertinent Information**<br>• **Age**<br>○ Variable<br>• **Dilated fallopian tube filled with blood**<br>• **Causes**<br>○ Endometriosis<br>○ Obstructive congenital conditions<br>○ Pelvic inflammatory disease<br>○ Ectopic pregnancy | **MRI features**<br>• **Blood-filled tubular adnexal structure**<br>• **T1WI**<br>○ Tubular T1-hyperintense adnexal structure, with T1-hyperintense signal persisting after fat saturation<br>• **T2WI**<br>○ Variable signal<br>○ May show T2-hypointense signal (T2-shading) if there is chronic hemorrhage<br>• **DWI**<br>○ May show diffusion restriction due to hemorrhagic fluid<br>• **CE**<br>○ Smooth wall enhancement |
| **UTERINE** | **Leiomyomas with red or cavernous degeneration** | |
| | **Pertinent information**<br>• **Age**<br>○ Usually, premenopause<br>• **Red or cavernous degeneration from a hemorrhagic infarction**<br>○ Pregnancy<br>○ Oral contraceptives<br>○ Uterine artery embolization<br>• **Asymptomatic or pelvic pain** | **MRI features**<br>• **Well-circumscribed myometrial lesion**<br>• **T1WI**<br>○ Diffusely or rim-like T1-hyperintense<br>• **T2WI**<br>○ Diffusely or rim-like T2-hypointense<br>• **DWI**<br>○ May show diffusion restriction due to hemorrhage<br>• **CE**<br>○ Subtraction postcontrast images are essential for diagnosis and show no enhancing solid tissue<br>▪ If enhancing solid tissue is present, differentiation from malignancy, most commonly leiomyosarcoma, is critical |
| | **Accessory Cavitary Uterine Mass (ACUM)** | |
| | **Pertinent information**<br>• **Age**<br>○ Typically, <30 years<br>• **Rare congenital Müllerian anomaly**<br>○ Non-communicating cavity lined by the functional endometrium and filled with chronic blood products. The cavity is surround by the smooth-muscles and located | **MRI features**<br>• **Well-circumscribed blood-filled cavity with smooth muscle wall, located in the uterus at the round ligament insertion**<br>• **T1WI**<br>○ Centrally T1-hyperintense (blood-filled cavity); peripherally T1-intermediate wall (smooth muscle)<br>• **T2WI**<br>○ Centrally T2-shading |

| | | |
|---|---|---|
| | in the myometrium at the round ligament attachment site<br>• **Symptoms: chronic pelvic pain, dysmenorrhea, infertility**<br>• **Laparoscopic surgical excision** is the definitive treatment to relive symptoms | ○ Peripherally, T2-indetermiate to hypointense wall<br>• **DWI**<br>○ May show diffusion restriction due to hemorrhage<br>• **CE**<br>○ Smooth wall enhancement |
| | **Hematometra, hematocolpos, or hematometrocolpos** | |
| | **Pertinent information**<br>• **Age**<br>○ Variable<br>• **Blood-filled dilated endometrial cavity, vagina, or both**<br>• **Causes**<br>○ Congenital Müllerian duct anomalies<br>▪ Present at puberty<br>○ Imperforated hymen<br>▪ Present at puberty<br>○ Cloacal malformation<br>○ Cervical or vaginal stenosis due to scarring<br>○ Obstructing tumor | **MRI features**<br>• **Dilated blood-filled endometrial cavity and/or vagina**<br>• **T1WI**<br>○ T1-hyperintense signal that persists after fat saturation if there is chronic hemorrhage<br>• **T2WI**<br>○ May show T2-hypointense (T2-shading) if there is chronic hemorrhage<br>• **DWI**<br>○ May show diffusion restriction due to hemorrhage<br>• **CE**<br>○ Subtraction postcontrast images are essential to exclude enhancing solid tissue as the cause of hemorrhage |

**Note:--Abbreviations:** CE, contrast-enhanced; DWI, diffusion-weighted imaging; LM, leiomyoma; T1WI, T1-weighted imaging; T2WI, T2-weighted imaging
**References:** 10, 19, 39, 44, 64-68

**Table S8. Most common gynecologic conditions presenting as cysts (simple or proteinaceous fluid) without solid tissue at female pelvic MRI, organized by their origin.**

| | | |
|---|---|---|
| **OVARIAN** | **Serous cystadenoma** | |
| | **Pertinent Information**<br>● **Age**<br>○ Pre- and postmenopause<br>● **The most common benign epithelial ovarian tumor, lined with tubal-type epithelium** | **MRI features**<br>● **Unilateral or bilateral simple unilocular cyst with occasional thin septa; persist over time, unlike premenopausal functional ovarian cysts that resolve over time**<br>● **T1WI**<br>○ T1-hypointense<br>● **T2WI**<br>○ Unilocular cyst with T2-hyperintense (simple) fluid<br>○ Occasional thin septa<br>● **DWI**<br>○ No diffusion restriction<br>● **CE**<br>○ Smooth wall enhancement |
| | **Mucinous cystadenoma** | |
| | **Pertinent Information**<br>● **Age**<br>○ Pre- and postmenopause<br>● **Benign epithelial tumors lined with mucinous gastrointestinal-type epithelium**<br>● **10% occur with a mature teratoma or Brenner tumor**<br>● **Large and unilateral**<br>○ If bilateral and/or smaller (<10 cm), consider ovarian metastases | **MRI features**<br>● **Large unilateral multilocular cyst with locules of variable SI, resembling stained glass**<br>● **T1WI**<br>○ Multilocular cyst with locules of variable SI<br>▪ T1-hyperintense due to mucin<br>● **T2WI**<br>○ Multilocular cyst with locules of variable SI<br>▪ T2-hypointense due to mucin<br>● **DWI**<br>○ No diffusion restriction except when there is high-viscosity mucin<br>● **CE**<br>○ Enhancement of the smooth wall and septa |
| | **Hydrosalpinx** | |

Back

| | | |
|---|---|---|
| **PARA-OVARIAN** | **Pertinent information**<br>● **Age**<br>○ Pre- or postmenopause<br>● **Dilated FT filled with fluid due to obstruction at the fimbriated end**<br>● **Causes**<br>○ PID<br>○ Less common<br>▪ Endometriosis<br>▪ Adhesions from surgery<br>▪ Tumor | **MRI features**<br>● **Dilated, fluid-filled, C- or U-shaped tubular structure with a smooth wall and incomplete septa (endosalpingeal folds), separate from the uterus and ovaries**<br>● **T1WI**<br>○ T1- hypointense<br>● **T2WI**<br>○ T2-hyperintese tubular structure with thin wall and incomplete septa (endosalpingeal folds)<br>● **DWI**<br>○ No diffusion restriction<br>● **CE**<br>○ Enhancement of smooth wall and incomplete septa (endosalpingeal folds) |
| | **Para-ovarian cyst** | |
| | **Pertinent information**<br>● **Age**<br>○ Pre- or postmenopause<br>● **Located within the mesosalpinx** | **MRI features**<br>● **Unilocular simple cyst adjacent to but separate from the uterus and ovary**<br>● **T1WI**<br>○ T1- hypointense (simple) fluid<br>○ May show variable T1-SI after hemorrhage<br>● **T2WI**<br>○ T2-hyperintense (simple) fluid<br>○ Variable T2-SI after hemorrhage<br>● **DWI**<br>○ No diffusion restriction unless hemorrhage is present<br>● **CE**<br>○ Smooth wall enhancement |
| | **Peritoneal Inclusion Cyst** | |
| | **Pertinent Information**<br>● **Age**<br>○ Premenopausal (most common)<br>● **Asymptomatic or associated with pelvic pain**<br>● **Benign**<br>○ Results from prior peritoneal insult, resulting in reactive proliferation, adhesions, and impaired fluid absorption in the presence of active ovaries<br>○ Surgery<br>○ Trauma<br>○ PID | **MRI features**<br>● **Cystic lesion with septations (caused by adhesions), conforming to the peritoneal cavity shape, with the ovary suspended centrally or at the margin**<br>● **T1WI**<br>○ T1-hypointense (simple) fluid<br>○ May show variable T1-SI within locules after hemorrhage<br>● **T2WI**<br>○ T2-hyperintense (simple) fluid<br>○ May show variable T2-SI within locules after hemorrhage<br>● **DWI** |

| | | |
|---|---|---|
| | ○ Endometriosis | ○ No diffusion restriction except in hemorrhagic locules<br>● **CE**<br>○ Smooth wall and septal enhancement |
| **UTERINE** | **Nabothian cysts (tunnel clusters)** | |
| | See **Table S3** | See **Table S3** |

**Note:--Abbreviations:** CE, contrast-enhanced; DWI, diffusion-weighted imaging; FT, fallopian tube; T1WI, T1-weighted imaging; T2WI, T2-weighted imaging; PID, pelvic inflammatory disease; SI, signal intensity
**References:** 36, 39, 69-71

**Table S9. Most common gynecologic conditions presenting as cystic or solid lesions with dark-T2/dark-DWI solid tissue at female pelvic MRI, organized by their origin**

| | | |
|---|---|---|
| **OVARIAN** | **Fibroma (fibrothecoma)** | |
| | **Pertinent Information**<br>• **Age**<br>  ○ Middle-aged women<br>• **Most common sex-cord stromal tumor, benign**<br>• **Fibrous tissue and theca cells**<br>  ○ Theca cell can secrete estrogen, resulting in endometrial polyps, hyperplasia and/or carcinoma<br>• **Meigs syndrome (rare)**<br>  ○ Pleural effusions<br>  ○ Ascites<br>  ○ Ovarian mass (most commonly a fibroma)<br>• **Unilateral**<br>  ○ If bilateral, consider Gorlin (basal cell nevus) syndrome | **MRI features**<br>• **Typically, a unilateral, well-circumscribed solid lesion with dark-T2/dark-DWI solid tissue, showing a T2-blackout pattern; careful evaluation of the endometrium is recommended to assure the absence of concurrent endometrial hyperplasia or endometrial cancer.**<br>• **T1WI**<br>  ○ T1-iso to hypointense<br>• **T2WI**<br>  ○ T2-hypointense similar to skeletal muscle<br>  ○ Larger lesions may show T2-hyperintense areas due to edema and cystic change<br>• **DWI**<br>  ○ Hypointense on both DWI and ADC map<br>• **CE**<br>  ○ Mild progressive enhancement |
| | **Brenner tumor** | |
| | **Pertinent Information**<br>• **Uncommon epithelial-stromal tumor, most are benign**<br>  ○ Composed of fibrous stroma with calcifications and transitional cells<br>  ○ Most are unilateral and nearly always benign<br>• **May coexist with other epithelial tumors, most commonly mucinous cystadenoma** | **MRI features**<br>• **Unilateral, small (<5 cm), well-circumscribed solid lesion with dark-T2/dark-DWI solid tissue, showing a T2-blackout pattern; calcifications on CT (~50%)**<br>• **T1WI**<br>  ○ T1-iso to hypointense<br>• **T2WI**<br>  ○ T2-hypointense similar to skeletal muscle<br>  ○ May be associated with a mucinous cystadenoma<br>• **DWI**<br>  ○ Hypointense on both DWI and ADC map<br>• **CE**<br>  ○ Mild progressive enhancement |
| | **Cystadenofibroma** | |
| | **Pertinent Information**<br>• **Age**<br>  ○ Pre- or postmenopause | **MRI features** |

Back

| | | |
|---|---|---|
| | • **Benign epithelial ovarian tumor with fibrous stroma**<br>• Asymptomatic or non-specific symptoms<br>• Unilateral | • **Unilocular or multilocular cystic lesion with dark-T2/dark-DWI solid tissue and a T2 blackout pattern**<br>• **T1WI**<br>  ○ T1-iso to hypointense<br>• **T2WI**<br>  ○ T2-hyperintense cystic component<br>  ○ T2-hypointense solid tissue<br>  ▪ Occasionally with interspersed tiny cystic foci, known as "black-sponge"<br>• **DWI**<br>  ○ Hypointense solid tissue on both DWI and ADC map<br>• **CE**<br>  ○ Slow, progressive enhancement of solid tissue |
| **UTERINE** | **Leiomyoma** | |
| | **Pertinent Information**<br>• **Age**<br>  ○ Variable<br>• **Most common gynecologic and uterine neoplasms**<br>  ○ Lifetime prevalence 70%; higher in black and brown women<br>• **Benign smooth muscle tumors**<br>• **Causes**<br>  ○ Hormonally driven; enlarge before menopause and regress after<br>  ○ Hereditary leiomyomatosis and renal cell carcinoma syndrome<br>• **Most common form**<br>  ○ Conventional, 80–90% LM<br>• **Most common degeneration**<br>  ○ Hyalinization, 60% | **MRI features**<br>• **Single or multiple well-circumscribed solid lesion(s), with dark-T2/dark-DWI solid tissue, showing a T2-blackout pattern*****<br>• **T1WI**<br>  ○ T1-iso to hypointense<br>• **T2WI**<br>  ○ Uniformly T2-hypointense, similar to skeletal muscle*<br>  ○ May show T2-hyperintense rim due to edema<br>• **DWI**<br>  ○ Hypointense on both DWI and ADC map<br>• **CE**<br>  ○ Conventional LM<br>  ▪ Early avid enhancement, similar to the myometrium<br>  ○ Hyalinized LM<br>  ▪ Enhances less than the myometrium<br>***Note: Non-dark T2/non-dark DWI solid tissue can be seen with histologic variants or certain types of degeneration. In such cases, follow the algorithmic approach outlined in section "Cystic or Solid Lesions with Non-Dark T2/Non-Dark DWI Solid Tissue; non-adnexal lesions". |
| | **Deep Endometriosis** | |

| | | |
|---|---|---|
| **PARA-UTERINE/OVARIAN** | **Pertinent information**<br>• **Age**<br>  ○ Most common in premenopausal women<br>• **Most severe form of endometriosis**<br>• **Multifocal, predominantly in the pelvis**<br>• **Most common sites**<br>  ○ Uterosacral ligaments/torus uterinus<br>  ○ Rectosigmoid colon<br>  ○ Posterior uterine surface<br>  ○ Posterior vaginal fornix<br>  ○ Round ligaments<br>  ○ Urinary bladder<br>  ○ Ovarian surface<br>• **Look for other features of endometriosis**<br>  ○ Endometriomas<br>  ○ Hematosalpinx | **MRI features**<br>• **Dark-T2/dark-DWI thickening, stellate or smooth nodules, or infiltration; can tether adjacent structures and cause architectural distortion**<br>• **T1WI**<br>  ○ T1 iso- to hypointense<br>  ○ May contain T1-hyperintense foci that persist after fat saturation<br>  ▪ Hemorrhage in ectopic endometrial glands<br>• **T2WI**<br>  ○ T2-hypointense thickening, stellate or smooth nodules, or infiltration; may see tethering and architectural distortion<br>  ▪ Uterine retroflexion and/or lateral deviation<br>  ▪ Adenomyosis-like infiltration of the myometrium with an outside-in pattern of involvement, sparing the junctional zone<br>  ▪ Bowel angulation<br>  ▪ “Kissing ovaries” (touching ovaries situated posterior to the uterus)<br>  ○ May contain T2-hyperintense foci<br>  ▪ Ectopic endometrial glands<br>• **DWI**<br>  ○ Hypointense on both DWI and ADC map, except in areas with hemorrhage<br>• **CE**<br>  ○ Mild slow progressive enhancement, typically due to fibrosis<br>  ○ More avid enhancement may be seen with inflammation |

**Note:--Abbreviations:** CE, contrast-enhanced; CT, computed tomography DWI, diffusion-weighted imaging; LM, leiomyoma; SI, signal intensity; T1WI, T1-weighted imaging; T2WI, T2-weighted imaging
**References:** 10, 36, 64, 72-74

**Table S10. Most common gynecologic conditions presenting as cystic or solid lesions with non-dark T2/non-dark DWI soft tissue at female pelvic MRI, organized by their origin from the adnexa**

| | | |
|---|---|---|
| | **Dysgerminoma** | |
| | **Pertinent Information**<br>• **Age**<br>  ○ <30 years<br>• **Most common malignant OGCT; ovarian counterpart of testicular seminoma**<br>• **Tumor markers**<br>  ○ Elevated LDH<br>  ○ Rarely, β-hCG<br>• **Unilateral, with up to 10% bilateral** | **MRI features**<br>• **Unilateral non-dark T2/non-dark DWI solid lesion, divided into lobules by fibrovascular septa**<br>• **T1WI**<br>  ○ T1-iso-to-hypointense<br>• **T2WI**<br>  ○ T2-intermediate solid lesion, divided into lobules by T2-hypointense fibrovascular septa<br>• **DWI**<br>  ○ Diffusion restriction: hyperintense on high b-value DWI and hypointense on the ADC map<br>• **CE**<br>  ○ Enhancing solid lesion with avidly enhancing fibrovascular septa |
| | **Sertoli and Sertoli–Leydig cell tumors** | |
| | **Pertinent Information**<br>• **Age**<br>  ○ Typically, <30 years<br>• **Sex-cord stromal tumor**<br>  ○ Can be benign or malignant<br>• **Most common ovarian tumor associated with increased testosterone** resulting in<br>  ▪ Virilization<br>  ▪ Oligomenorrhea or amenorrhea | **MRI features**<br>• **Unilateral heterogenous solid lesion with non-dark T2/non-dark DWI solid tissue**<br>• **T1WI**<br>  ○ T1-iso-to-hypointense<br>• **T2WI**<br>  ○ Heterogeneous solid lesion with T2-intermediate solid tissue and occasional small cystic foci<br>• **DWI**<br>  ○ Diffusion restriction: hyperintense on high b-value DWI and hypointense on the ADC map<br>• **CE**<br>  ○ Enhancing solid tissue |
| | **Serous borderline tumor** | |
| | **Pertinent Information**<br>• **Age**<br>  ○ Premenopause<br>• **Most common BT (50–70%)**<br>  ○ All BT: Increased epithelial proliferation and nuclear atypia without stromal invasion | **MRI features**<br>• **Unilateral or bilateral cystic lesions (occasionally solid) with papillary projections; peritoneal implants may be present**<br>• **T1WI**<br>  ○ T1-iso to hypointense<br>• **T2WI**<br>  ○ Unilocular cystic lesion (occasionally solid) with papillary projections |

Back

| | | |
|---|---|---|
| **OVARIAN** | ○ Intermediate step from serous cystadenoma to LGSC<br>○ *BRAF*, *KRAS* mutations<br>• **Types**<br>○ Typical<br>▪ Hierarchical branching papillae with stromal cores<br>○ Micropapillary-cribriform (more aggressive; direct precursor of LGSC)<br>▪ Micropapillae without stromal cores<br>• **Asymptomatic or nonspecific symptoms**<br>• **CA-125 level may be elevated**<br>• **Bilateral tumors and/or peritoneal implants in 30%** | showing intra- or extra-cystic growth, or both<br>▪ **Sea anemone–like appearance is diagnostic:** T2-hyperintense papillary architecture with T2-hypointnese internal branching<br>▪ Small mural nodules<br>• **DWI**<br>○ Moderate-to-high SI on DWI and relatively high SI on the ADC map<br>• **CE**<br>○ Enhancing solid tissue |
| | **Mucinous borderline tumor** | |
| | **Pertinent Information**<br>• **Age**<br>○ Premenopause<br>• **2nd most common subtype of BT, after serous BT**<br>○ No stromal invasion<br>○ Gastrointestinal differentiation<br>○ Intermediate step from mucinous cystadenoma to mucinous carcinoma<br>○ *KRAS* mutations<br>• Asymptomatic or nonspecific symptoms<br>• **CA19-9 level may be elevated**<br>• **May be associated with mature teratoma or Brenner tumor**<br>• **Unilateral and large; If bilateral and small (<10 cm), should consider ovarian metastases** | **MRI features**<br>• **Large unilateral multilocular cystic lesions with locules of variable SI; cystadenomas, BTs, and carcinomas may overlap in their imaging appearance**<br>• **T1WI**<br>○ Multilocular cystic lesion with locules of variable SI due to mucin<br>• **T2WI**<br>○ Multilocular cystic lesion with locules of variable SI due to mucin<br>○ May see honeycomb locules (microcysts) or T2-intermediate solid tissue (mural nodules, irregular septations, or irregular wall)<br>• **DWI**<br>○ Moderate-to-high SI on DWI and relatively high SI on ADC map<br>• **CE**<br>○ Enhancing solid tissue |
| | **Seromucinous borderline tumor** | |
| | **Pertinent Information**<br>• **Age**<br>○ Premenopause<br>• **Rare subtype of BT**<br>• **This BT type is associated with endometriosis** | **MRI features**<br>• **Similar appearance to serous BT, except for T1-hyperintense blood due to its origin in an endometrioma**<br>• **T1WI** |

| | | |
|---|---|---|
| | ○ Additional BTs associated with endometriosis include<br>▪ Endometroid<br>▪ Clear cell<br>• **Similarly to serous BT, can be bilateral and associated with peritoneal implants** | ○ T1-hyperintense due to chronic hemorrhage<br>• **T2WI**<br>○ T2-hypointense cystic component (T2-shading) due to chronic hemorrhage<br>○ T2-hyperintense papillary architecture with T2-hypointnese internal branching (PA-IB)<br>• **DWI**<br>○ Moderate-to-high SI on DWI and relatively high SI on the ADC map<br>• **CE**<br>○ Enhancing solid tissue |
| | **Granulosa cell tumor** | |
| | **Pertinent Information**<br>• **Age**<br>○ Adult type: postmenopause (most common)<br>○ Juvenile type: <30 years<br>• **Most common malignant sex-cord stromal tumor**<br>• **Most common ovarian tumor, associated with increased estrogen**<br>▪ Abnormal uterine bleeding<br>▪ Endometrial polyps, hyperplasia, and/or carcinoma<br>• **Inhibin-B level may be elevated**<br>• **Prone to late recurrences** | **MRI features**<br>• **Variable in appearance; classically, a unilateral multilocular cystic lesion with non-dark T2/non-dark DWI solid tissue; may have 'sponge-like' appearance due to cystic components, including hemorrhage**<br>• **T1WI**<br>○ T1-iso-to-hypointense with T1-hyperintense hemorrhage<br>• **T2WI**<br>○ Hyperintense cystic portion with fluid-fluid levels if hemorrhage is present and intermediate SI solid tissue<br>○ The endometrium may show thickening and heterogeneous hypo-intense SI due to polyps, hyperplasia, or carcinoma<br>• **DWI**<br>○ Diffusion restriction in solid tissue or hemorrhagic areas<br>• **CE**<br>○ Enhancing solid tissue |
| | **High-grade serous ovarian cancer** | |
| | **Pertinent Information**<br>• **Age**<br>○ Postmenopause<br>• **Prevalence:**<br>○ Accounts for 70% of all ovarian carcinomas<br>○ Most common epithelial ovarian carcinoma<br>• **Classification**<br>○ Primary ovarian, fallopian, and peritoneal carcinomas | **MRI features**<br>• **Often bilateral solid lesions or cystic lesions with solid tissue; frequently associated with peritoneal implants, ascites, and enlarged lymph nodes**<br>• **T1WI**<br>○ T1-iso-to-hypointense<br>• **T2WI**<br>○ Variable SI cystic portion and T2-intermediate solid tissue<br>○ T2-intermediate peritoneal implants |

| | | |
|---|---|---|
| | are grouped due to similar presentation, treatment, and prognosis<br>○ FIGO staging system<br>• **Origin**<br>○ Fimbriated end of the fallopian tube (with serous tubal intraepithelial carcinoma as a precursor lesion)<br>• **Molecular features**<br>○ Ubiquitous *TP53* mutation<br>○ Associated with HBOC syndrome (*BRCA* mutations; see **Table 1**)<br>• **Presentation**<br>○ Typically diagnosed at advanced stages due absent early symptoms and rapid peritoneal spread<br>• **Biomarkers**<br>○ CA-125 level is frequently elevated | ○ T2-hyperintense ascites<br>• **DWI**<br>○ Diffusion restriction in adnexal solid tissue and peritoneal implants<br>○ Hyperintense enlarged lymph nodes<br>• **CE**<br>○ Enhancing adnexal solid tissue, peritoneal implants and enlarged lymph nodes |
| | **Endometriosis-associated malignancy** | |
| | **Pertinent Information**<br>• **Age**<br>○ Pre- or postmenopause<br>• **Prevalence**<br>○ 1% of patients with endometriosis<br>• **Risk factors**<br>○ Long-standing endometrioma<br>○ Estrogen-only hormone replacement therapy<br>• **Most common sites**<br>○ 75% arise from endometrioma<br>○ 25% arise from deep endometriosis, typically in<br>▪ Rectovaginal septum<br>▪ Rectosigmoid colon<br>• **Most common associated tumors**<br>○ Carcinoma<br>• Endometrioid (most common)<br>• Clear cell<br>○ Borderline tumor | **MRI features**<br>• **Cystic lesion with non-dark T2/non-dark DWI solid tissue and variable SI fluid; fluid is less T1-hyperintense and shows less or no T2-shading compared with endometrioma due to hemodilution by secretions from tumor cells; additional imaging findings of endometriosis**<br>• **T1WI**<br>○ Variable T1-SI cystic portion (less T1-hyperintense than endometrioma due to hemodilution by secretions from tumor cells)<br>○ T1-iso-to-hypointense solid tissue<br>• **T2WI**<br>○ Cystic portion<br>▪ Reduction or loss of T2-shading due to hemodilution by secretions from tumor cells<br>▪ T2-intermediate solid tissue<br>• **DWI**<br>○ Diffusion restriction in solid tissue<br>• **CE**<br>○ Subtraction post-contrast images are essential for detecting the presence of solid tissue |

| | | |
|---|---|---|
| | • Seromucous, endometrioid, clear cell<br>• **Classification**<br>○ FIGO staging system | ○ Enhancing solid tissue |
| | **Ovarian metastases** | |
| | **Pertinent Information**<br>• **Age**<br>○ Pre- or postmenopause<br>• **Clinical history**<br>○ Primary malignancy<br>○ Occasionally as initial presentation of occult primary malignancy<br>• **Common primary sites**<br>○ Colon (most common, 30%)<br>○ Endometrial cancer (second most common)<br>○ Gastric, breast, appendix, pancreaticobiliary<br>• **Krukenberg tumors**<br>○ Type of ovarian metastases, accounting for 50% of cases<br>○ Caused by mucin-secreting signet ring cells<br>○ Most common primary sites<br>• Gastric (most common)<br>• Colon<br>• **Clinical presentation**<br>○ Typically, bilateral rapidly growing lesions | **MRI features**<br>• **Bilateral, rapidly growing solid or cystic lesions with non-dark T2/non-dark DWI solid tissue**<br>• **T1WI**<br>○ Variable SI<br>• **T2WI**<br>▪ T2-hyperintense cystic portion due to mucin secreted by tumor cells (Krukenberg tumors)<br>▪ T2-intermediate solid tissue<br>• **DWI**<br>○ Diffusion restriction in solid tissue<br>• **CE**<br>○ Enhancing solid tissue |

**Note:--Abbreviations:** ADC, apparent diffusion coefficient; β-hCG; beta-human chorionic gonadotropin; BT, borderline tumor; CE, contrast-enhanced; DWI, diffusion-weighted imaging; FIGO, the International Federation of Obstetrics and Gynecology; LDH, lactate dehydrogenase; LGSC, low grade serous carcinoma; OGCT, ovarian germ cell tumor; T1WI, T1-weighted imaging; T2WI, T2-weighted imaging; SI, signal intensity.
**References:** 10, 36, 62, 69, 72, 75-78

**Table S11. Most common gynecologic conditions presenting as solid or cystic lesions with non-dark T2/non-dark DWI solid tissue at female pelvic MRI, organized by their origin from non-adnexal structures**

| | | |
|---|---|---|
| U T E R | **Endometrial carcinoma** | |
| | **Pertinent Information**<br>• **Age**<br>○ Typically, postmenopause<br>• **Second most common gynecologic cancer worldwide (after cervical cancer)**<br>• **Main risk factors**<br>○ Hyper-estrogenic state<br>▪ Obesity<br>▪ Early menarche<br>▪ Late menopause<br>▪ Chronic anovulation with polycystic ovary syndrome<br>▪ Tamoxifen<br>○ Lynch syndrome (**Table 1**)<br>• **Symptoms**<br>▪ Abnormal uterine bleeding<br>• **Staged with the 2023 FIGO staging system based on:**<br>○ Traditional anatomic extent<br>○ Pathologic features<br>○ Molecular profiling<br>• **Main histologic subtypes**<br>○ Endometrioid (most common)<br>○ Non-endometrioid | **MRI features**<br>• **Non-dark T2/non-dark DWI solid tissue centered in the endometrium with diffusion restriction**<br>• **Imaging in the sagittal plane and oblique plane (perpendicular to the endometrial cavity) is essential for accurate staging**<br>• **T1WI**<br>○ T1-iso-to-hypointense<br>• **T2WI**<br>○ T2-intermediate; lower than the normal endometrium but higher than the junctional zone<br>• **DWI**<br>○ Diffusion restriction<br>• **CE**<br>○ Usually enhances less than the myometrium on all post-contrast phases<br>○ Images acquired within 60 seconds post-contrast administration may help exclude myometrial invasion by demonstrating smooth, avid enhancement of the junctional zone<br>○ Images acquired 90–120 seconds post-contrast administration provide superior tumor-myometrium contrast for assessing the presence and depth of myometrial invasion<br><br>**Note: Across imaging sequences and planes**<br>• An interruption in the smooth tumor-myometrial inface suggests myometrial invasion; myometrial invasion is classified as superficial if it involves <50% of the myometrial thickness and deep if it involves ≥50%<br>• An interruption in the smooth tumor-cervical stroma interface suggests cervical stromal invasion |
| | **Leiomyosarcoma** | |
| | **Pertinent Information**<br>• **Age** | **MRI features**<br>• **Typically presents as a heterogeneous large solid myometrial lesion with** |

Back page 19

Back page 23

| | | |
|---|---|---|
| I<br>N<br>E | ○ Typically, peri- and postmenopause<br>• **Rare, most common uterine sarcoma**<br>• **Same symptoms as with more common uterine leiomyomas**<br>○ Pelvic pain<br>○ Pelvic pressure<br>○ Abnormal vaginal bleeding<br>• **Growth of a myometrial mass after menopause is highly suspicious for uterine leiomyosarcoma** | **irregular margins (angular margins, soft tissue protrusions), hemorrhage, and necrosis**<br>• **T1WI**<br>○ T1-iso-to-hypointense solid lesion with frequent T1-hyperintense areas due to hemorrhage or hemorrhagic necrosis<br>• **T2WI**<br>○ Heterogenous T2-intermediate solid tissue (excluding hemorrhage and necrosis)<br>• **DWI *****<br>○ Hyperintense enhancing solid tissue (excluding non-enhancing hemorrhage and necrosis) with SI equal to or greater than that of the endometrium or lymph nodes<br>○ ADC of enhancing solid tissue (excluding non-enhancing hemorrhage and necrosis) ≤$0.9\times10^{-3}$ $mm^2/s$<br>• **CE**<br>○ Enhancing solid lesion with frequent central necrosis<br><br>*** Cellular leiomyomas may show diffusion restriction with ADC ≤$0.9\times10^{-3}$ $mm^2/s$. However, unlike leiomyosarcomas, they are typically well-circumscribed, homogeneous T2-intermediate solid masses without hemorrhage or necrosis |
| | **Cervical carcinoma (excluding gastric-type adenocarcinoma subtype)** | |
| | **Pertinent Information**<br>• **Age**<br>○ Pre- or postmenopause<br>• **The most common gynecologic cancer worldwide and fourth most common cancer in women worldwide**<br>• **Main risk factors**<br>○ Chronic HPV infection<br>○ HIV infection<br>• **Symptoms**<br>▪ Asymptomatic, detected at routine screening<br>▪ Pelvic pain, pain with intercourse, vaginal bleeding or discharge | **MRI features**<br>• **Typically presents as a solid lesion with non-dark T2/non-dark DWI solid tissue centered in the endocervical canal and invading into the cervical stroma**<br>• **Imaging in the sagittal plane and oblique plane (perpendicular to the cervix) is essential for accurate staging**<br>• **T1WI**<br>○ T1-iso-to-hypointense<br>• **T2WI**<br>○ T2-intermediate, higher than the cervical stroma<br>• **DWI**<br>○ Diffusion restriction<br>• **CE**<br>○ Typically, hypoenhancing |

| | | |
|---|---|---|
| | • **Staged with the 2018 FIGO staging system, based on traditional anatomic extent**<br>○ Both imaging findings and pathologic features can be used for staging, with pathologic findings taking precedence over imaging<br>• **Main histologic subtypes**<br>○ Squamous cell carcinoma (80%)<br>○ Adenocarcinoma<br>○ Other rare histologic subtypes | ○ Small tumors may show early avid enhancement<br>**Note:**<br>• An oblique plane perpendicular to the cervix is essential to evaluate for parametrial invasion. Parametrial invasion is indicated by full-thickness cervical stromal invasion (i.e., loss of the T2-hypointense outer rim of the cervical stroma) and a nodular or spiculated tumor-parametrium interface<br>• Adding DWI to T2WI improves diagnostic accuracy for detecting parametrial invasion |
| | **Gastric-type adenocarcinoma of the cervix** | |
| | **Pertinent Information**<br>• **Age**<br>○ Pre- or postmenopause<br>• **Prevalence**<br>○ 10% of cervical adenocarcinomas<br>• **Causes**<br>○ HPV-independent<br>○ Peutz–Jeghers syndrome<br>• 10% of patients with gastric-type adenocarcinoma<br>• **Mucinous tumors with variable differentiation**<br>○ Minimal deviation adenocarcinoma (adenoma malignum) is a well-differentiated subtype with benign appearing endocervical glands that extend deeply into the cervical stroma<br>• **Symptoms**<br>○ Copious watery discharge<br>○ Abnormal vaginal bleeding<br>• **Diagnosis**<br>○ Challenging, requires a cone biopsy<br>• **Prognosis**<br>○ Poor prognosis due to early peritoneal spread and treatment resistance | **MRI features**<br>• **Solid or multilocular cystic endocervical lesion with non-dark T2/non-dark DWI solid tissue, extending deeply into the cervical stroma; may show peritoneal spread**<br>• **T1WI**<br>○ T1-iso to hypointense endocervical lesion<br>• **T2WI**<br>○ Endocervical lesion with T2-hyperintense cysts/cystic component and T2-intermediate solid tissue<br>• **DWI**<br>○ Diffusion restriction in solid tissue<br>• **CE**<br>○ Enhancing solid tissue |
| **V U** | **Vulvar carcinoma** | |
| | **Pertinent Information**<br>• **Age** | **MRI features** |

| | | |
|---|---|---|
| **LVA-PERINEUM** | ○ Peri- or postmenopause<br>• **Rare gynecologic malignancy**<br>• **Main risk factors**<br>○ Chronic HPV infection<br>○ HIV infection<br>○ Lichen sclerosus (skin condition)<br>• **2009 FIGO staging system, based on traditional anatomic extent**<br>• **Most prevalent histology**<br>○ Squamous cell carcinoma<br>• **Clinical examination**<br>○ Lesion size and number; distance to the midline; vaginal, urethral, or anal involvement,<br>○ Palpation of groin regions to check for enlarged inguinofemoral LNs<br>• **Punch biopsy**<br>○ Diagnosis<br>○ Depth of stromal invasion<br>• **Most important prognostic factor**<br>○ Inguinofemoral LN status<br>○ Influenced by tumor size, depth of stromal invasion, and LVSI | • **Solid lesion with non-dark T2/non-dark DWI solid tissue centered in the vulva and/or perineum**<br>• **Imaging in the sagittal plane, coronal or coronal oblique plane parallel to the urethra, and axial or axial oblique plane perpendicular to urethra are critical for accurate staging**<br>• **Adding fat saturation to coronal and axial images can facilitate assessment of local tumor extent**<br>• **T1WI**<br>○ T1-iso-to-hypointense<br>• **T2WI**<br>○ T2-intermediate<br>○ Fat-saturation improves delineation of local tumor extent<br>• **DWI**<br>○ Diffusion restriction<br>• **CE**<br>○ Enhancing primary tumor and inguinofemoral LN metastases without or with central necrosis<br>**Note:**<br>• MRI is recommended for tumors >2 cm with >1 mm stromal invasion or when there is close proximity to or potential involvement of the urethra, vagina, or anus<br>• The primary goal is to evaluate local tumor extent and assess bilateral groin regions for inguinofemoral LN metastases |
| | **Aggressive Angiomyxoma** | |
| | **Pertinent Information**<br>• **Age**<br>○ Premenopause<br>• **Rare aggressive mesenchymal tumor**<br>○ Propensity for local recurrence<br>• **Collagen fibrils within a myxoid stroma, creating an internal laminated appearance** | • **Large solid lesion in the perineum or vulvovaginal region with a laminated appearance, straddling levator ani muscles**<br>• **T1WI**<br>○ T1-iso-to-hypointense lesion<br>• **T2WI**<br>○ T2-hyperintense myxoid stroma with T2-hypointense collagen bands, creating a laminated appearance<br>• **DWI**<br>○ No diffusion restriction due to myxoid content<br>• **CE**<br>○ Avid enhancement |

**Note:--Abbreviations:** ADC, apparent diffusion coefficient; CE, contrast-enhanced; DWI, diffusion-weighted imaging; FIGO, International Federation of Gynecology and Obstetrics; HIV, human
**References:** 8, 9, 20-25, 79-82